1977

Determination of undrained shear strength of marine clays by combined vane and direct shear analysis.

Foster, James Edward

University of Washington

DETERMINATION OF UNDRAINED SHEAR STRENGTH OF MARINE CLAYS BY COMBINED VANE AND DIRECT SHEAR ANALYSIS

JAMES EDWARD FOSTER

1977

DETERMINATION OF UNDRAINED SHEAR STRENGTH OF MARINE CLAYS BY COMBINED VANE AND DIRECT SHEAR ANALYSIS

BY

JAMES EDWARD FOSTER

A thesis submitted in partial fulfillment
of the requirements for the degree of

Master of Science in Civil Engineering

University of Washington
1977

Approved by _____
(Chairman of Supervisory Committee)

Program Authorized
to Offer Degree _____

Date _____

In presenting this thesis in partial fulfillment of the requirements for a Master's degree at the University of Washington, I agree that the Library shall make its copies freely available for inspection. I further agree that extensive copying of this thesis is allowable only for scholarly purposes. It is understood, however, that any copying or publication of this thesis for commercial purposes, or for financial gain, shall not be allowed without my written permission.

Signature _____

Date _____

TABLE OF CONTENTS

LIST OF TABLES

LIST OF FIGURES

LIST OF PLATES

ACKNOWLEDGEMENTS

The author wishes to express his profound appreciation to Professor Mehmet A. Sherif, the Chairman of his Supervisory Committee, for his dynamic and unselfish guidance and encouragement. In addition, the author wishes to thank the other members of his Committee, Professor Richard H. Meese and Dr. Isao Ishibashi for their suggestions and guidance. Thanks are also extended to Mr. Bob Bea of the Shell Oil Company and Dr. Leland Kraft, McClellan Engineers, Inc. for their assistance in obtaining the Gulf of Mexico sample and to Dr. Armand Silva and Mr. Dave Calnan, University of Rhode Island for their assistance in obtaining the Atlantic Ocean samples. Gratitude is also extended to the U.S. Navy for having funded my pursual of this Master of Science degree.

Finally, the author expresses his sincere gratitude to his wife, Susan, daughter, Carrie and son, Travis for their patience and help in the preparation of this thesis.

CHAPTER I

INTRODUCTION

With the rapid increase in offshore exploration and construction in the 1970's, the need to determine quality geotechnical properties of marine sediments has greatly increased. Since the initial stages of off-shore developments in shallow Gulf of Mexico waters in the late 1940's, submarine soil testing has been required in progressively deeper water. Testing is presently being accomplished in water depths exceeding 1000 feet (Bhushan, et. al. ref. 3) from dynamically positioned drillships and samples have been taken from depth exceeding 3 miles (ref. 20). As the water depths increase, the structures being constructed are designed to resist larger and larger vertical and lateral loads, amplifying the requirement for quality geotechnical property determination for the design of their foundations. There are no standardized procedures for obtaining geotechnical properties and there is no agreement within the off-shore design/construction community as to what tests (in-situ or laboratory) are the best for determining geotechnical properties. Eide (ref. 5) in his comprehensive review of applications of soil mechanics to off-shore structures in 1974, pointed out that most of the available drilling and sampling techniques were rather crude and result in significant disturbance of the sample, hence results of tests on such samples show great scatter making the selection of design parameters very difficult.

Presently, empirical formulas are being used almost exclusively for designing seafloor foundations on marine clay.

McClellan (ref. 11) presented design procedures which are currently being utilized by McClellan Engineers, Inc. for ocean foundations. These procedures which have been generally accepted by the profession involve equations of the following types:

$$Q_s = \lambda(\bar{\sigma}_m + 2\,C_m)\,A_s \qquad 1\text{-}1$$

where: Q_s = total friction capacity of a pile

λ = frictional capacity coefficient

$\bar{\sigma}_m$ = mean effective vertical pressure for depth of pile embedment

C_m = mean undrained shear strength for depth of pile embedment

A_s = surface area of embedded pile

Valent in ref. (7) presented the following equation for the uplift resistance of an embedded plate (anchor) in cohesive soils:

$$Q_u = N_{cu}\,C\,A\,(0.84 + 0.16\,B/L) \qquad 1\text{-}2$$

where: Q_u = total uplift capacity of a plate

N_{cu} = uplift capacity factor

C = undrained shear strength near the plate elevation

A = projected area of the plate

B = one-half the width of the plate

L = the length of the plate

Hermann in ref. (6) presented the following equation for the bearing capacity of a footing on the ocean floor:

$$q_{ult} = K_1\,N_c\,C + K_2\,\gamma N_\gamma\,B + N_q\gamma\,D \qquad 1\text{-}3$$

where: q_{ult} = the ultimate bearing capacity of the footing

K_1, K_2 = shape coefficients

N_c, N_γ, N_q = bearing capacity factors

C = cohesive strength

γ = submerged soil density

B = width or diameter of footing

D = depth of footing base below mudline

The value of C, the undrained shear strength, is the key value in each of the above equations. There is no agreement as to the best method for determining C. In this paper, the author will focus on one procedure for determining undrained shear strength of marine clays by utilizing combined vane and direct shear tests which will provide quality, economical data from relatively "undisturbed" samples. Furthermore, an attempt is made to corroborate the equipment and test procedures used by Webb (ref. 21) and to expand his data and theory for shear strength envelope to determine application to a general case versus a specific case. This investigation will study the relationship between the direct shear test and the vane shear test as determined from a combined analysis of clay samples from the Pacific Ocean, the Gulf of Mexico and the Atlantic Ocean.

The equipment used was: a) direct shear device modified to receive a relatively "undisturbed" marine sample, to have a refined vertical loading system, and to provide electronic printout of data, b) vane shear device modified to provide constant and controlled strain and electronic printout of data.

Consolidated undrained (CU) tests were conducted on samples that were consolidated under varying normal loads in the direct shear machine. These direct shear tests were followed immediately by vane shear tests on those same samples, performed

while the samples remained in the direct shear box. The data was plotted and analyzed and a general theory proposed that will describe the entire strength envelope of marine clays utilizing only two samples. Acceptance of this theory will greatly reduce the number of samples and testing required to determine the strength envelope of a marine clay.

CHAPTER II

DISCUSSION OF SHEAR STRENGTH

II - 1 Methods of Collecting and Analyzing Data

For determining the shear strength of today's marine clay, the vane shear and penetrometer tests are primarily utilized in-situ, while the vane shear and triaxial test are most often used in the laboratory. For terrestial soils, the triaxial test is considered to provide the best results because it has better control over stress, strain, pore pressure measurement and it does not have a pre-determined failure plane. However, primarily due to sampling methods, recovery and handling, the triaxial shear strength test is not as reliable when dealing with marine soils. In the marine environment we are forced to cope with materials whose moisture contents are near or exceed the liquid limit (figure 1). Historically, the direct shear test on a marine clay has been thought to be unreliable because of unknown drainage conditions. However, the author feels that under controlled conditions the direct shear test can provide reliable results. The direct shear test utilized in conjunction with the vane shear test will be investigated in this paper.

The cone penetration device is widely used to determine shear strength of marine clays. There are several types of penetrometers, all of which basically involve transcribing the penetration energy to values for shear strength. Figure 2 is representative of a typical cone penetrometer. This method has the distinct advantage of providing a continuous strength profile with depth. The cone penetrometer is usually used in conjunction

with a vane shear device. The vane is essentially used to "calibrate" the penetrometer profile. Such a system is used by the Naval Civil Engineering Laboratory (NCEL) on the DOTIPOS (Deep-Ocean Tests in Place and Observation System) retrievable platform. Figure 3 represents correlations resulting from this type of combined testing.

Soil "Sensitivity" is important when considering the shear strength of marine clays. Sensitivity is defined as the "undisturbed" shear strength divided by the "remolded" shear strength (figure 4). Table 1 indicates the range of values of sensitivity. Some highly sensitive clays have little or no strength after being disturbed. There appears to be a close relationship between liquidity index and sensitivity (Buchan, et. al., ref. 15); sensitive clays with high moisture content have liquidity indices much greater than one. It has been shown that abrupt changes in moisture content bring about abrupt changes in sensitivity (Buchan, et.al., ref. 15).

In general, shear strength and bulk density increase with depth below the mudline, while water content and void ratio decrease. Table 2 gives a good indication as to the typical magnitudes of shear strength values that can be expected. Shear strengths of marine clays range from values as low as 0.1 psi to values exceeding 5.0 psi, at water contents ranging between 30% and 300% (Noorany, ref. 13). Calcareous oozes indicate an undrained shear strength of 0.5 to 2.5 psi. These values are surprisingly low for such deep burial (400-500 feet below mudline) and are probably the result of a high degree of disturbance (Noorany, ref. 13). Attempts have been made to simulate in-situ

conditions by consolidating in a triaxial cell at effective over-burden pressure. The results were values for strength in excess of 10 times the undrained vane strength. The difference again was attributed to disturbance and change in the stress system as a result of sampling.

II - 2 Effects of Loading History on Shear Strength

Noorany (ref. 13) summarized the relationship between shear strength and consolidation for marine sediments. There are areas in the oceans where sediments accumulate at such a high rate that there is not adequate time for consolidation; pore pressure builds up, resulting in a soil that has very little strength for great depths. These sediments are termed under-consolidated. The area off the mouth of the Mississippi River is such a region, having an estimated deposition of approximately 1,500,000 tons of material daily. Shear strength values determined in 250 feet of underconsolidated clay near the South Pass area of the Gulf of Mexico showed little change in strength with depth and was nearly equal to the determined cohesion of that clay (Noorany, ref. 13). Terzaghi calculated that for an underconsolidated marine soil, slopes of 10° could be subject to failure if that sediment reached a depth of 47 feet (ref. 12).

Normally consolidated clays exhibit ratios of unconsolidated undrained shear strength, C_{μ}, to effective over-burden pressure, P'_{o}, in the range of 0.1 to 0.4. This ratio for the Gulf of Mexico prodeltaic clays averages 0.31. The value of shear strength previously mentioned for calcareous oozes were also representative of normally consolidated marine clays.

Overconsolidated and "apparently" overconsolidated clays exhibit higher shear strengths; clays of the South Timbalier area of the Gulf of Mexico have C_μ values of almost 10 psi. Table 3 shows typical values for some overconsolidated clays. It should be noted that the C_μ/P'_o ratio looses meaning near the mudline as P'_o approaches zero. Overconsolidation is usually associated with removal of overburden, however, massive erosion of the continental shelf or the abyssal plain is unlikely. Figure 5 showing e-log P curves for Gulf of Mexico sediments, indicates consolidation behavior similar to that for overconsolidated clays. This behavior is attributed to the cementation brought about by the chemical alteration of the volcanic or carbonate fraction of the sediment.

The terms "under", "over" and "normally" consolidated, although appropriate for land and shallow water soil mechanics, are not necessarily appropriate for deep water sdeiments (Richards, ref. 15). It is known that any factor that imparts unusual structural strength to a soil will result in an e-log P diagram that appears to represent an overconsolidated condition. It has been further shown that complete remolding of samples reduces the consolidation curves to near straight lines (figure 6).

II - 3 Laboratory Vs. In-Situ Results for Shear Strength

Since the initial attempts at marine soils investigations it has been known that in-situ values differ from laboratory values despite extreme care to simulate seafloor conditions. The reasons for these deviations and ways to correct them are the objects of tremendous research effort. Numerous papers on this

subject are presented each year at the Annual Offshore Technology Conference in Texas. Some of the factors producing deviation in laboratory vs. in-situ values were summarized by True (ref. 17) and include the following:

1. Replacement of in-situ stress with uniform hydrostatic effective stress.
2. Mechanical sampling disturbance; hydrostatic stresses and soil structure are changed by disturbance from sampling, transporting, storage, trimming, and test sample preparation. The result is decreased shear strength and compressibility.
3. Pore water expansion: sea water expands 0.5%/1000 m., thus a sample from 3500 meters has a pore pressure expansion of approximately 2%. The result is a reduction of effective stress, strength and compressibility.
4. Changes in pressure affect dissolved pore water gases.
5. Changes in temperature causes direct changes in stresses and strength.
6. Changes in temperature and pressure can cause rapid decomposition or growth of organic matter in the soil.

II - 4 Theories For Shear Strength

Shear strength as defined in terms of soil failure, has long been the subject of discussion and disagreement. The development of shear strength concepts began with Coulomb in 1776. Since that time, complicated apparatus has been developed in order to more fully define the elements of shear strength. For this study, the direct shear test was combined with the vane shear

test to determine the strength envelope. Both of these tests generate enforced failure planes between stationary and moving equipment or sample sections. A well-defined peak in the shear stress versus strain curve (figure 7) is usually considered to be the shear strength of a soil. The shape of this curve is very much dependent on loading type, shearing rate, and drainage conditions (Hvorslev, ref. 1).

Coulomb's first expression of soil failure criteria was:

$$\tau_f = C + \sigma_f \tan \phi \qquad 2\text{-}1$$

Where τ_f is the shear stress at failure, C is cohesion, σ_f is the normal stress applied at failure, and ϕ is the angle of internal friction. Coulomb considered C and ϕ to be constant for a given soil and that simple tests could be used for their determination. Subsequent investigations have shown these parameters to vary widely depending on such factors as initial water content, shearing rate and anisotropy (Wu, ref. 22).

Casagrande, as well as Terzaghi, concluded that normal stress, σ_f, should be replaced by effective normal stress, σ_f' where:

$$\sigma_f' = \sigma_f - \mu \qquad 2\text{-}2$$

with the pore water pressure, μ, equal to zero in fully drained tests. Terzaghi expressed the soil failure criteria in terms of effective stresses as opposed to total stresses. The Terzaghi failure criteria appears as

$$\tau_f = C' + \sigma_f' \tan \phi' \qquad 2\text{-}3$$

where C' and ϕ' are the effective cohesion and effective angle

of internal friction. This function is illustrated as a part of figure 8. The line OAC represents the shear strength line for a normally consolidated clay with C' = 0 and $\phi = \phi'_s$. Preconsolidation of a clay has considerable effect on the representation of shear strength. The line BA is the shear strength curve for a clay preconsolidated at a pressure of σ'_p and exhibits an angle of internal friction of ϕ'_r. Preconsolidation to pressures other than σ'_p produce shear strength lines represented by the dashed line parallel to BA. The significance of this is that C' is proportional to the preconsolidation pressure σ'_p in the following manner:

$$C' = \sigma'_p \tan\phi'_c \qquad 2\text{-}4$$

therefore equation 2-3 would appear as (Hvorslev, ref. 1)

$$\tau_f = \sigma'_p \tan \phi'_c + \sigma'_f \tan \phi'_r \qquad 2\text{-}5A$$

For a normally consolidated clay, this formula can be modified further such that

$$\tau_f = \sigma'_f \tan \phi'_c + \sigma'_f \tan \phi'_r \qquad 2\text{-}5B$$

Hvorslev referred to this presentation as the Krey-Tiedman failure criteria. The general concept was proposed initially by Krey and subsequently extended by Tiedman. It should be noted that equations 2-4 and 2-5, as well as their representation in figure 8, are based upon results of fully drained direct shear tests on normally and overconsolidated clays. The first term on the right side of equation 2-5B can be referred to as the cohesion component and the second term as the friction component,

thus the anomally of having two angles of internal friction, ϕ_s' and ϕ_r', for the same clay and no cohesion for a normally consolidated clay is thereby eliminated (Hvorslev, ref. 1).

Terzaghi (Wu, ref. 22) determined that the stress or loading history of a sample affects the determined shear strength. Hvorslev (ref. 1) summarized this effect which is represented in figure 9. This figure indicates different values of σ_p' and σ_f'. The unloading and reloading of a sample produces the hysteresis loop shown in figure 9. It is evident that the idealized straight lines represented in figure 8 are actually complex curves.

The dashed line, DE, in figure 9 represents a slight double curvature noted by several researches (Wu, ref. 22) from tests on undisturbed samples. D represents the strength of a sample at pressure σ_d' that was preconsolidated at σ_p'. If tests are performed at values of normal pressure greater than σ_d', the strength line will pass to the reloading curve of the hysteresis loop.

Hvorslev (ref. 1) conducted exhaustive studies using direct shear tests on Vienna and Little Belt clays in order to better define the effect of over-consolidation. Hvorslev summarized his results in an equation very similar to the Krey-Tiedman formula

$$\tau_f = C_e' + \sigma_f' \tan \phi_e' \qquad 2\text{-}6$$

where C_e' and ϕ_e' are the "true cohesion" and "true angle of internal friction". Hvorslev concluded that C_e' is a function of water content only while ϕ_e' is constant for a given soil. In order to separate the two strength components, it is necessary

to conduct tests on a series of samples having the same water content at failure, but different effective stresses. This can be accomplished by using the consolidation, unloading, and reloading technique illustrated in figure 10. It has also been shown that the true cohesion at any water content is proportional to the equivalent consolidation pressure, σ_e. In the triaxial test, σ_e is the consolidation pressure producing that water content in a normally consolidated sample (Bishop and Henkel, ref. 2). Only drained or consolidated-undrained tests with pore pressure measurements can be used to evaluate the true cohesion.

Besides being difficult to determine, the parameters of the Hvorslev failure criteria were formulated based upon drained direct shear tests that considered only peak shear stress as the failure strength. It is therefore questionable as to the application of this criteria to other test results (Wu, ref. 22).

A change in void ratio or water content causes a change in the shear strength of a clay, therefore a complete expression of shear strength should include consolidation characteristics. The semi-logarithmic plot of the consolidation diagram (ω% vs. Log P) of a normally consolidated clay is usually straight (Hvorslev, ref. 1). Figure 11 shows the consolidation diagram for a sample consolidated normally, unloaded, and then reloaded.

As an alternative to the Hvorslev method of determining shear strength, Webb (ref. 21) has proposed a simple theory for determining the undrained shear strength envelope of marine soils. He ran a series of "combined" vane and direct shear tests on naturally occurring marine soils. A sample specimen was consolidated and sheared in the direct shear machine under a normal

stress equal to that consolidation pressure. The normal load was immediately removed and a vane shear test was run. The data derived from one direct shear test and the subsequent vane shear test is referred to as one "combined" shear strength plot. Because the vane shear tests are conducted at zero normal stress, their resulting shear strength can be thought of as being a function of "preconsolidation" pressure.

When plotting shear stress versus normal stress (direct shear) or consolidation pressure (vane shear), Webb found the vane shear plot to be linear over all values of consolidation pressure. The direct shear plot was higher and roughly parallel to the vane shear plot for $\sigma_n < P_c$ (preconsolidation pressure) and for $\sigma_n > P_c$ the slope of the plot increased and passed through the origin when extended back. This last portion of the direct shear plot is usually interpreted as representing the strength of normally consolidated samples. These observations of his experimental results led Webb to suggest a "combined" analysis of shear strength that utilizes direct and vane shear tests on only two samples to determine the complete strength envelope. The terms, definitions and relationships of this theory are depicted on fig. 12. The plot of direct shear strength vs. normal stress was referred to as the "Total Failure Stress Envelope". The plot of vane shear strength vs. consolidation pressure was termed the "Cohesion Line," since the vane test measures only sample cohesion. The angle of slope of the cohesion line was designated as ϕ_c, while the angle of slope of the normally consolidated portion of the total failure stress envelope was referred to as ϕ_n. The value of shear stress at σ_n equal to

zero was termed C_d. C_v was the value of vane shear stress at consolidation pressure equal to zero. The difference in the terms C_d and C_v is referred to as ΔC. The value of σ_n above which the total failure stress envelope is linear is termed the "apparent" precompression stress, P_c.

The factor that made this theory possible was the observation that the total failure stress envelope, as defined by the direct shear test results, is roughly parallel to the cohesion line for values of σ_n less than P_c. As illustrated in figure 12, the angle of slope of the total failure stress envelope is ϕ_c for σ_n less than P_c. Therefore, the entire total failure stress envelope can be drawn if C_d, ϕ_c, and ϕ_n are known. It follows that only two "combined" shear strength tests are required to generate the total failure stress envelope; one test at σ_n and consolidation pressure equal to zero and the other at σ_n and consolidation pressure greater than P_c. A preliminary estimate of P_c is required to ensure that σ_n for the second data point is greater than P_c. This method gives four data points; two direct shear strengths and the two vane shear strengths, C_d and C_v. ϕ_c is determined by connecting C_v with the vane shear strength at the higher consolidation pressure. A line is drawn from the origin to the direct shear strength value at the higher value of σ_n. This enables the determination of ϕ_n. Finally, a line is drawn from C_d, at an angle of slope ϕ_c, to intersect the line drawn through the origin. The result is the total failure stress envelope that would have resulted from a series of direct shear tests at progressively increasing values of normal stress.

Mathematical descriptions of this theory are as follows:

a) For $\sigma_n < P_c$ $\quad \tau_f = C_d + \sigma_n \tan \phi_c$ 2-7

b) For $\sigma_n > P_c$ $\quad \tau_f = C_d + P_c \tan \phi_c + (\sigma_n - P_c) \tan \phi_n$ 2-8

c) For $\sigma_n > P_c$ $\quad \tau_f = C_v + \sigma_n \tan \phi_c + \Delta C + (\sigma_n - P_c)(\tan \phi_n - \tan \phi_c)$ 2-9

Where τ_f = the maximum shear stress at failure.

The purpose of this investigation will be to validate this theory. Test apparatus and procedures similar to those used by Webb will be utilized. A general set of samples will be used to determine general applicability of the theory.

CHAPTER III

DISCUSSION OF DIRECT AND VANE SHEAR APPARATUS AND TESTS

As outlined in the introduction, this study uses the direct shear test in conjunction with the vane shear test in a combined strength analysis of marine clays. Both tests have been subject to criticism and praise. This chapter will outline the advantages, disadvantages, apparatus, application, and the test procedure associated with both tests.

III - 1 Direct Shear Test

The direct shear test is one of the simplest soil strength tests known as well as being the oldest; it was first used by Coulomb in 1776 (Lambe and Whitman, ref. 10). The cylindrical or triaxial shear test and the torsional shear test are the other commonly used methods for soil shear strength determination. The vane shear and cone penetrometer tests were previously discussed and continue to have limited use.

The torsional shear test is more commonly used in Europe. In this test, a cylindrical soil sample is twisted by applying a twisting moment at the top and bottom (figure 13). A lateral stress can be applied to the sample if desired. During the direct shear and triaxial shear tests, the sample becomes badly deformed causing non-uniform stress and strain thus making the measurement of the failure surface area difficult. The torsional shear test has the advantage in that the cross-section remains more nearly constant during shear (Lambe, ref. 9). This advantage is out-weighed by the fact that the shear displacements vary with radius, promoting progressive failure of the soil

sample. The use of an annular sample somewhat reduces this problem. The torsional shear test has the definite disadvantage of requiring considerable specimen handling for test preparation.

The triaxial test involves the axial loading of a cylindrical sample (figure 13) that is usually encased in a rubber membrane. Uniform pressure is applied using a pressure cell containing the sample and surrounding fluid.

The direct shear test requires the placing of a soil sample in a container having fixed and movable sections. The test is performed by displacing the sections of the container relative to each other. During this displacement, the soil is sheared along one or more internal surfaces. The only resistance to that shearing is provided by the soil. There are several types of direct shear tests and apparatus with their names being derived primarily by the design of the soil container or the shape of the shear surface. These include (figure 14):

1. 2-piece single shear box
2. single or double ring shear apparatus
3. annular or "punching" shear apparatus.

The annular direct shear test provides a more nearly constant shear area than does the box or ring shear test, and consequently, more uniform strains (Lambe, ref. 9). The test is more complex to perform and the specimen is more difficult to prepare than those of the box or ring shear type of test.

In the double ring shear apparatus, the shearing force is applied to a central, movable ring (figure 14). Samplers have been designed such that their liners are composed of continuous close fitting rings (Lambe, ref. 9). These rings fit directly

into the ring shear device. This eliminates the transfer of the sample from the liner to the shear apparatus, as well as any required sample trimming. This advantage is somewhat questionable because the sampler is necessarily thick walled having a high area ratio, A_r (Terzaghi and Peck, ref. 18). High area ratios result in "disturbed" (A_r greater than 20%) samples, increasing the danger of remolding and weakening the soil before testing.

Of the three direct shear tests discussed, the 2-piece simple shear box is the most used in the United States. A basic representation of the simple shear box appears in figure 14. The soil to be tested fills the two sections of the box and is fitted with a plate on top and bottom. The plates can be pervious or impervious depending on the nature of the direct shear test being conducted. Usually the lower section of the shear box is fixed and the upper section is allowed to move. The reverse arrangement is sometimes used although is is considered to give too high values for shearing resistance because of restraint to sample expansion (Tschebotarioff, ref. 19). In either case, a normal force, N_1 is applied to the upper plate distributing that force over the soil surface. A lateral load, P_1 is applied to the movable section of the shear box. The direct shear test is further designated by the manner in which loading is applied and displacement measured. The test can be either a stress-controlled direct shear test or a strain-controlled direct shear test.

In the case of the stress-controlled direct shear test, the lateral force is applied in discrete increments, often by using dead weights. Shear displacement is recorded as a function of time until it ceases or until failure occurs. Failure is in-

dicated by a rapid increase in displacement. The stress-controlled test is preferable in those situations requiring very low rates of loading. The load can be kept constant for any given period of time. It is more difficult to obtain a value for ultimate strength due to the rapid shear displacement that occurs immediately following the exceeding of the maximum shear resistance of the soil (Lambe, ref. 9). This test is used for most soil mechanics applications.

The strain-controlled direct shear test is used mostly for research (Jumikis, ref. 8), but has some practical applications. Normally, controlled and constant strain (shear displacement) is applied to the movable box section by means of a gear assembly that is either manual or motorized. The force is usually determined by using a calibrated proving ring and is recorded as a function of time or displacement. This type of direct shear test has the advantage of providing a good measurement of both peak and ultimate shear resistance (Lambe, ref. 9). The stress-controlled test requires the manual regulation of loading and is thus more difficult to conduct.

Jumikis (ref. 8) summarized the disadvantages of the direct shear test as follows:

1. The shear area in a direct shear test is constantly changing causing unequal distribution of shear and normal stresses over the potential sliding surfaces. This makes the stress conditions across the sample very complicated.
2. The water content of saturated samples of many types changes rapidly as the result of changes in stress.

3. There is question as to the effect of the lateral restraint of the walls of the shear box. The stress conditions produced thus do not correspond to conditions in a foundation. The shear stress obtained by dividing shear force by rupture area is only approximate.
4. The time required to remove the sample from the test apparatus can effect the water content determination. Also, the water content at the sample boundaries show different values than the sample interior. (Hvorslev, ref. 1).
5. The complete state of stress at any time prior to failure is unknown.
6. The majority of "undrained" tests using the direct shear test are not completely undrained. There appears to be no way to determine to what degree these tests approach undrained conditions. Ultimate strength is more affected by this unknown merely because of the longer time required to reach ultimate shearing resistance (Lambe, ref. 9).

The advantages of the direct shear test comprise a short but important list, especially as it concerns marine clays.

1. The direct shear test offers a simplicity of operation requiring less test time and sample handling.
2. The smaller height of sample used in the direct shear test requires less drainage time. This facilitates more rapid Q_c or S tests. The shear rate can be larger than that used in the triaxial test.
3. The direct shear test requires much less sample than

does the triaxial test.

The direct shear apparatus used in this study was a strain-controlled single shear box type. The complete apparatus appears on Plate 1.

III - 2 Direct Shear Apparatus

The direct shear apparatus (Plate 1) was originally designed and built by the Department of Civil Engineering of the University of Washington and was modified slightly to conform to the requirements of this study. This system is designed to perform strain-controlled direct shear tests.

Shear displacement is provided by a variable-speed motor coupled directly to a multiple output shaft gear box. This combination is manufactured by Karol Warner, Inc., and provides for a wide range of rotational speeds by the proper selection of output shaft and motor speed. The output shaft is coupled to a gearbox mounted on the direct shear test stand. This gear arrangement translates the rotational motion into the transverse motion used to provide shear displacement in the shear box. The various output shaft and motor speeds were calibrated against shear displacement as a function of time. The strain (shear displacement) rate can be accurately controlled from 0.001 in/min. to 0.5 in/min. (Webb, ref. 21). The gearbox offers output rotational rates that increase in steps of 10. The output shaft designated as 1/10 rotates at 1/10 the rate of the variable speed motor. Using a motor setting of 55 and the 1/10 output shaft, a translational displacement rate of the shear box of 0.06 in/min. was observed.

The majority of commercially manufactured strain controlled direct shear machines use calibrated proving rings to measure the shearing force applied to the sample. The system used in this study employs a BLH Electronics, Inc., Type U3G1 load cell (Plate 2) between the second gear assembly and the shear box. This load cell was calibrated using a proving ring and the Gould strip recorder (Plate 3). The calibration refers only to this particular load cell-strip recorder combination at the strain gage conditioner and chart sensitivity settings specified. The calibration appearing in the appendix as figure A-1 was determined by Webb (ref. 21) and verified by the author. The strip recorder provided for more accurate determination of force vs. displacement. It has the added advantages of making the recording of the test easier as well as providing an immediate and permanent visual presentation of the test data.

The direct shear box is shown on Plates 4 and 5. The area of the shear box in its original configuration was 9 in^2. The top portion of the box is fixed and the bottom is free to move. There is a porous stone at the bottom of the lower section allowing drainage. The shearing surface is 0.5 inches above this stone. The samples used in this study have a round cross-section. Ring adapters (Plate 4) were designed to fit inside the square shear box and accept the samples directly from their liner. Plate 5 shows the ring adapters in place along with the vertical pressure plate. Adapters were designed for liners with a 2.62 in. inside diameter as used to collect Pacific sample KK076 and a 2.00 in. inside diameter for the Gulf of Mexico and Atlantic samples. The Gulf of Mexico samples were approximately 2.25 in.

in diameter and were trimmed to 2.00 in. with a thin-walled cutter. The atlantic samples were 2.00 in. in diameter.

The air pressure operated vertical loader, apparent in Plate 1, used for conventional applications of the direct shear test, proved inappropriate for this study. This loader did not allow for accurate control of small values of normal load. A simple lever arm system was designed to replace the air loader (Plates 1, 6 and 7). The arm has a lever ratio of 10 to 1. By knowing the cross-sectional area of the ring adapters, the desired normal load was easily applied by placing the proper weights in the tray.

The area of sample resisting shear was reduced as a function of displacement as the test progressed. This area is easily determined when the shear box has a rectangular or square section. This determination was more difficult for overlapping circular sections as was the case in this study. This area is plotted as a function of displacement in the appendix, figure A-2 for the 2.62 in. samples and figure A-3 for the 2.00 in. samples and was based upon the following relationship:

$$A = R^2 \left\{ \frac{\pi \cos^{-1} \frac{X}{2R}}{90^\circ} - \sin \left[2\cos^{-1} \left(\frac{X}{2R} \right) \right] \right\} \qquad 3\text{-}1$$

where A is the coincidental or "common" area of two overlapping circles of radius R, as a function of displacement, X.

III - 3 Vane Shear Tests

Granular soils that are free draining and contain significant amounts of water, present little problem when determining

shear strength, either in the field or the laboratory. With marine clays, the foundation engineer is confronted with the problem of determining the strength of a saturated clay with very low permeability that does not allow free drainage. The pore pressures associated with shear stress application do not readily dissipate in such materials. The time required for dissipation of these pore pressures, with its accompanying increase in shear resistance, is a function of the boundary constraints, dimensions, and consolidation characteristics of the particular clay material.

When testing a saturated clay using the unconfined compression test or triaxial test with the minor and the intermediate principal stresses equal to zero, the result is the $\phi = 0$ condition described by Terzaghi (ref. 18). The shear strength under these conditions is described by the equation:

$$S = C = \tfrac{1}{2}q_u \qquad 3\text{-}2$$

Where S is the shear strength, C is the cohesion, and q_u is the ultimate unconfined compressive strength. There are relatively quick, uncomplicated strength tests available when the undrained condition exists, whether in the field or the laboratory. The test that fulfills these needs is the vane shear test. The vane test is analogous to the Q test, if carried out rapidly enough. The vane test, in its simplest form, consists of pushing a four bladed vane, mounted on the end of a thin rod, into the soil with as little disturbance as possible. The vane is rotated and the torque required to turn the vane is recorded as a function of vane rotation. In more refined field vane shear tests

the vane is pushed into the soil inside a shield and is protruded only at the time of the test (ref. 18). Elaborate laboratory vane devices are available that can control boundary conditions and stress-strain rates during testing.

Investigation has shown that the soil fails along a cylindrical surface circumscribed by the outer vane edges. Both the top and bottom of the vanes are included as failure surfaces in most vane shear tests. The relationship between angular rotation and torque must be known along with applied torque and vane dimensions in order to determine shear strength. The relationship is expressed by the formula:

$$M = \pi\tau \left(\frac{D^2H}{2} + \frac{D^3}{6}\right) \qquad 3\text{-}3$$

where M = net applied torque, $\tau = C = q_u/2$ = shear strength, D = vane diameter, and H = vane height.

If the top of the vanes are not into the soil enough to contribute to the resistance, the formula appears as:

$$M = \pi\tau \left(\frac{D^2H}{2} + \frac{D^3}{12}\right) \qquad 3\text{-}4$$

The test and formulas make the assumption that the failure is a right circular cylinder with a diameter equal to the vane blade diameter, D, in which the stress distribution at maximum torque is everywhere equal on the surface of the cylinder.

Sensitivity can be determined using the vane shear test. The vane is rotated several times after determining the "undisturbed" strength and then allowed to consolidate. The test is then repeated thus measuring "remolded" strength from which the

sensitivity is determined. Values for sensitivity determined in this manner differ from those determined if the sample is remolded by kneading (ref. 18).

Sibley and Yamane invented (1965) a small, convenient, hand-held vane shear device known as the TORVANE. It has gained wide acceptance and is widely used, both in the field and laboratory. The vanes are pushed to their full height into the soil and torque is applied by turning the upper knob until the soil fails. The value of C is read directly from the scale on the top of the TORVANE. Typically, the scale is calibrated so that one revolution of the pointer corresponds to C = 1 tsf. In spite of several modifications, the TORVANE cannot be used accurately on saturated clays with a q_u much greater than 1 tsf or on materials that contain pebbles, sandy layers, or any other secondary structure (ref. 14). A larger vane attachment is available to obtain more accurate values for C less than 0.25 tsf. Also available are miniature torque wrenches that can give torque directly and with fair accuracy.

The TORVANE is the object of considerable criticism including: 1) it only samples the surface of the unit, 2) there is poor control over the rate of shear, and 3) it is not firmly mounted, thus allowing for something other than a cylindrical shear surface. The TORVANE should be used with some discretion with these objections in mind. Its primary uses should be to make preliminary estimates of shear strength, to compare materials, or to identify soils that require further testing.

More elaborate vane shear devices are available for the laboratory. One manufactured by the Leonard Farrell and Co., Ltd. and another by Wykham-Farrance Engineering, Ltd. are the

most commonly used. The devices operate using the same principals and assumptions, but allow for more accurate determination of torque and vane rotation than devices such as the TORVANE. Torque is applied through interchangeable, calibrated springs with different spring constants; the proper spring being determined by the soil being tested. The Wykham-Farrance machine is available with a motor driven vane. It is this machine that was modified for this study. The modifications will be discussed in detail in subsequent pages.

Neil Monney (ref. 7) has recently experimented with the vane shear test. Monney listed several serious deficiencies with the vane shear test that include:

1. the test is not applicable to granular soils
2. the failure surface is predetermined and oriented
3. the failure surface is not a perfect cylinder
4. the confining pressure is unknown in the laboratory test
5. the vane size is not standardized
6. the drainage conditions are not known
7. the rate of shear is not standardized

Monney concerned himself with item 7. He hypothesized that since a saturated clay behaves as a visco-elastic material, it should exhibit an increase in strength as the shear rate is increased. The rate of shear used by most researchers and engineers ranges from 1°/min. to 90°/min. with 6°/min. being most common. In Monney's study, Wykham-Farrance machine was modified in a manner similar to that used during this study. Saturated clay was tested for "undisturbed" and "remolded" values over ranges of angular strain rate up to 720°/min. and the following was ob-

served:

1. Vane shear strength varies significantly with ranges of angular strain rate commonly used by engineers and researchers.
2. The shear rate should be standardized.
3. The standardized rate should be 90°/min.

These conclusions leave considerable room for discussion. It is not apparent how different soils or vane sizes would have affected the results. Values of strength determined at 90°/min. strain rate may not be appropriate to evaluate every foundation performance; different strain rates could be more appropriate for different applications.

The ASTM is presently considering several vanes and test procedures for standardization of the laboratory vane shear test. A field vane shear test using a larger vane is standardized as ASTM #D-2573.

III - 4 Vane Shear Apparatus

The basic vane shear apparatus used for this study was the Wykham-Farrance, Ltd., instrument previously mentioned. This machine was modified to transform this stress-controlled apparatus to a strain-controlled unit.

In its normal configuration, the above vane device has a small one-speed motor that drives a small gear assembly at the head of the instrument. This gear assembly is attached to the vane through a calibrated spring. During the test a torque is applied to the vane, the amount of which is determined by the angular deflection of the spring which is read at the head of

the instrument. The test is completed when the torque reaches the point where the soil fails as indicated by a sudden release of spring deflection. Uniform rate of shear is not possible using this arrangement.

The major modification to the Wykham-Farrance machine was the replacement of the spring with a plate mounted with strain gages in a configuration designed to measure torque on the vane shaft. The strain gage replacement is shown on Plate 8. The modified vane shear device is shown on Plate 9.

The variable-speed motor and multiple output shaft gear-box described for use with the direct shear machine has also been adapted for use on the vane shear machine. This apparatus was calibrated enabling the accurate selection of sustained vane rotation rates that range from 0.005°/min. to 100°/min.

The strain gage torque pick-up was also connected to the Gould strip recorder in order to get a detailed record of the test data. The torque pick-up was calibrated by alternately applying known values of torque and recording the movement on the strip chart. The calibration is expressed in terms of shear stress as a function of chart sensitivity and vane configuration, in the Appendix as figure A-4 as determined by Webb (ref. 21) and verified by the author.

CHAPTER IV

SAMPLES AND TEST PROCEDURE

IV - 1 Samples

In order for this investigation of shear strength characteristics of marine clays to be of a general nature, quality "undisturbed" samples were obtained from three areas with vastly different geographic location and sedimentation and loading history. The three samples were from the Pacific Ocean, Gulf of Mexico and the Atlantic Ocean. The samples from the Pacific Ocean were supplied by the U.S. Naval Civil Engineering Laboratory, Port Hueneme, California, and were collected by the Hawaii Institute of Geophysics in late 1973. The samples from the Gulf of Mexico were supplied by McClellan Engineers, Inc., Houston, Texas, and were originally collected for the Shell Oil Co. The samples from the Atlantic Ocean were supplied by the Ocean Engineering Department, University of Rhode Island and were collected by a research vessel from Worcester Polytechnical Institute.

IV - 1.1 Pacific Ocean Sample - KK076

This sample was from a 40 foot core taken in water in excess of 5000 meters in depth by a modified Ewing piston corer (ref. 20). Inside diameter of the polycarbonate core liner measured an average of 2.62 inches. The sample was taken northeast of the Hawaiian Islands at : Latitude 30° - 59' - 24" N

Longitude 149° - 50' - 6" W

KK076 was from an area of basaltic abyssal hills covered by a thin layer of deep-sea, pelagic clay (ref. 20). The material tested was from a depth in the core of 404-428 inches. At this

depth the material was a dark brown clay classified by the Unified Soil Classification System as OH (fig. 15). Table 4 summarizes the soil properties of KK076 as a function of depth of core.

IV - 1.2 Gulf of Mexico Sample - GM

This sample was taken in 167 feet of water on May 28, 1976, near Eugene Island in the Gulf of Mexico (exact location proprietary). The sample was part of a 24 inch long core taken at 30 feet below the mudline with a 2.25 in. inside diameter thin wall push tube. The material at this depth was a soft olive-gray clay classified by the Unified Soil Classification System as CH (fig. 15). The following properties were observed by McClellan Engineers, Inc., at the 30 ft. level:

Vane Strength	.15 tsf with water content = 56.7%
Liquid Limit	97%
Plastic Limit	33%
Plasticity Index	64%

IV - 1.3 Atlantic Ocean Sample - ATL

This sample was taken in 4935 meters of water near the Bahama Outer Ridge in the Atlantic Ocean at:

Latitude 28° - 17' - 54" N

Longitude 72° - 17' - 48" W

The sample specimens were part of a 136 foot, 2.0 inch diameter core, and were from approximately 11 meters below the mudline. The material at this depth was a soft-olive gray clay classified by the Unified Soil Classification System as OH (fig. 15). Table 5 lists the geotechnical properties of ATL as a function of depth

of core.

IV - 2 Test Procedure

The procedure used in this investigation consisted of sample preparation, consolidation, direct shear test and then immediate removal of normal load and vane test. For each test, a 1.5 inch section of sample is cut and the remainder quickly resealed and placed back under refrigeration. The direct shear ring adapters (Plate 4) were designed to match the inside diameter of samples KK076 and ATL, 2.62 inches to 2.00 inches respectively. A cutter was designed to trim sample GM from approximately 2.25 inches to 2.00 inches. Filter paper is placed in the bottom on the lower porous stone. The sample is pushed into the shear box directly from the liner in the case of K076 and ATL, and from the cutter in the case of GM. The outer portion of the shear box is filled with water in order to keep the porous stone moist and water is placed on the top of the sample to keep it from drying out or sticking to the top plate. The pressure plate and lever arm are attached and the desired normal stress is applied by adding weights to the tray (Plate 6).

The sample is allowed to consolidate at the total normal stress level overnight. A dial gage is placed (Plate 7) in order to monitor consolidation. The shearing of the sample proceeded after the consolidation had ceased, at a rate (i.e., 0.06 in/min) to ensure "undrained" test conditions.

Immediately prior to shearing the sample, the locking pins are removed from the direct shear box. The shear rate is adjusted and the load cell voltage, chart speed, and chart sensitivity

selected. The shear rate chosen for this study was 0.06 in/min. as utilized by Webb (ref. 21). The test commences after placing a dial gage to check the horizontal displacement of the shear box (Plate 6). The test is stopped after 0.3 inches of shear has taken place. The pins connecting the shaft from the load cell to the shear box (Plate 2) are removed and the zero point on the recording chart is checked for drift. The shear box is removed from the direct shear apparatus, the water emptied, and the box placed under the vane shear machine for the vane shear portion of the test. The vane is lowered into the surface of the sample .5 inch. At this depth, the vane does not pass through the direct shear surface. This is shown schematically as follows:

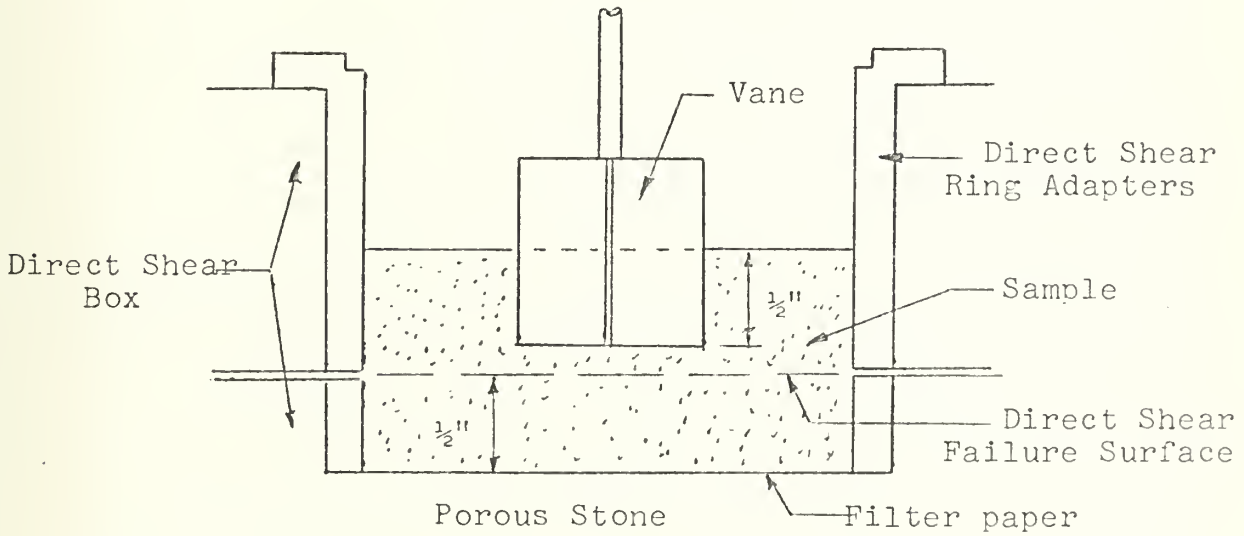

Before starting the vane shear test, the gear box output shaft and motor settings are changed in order to facilitate vane shear at the same rate as the direct shear. Per Webb (ref. 21), these rates are 7°/min. for vane shear and 0.06 in/min. for direct shear. The strain gage conditioner voltage is changed as is

the chart sensitivity. The chart is zeroed on a line of the chart and the test proceeds through a vane rotation of at least 30° (Plate 10). The vane is then raised out of the sample and the zero point checked for drift.

The final item is to determine the water content of the sample. The method used in this study is to take the water content sample down through the direct shear failure surface inclusive of the material sheared by the vane shear machine. This sample is immediately weighed and placed in an oven for drying and subsequent reweighing for water content determination.

CHAPTER V

EXPERIMENTAL RESULTS AND ANALYSIS

The first portion of the experimental work involved the calibration of the loading and recording devices (figures A-1 and A-4) of the direct and vane shear equipment and strip recorder setup. The primary work of this investigation was to verify the reliability and reproducibility of the test procedures described in Chapter IV and to run the "combined" direct and vane shear tests and analysis on a general set of samples in order to validate the theory proposed by Webb (ref. 20), as discussed in Chapter II. Figures A-5 through A-25 contain the data collected from running the "combined" vane and direct shear tests on the three samples. Sample shear strengths are represented by:

a) water content vs. log consolidation pressure

b) water content vs. log shear strength

c) shear strength vs. normal pressure and consolidation pressure.

These relationships are discussed in the following paragraphs.

V - 1 Water Content vs. Log Consolidation Pressure

Immediately following completion of the "combined" direct and vane shear tests, the water content was determined on each specimen as described in Chapter IV. These water content values were plotted against the log of the pressure used to consolidate each specimen prior to the direct shear test.

V - 1.1 Sample KK076

Water content as a function of laboratory consolidation pres-

sure for sample KK076 is depicted in figure 16. As anticipated and as previously discussed, the consolidation curve for this sample appears to be the reload portion of the curve of consolidation, figure 11. The "apparent" precompression stress, P_c, from this plot appears to be approximately 5.2 psi.

V - 1.2 Sample GM

Figure 17 indicates a plot of the water content of sample GM as a function of laboratory consolidation pressure. Results similar to those reported for sample KK076 were observed except that the change in slope of the curve at the "apparent" P_c was not as great as for sample KK076. The "apparent" P_c from this plot appears to be approximately 6.0 psi.

V - 1.3 Sample ATL

Figure 18 indicates a plot of the water content of sample ATL as a function of laboratory consolidation. Results similar to those reported for samples KK076 and GM were observed. The "apparent" P_c from this plot appears to be approximately 7.2 psi.

V - 1.4 Discussion of Water Content vs. Log Consolidation Pressure

The plot of water content vs. log consolidation pressure for all three samples indicate two distinct straight line segments with a change to a steeper negative slope at the apparent P_c for increasing consolidation pressure. This is the classical indication of an over-consolidated soil.

V - 2 Water Content vs. Log Shear Strength

Figures 19, 20 and 21 summarize the results of this part of

the investigation. There are both similarities and variances among the three plots. The water content was plotted against the log shear strength for the results obtained by both the direct shear test and the vane shear test. The water content vs. log direct shear strength for sample KK076 was a straight line over the whole range of normal stresses, while this plot for samples GM and ATL indicates two straight lines with a change of slope at $\omega\% = 70.4$, $\sigma_n = 5.5$ psi and $\omega\% = 159.0$ or $\sigma_n = 6.7$ psi, respectively. The water content vs. log vane shear strength for all samples was a straight line over the whole range of consolidation pressures. These plots, although not corresponding precisely with each other, did closely approximate the observations by Webb (ref. 21). The "apparent" P_c determined from this part of the investigation was 5.5 psi and 6.7 psi for samples GM and ATL respectively, compared with 6.0 psi and 7.2 psi as determined by the water content versus log consolidation pressure curves. These values compare favorably and appear to present evidence that the test apparatus, loading procedure, data collection system and data presentation worked as designed.

V - 3 "Combined" Shear Strength Analysis

A "combined" test consists of a direct shear test conducted at a normal stress equal to the consolidation pressure of a sample followed immediately by removal of normal load and a vane shear test. Because the vane shear tests are conducted at zero normal stress, their resulting shear strength can be thought of as being a function of "consolidation" pressure. The data derived from one direct shear test and the subsequent vane shear

test is referred to as one "combined" shear strength test.

Conventional techniques for presentation of shear strength data plot shear strength versus normal stress. The conventional technique was modified in this presentation by the addition of the vane shear data plotted on the same graph with shear strength as a function of consolidation pressure. The direct shear strength results were plotted versus normal stress. The results of the "combined" shear strength tests on samples KK076, GM and ATL are presented in figures 22, 23 and 24. These figures plot shear strength during direct shear and vane shear tests as a function of applied normal stress, σ_n and consolidation pressure. The results of the strength tests shown in figures 22, 23 and 24 exhibit several similarities. Above a certain value of σ_n, the plot of the direct shear data appears linear and when extended back, passes through the origin. The generally accepted interpretation is that this linear portion of the curve represents the strength of "normally" consolidated samples. Below this value of normal stress, a change in slope of the curve is apparent. These observations were evident for all three samples.

The "apparent" P_c determined by this part of the investigation was 5.2 psi, 5.9 psi and 6.7 psi for samples KK076, GM and ATL, respectively. A summary of "apparent" P_c values determined by the three different test methods is as follows:

	KK076	GM	ATL
1. Water content vs. log consolidation pressure	5.2 psi	6.0 psi	7.2 psi
2. Water content vs. log shear strength		5.5 psi	6.7 psi
3. Shear strength vs. normal pressure	5.2 psi	5.9 psi	6.7 psi

The values of "apparent" P_c determined experimentally are in relatively close agreement indicating consistency in the testing and analysis methods.

The direct shear strengths measured always exceeded the vane shear strength values at the consolidation pressures that corresponded to the normal stresses at which each direct shear test was conducted. The plots of the vane shear strength vs. consolidation pressure were approximately linear in the three samples although there was some scatter of data points. The vane shear strength plots did not exhibit the change in slope characteristic of the direct shear strength plots. The plots of direct shear strength, in the regions at low values of σ_n, seemed to be almost parallel with the plot of the vane shear data although the slope of the envelope was slightly greater for the direct shear values.

Similar observations by Webb (ref. 21) led him to propose the "combined" analysis of shear strength as described in Chapter II and as depicted on figure 12. Only two "combined" tests are required to determine the complete failure envelope; one test at σ_n and consolidation pressure equal to zero and the other at σ_n and consolidation pressure greater than P_c. The procedure outlined in Chapter II was used to analyze the results of the direct shear and vane shear tests on samples KK076, GM and ATL. The analyses are summarized in figures 25, 26 and 27. The complete failure envelope was drawn for each sample using only two "combined" shear strength tests. The remainder of the test results were plotted on the same figure for comparison. There was reasonably good correlation between the total shear strength envelope and the plotted data points. As previously mentioned,

the results of this investigation seem to indicate that the direct shear line between $\sigma_n = 0$ and $\sigma_n = P_c$ is not exactly parallel to the vane shear line in this area but is slightly steeper. Figures 22, 23 and 24 indicate the slope that best represents the direct shear data points in the region $\sigma_n = 0$ to $\sigma_n = P_c$ for samples KK076, GM and ATL. These figures indicate that the slope in the portion of the direct shear envelope for $\sigma_n < P_c$ is higher than ϕ_c obtained from the vane shear results by approximately 1.5°, 2.0°, 3.0°, respectively for samples KK076, GM and ATL. This would seem reasonable since theoretically the vane shear test only measures cohesion, therefore if the portion of the direct shear line for $\sigma_n < P_c$ were parallel to the vane shear line, it too, would only measure "cohesion". It is generally accepted that since the direct shear test is run under a normal stress that it measures both "cohesion" and "friction". Accordingly, it would be expected that the slope of the direct shear line for $\sigma_n < P_c$ would be greater than that of the vane shear test by the amount of the "frictional" component. Figure 28 illustrates this point. With the exception of ϕ_f, all the terms of figure 28 are the same as those of Webb's theory of "combined" analysis of shear strength as depicted on figure 12. ϕ_f is the angle of the slope of the friction component of the total failure envelope in the overconsolidated range of the plot for $\sigma_n < P_c$. Therefore, from the results of this investigation, it is felt that Webb's theory should be modified to reflect a "frictional" component in the portion of the direct shear line for $\sigma_n < P_c$. Based on limited data, this "friction" component should be approximately 2° - 3° for ϕ_f as shown on figure 28.

Another point that merits discussion is the fact that the cohesion value at $\sigma_n = 0$ obtained from the direct shear test, C_d, and the vane shear test, C_v, are considerably different for each of the three samples. Theoretically, these values should be equal so that ΔC is zero (refer to fig. 12). It was thought that perhaps the water content or the plasticity index might show some correlation between C_v and C_d because of the idea that the geometry of the failure planes seem to be a function of water content. Figures 29 and 30 plot the ratio of C_v/C_d versus water content and plasticity index at $\sigma_n = 0$ for the three specimens used in this investigation. The data is scattered and no real correlation can be drawn except that the ratio, C_v/C_d, is in the range 0.66 to 0.76. Another thought was that the two tests measure shear resistance along planes orthogonal to one another and that due to the platy shape of the clay particles the shear resistance along the horizontal plane might differ from that along a vertical plane. Limited testing was accomplished with the vane test in both the vertical and horizontal directions. It was found that the shear resistance along the horizontal plane was actually less than that along a vertical plane which would cause the C_v/C_d ratio to be further divergent and increase ΔC. The most likely explanation of the difference between C_d and C_v is in the failure mechanism of both tests and how it relates to the current theory. Presently, the shear stress of the direct shear test result is the shear force required to move the shear boxes relative to one another divided by the cross-sectional area of the sample. In the vane shear test the shear stress is taken as the torque required to turn the vane divided by the

first moment of the cylindrical area that the ends of the vanes transcribe. In this investigation a one-inch diameter, one inch deep vane was pushed one-half inch into the sample while running the vane shear test. As the test was performed and the soil failed, the vanes initially did not cut out a cylindrical section, but tension cracks commenced propulgating away from the ends of the vanes, and also from the ends of the vanes toward the interior of the vane shaft. This apparently weakened the sample so that with subsequent rotation of the vane the peak of the shear stress versus strain curve (fig. 7), was consistently lower by a constant amount than the direct shear line in the region $\sigma_n < P_c$.

As discussed and illustrated in Chapter I, present state-of-the-art criteria for designing marine foundations still consists mainly of empirical formulas. One of the key components of these formulas for bearing capacity, pile capacity or uplift capacity is the value of C, undrained shear strength. There are many methods for determining the undrained shear strength of a marine clay such as TORVANE, cone penetrometer, triaxial compression, vane shear, direct shear or fall cone. However, each of these tests has advantages and disadvantages, as described in Chapter II, with no general agreement as to which is better. The geotechnical engineer must use his own judgement, which may be affected by availability of test equipment, magnitude of proposed project, his own confidence in particular tests, etc. in choosing the undrained shear strength tests that he will specify. He will probably require that a combination of these methods be used in arriving at realistic values of C. The author feels that

by using the "combined" vane and direct shear method discussed in this paper, reliable data will be produced with considerable sample conservation and reduced time for testing, which makes the method attractive from an economical standpoint.

In summary, it is felt that the "combined" vane and direct shear analysis will provide an economical, consistent and realistic procedure to the geotechnical engineer for determining the undrained shear strength of marine clays. The method is simple, direct and does not require complicated equipment. It is highly reproducable and provides a permanent documentation of test results. As in most laboratory analysis, it is mandatory that rigorous adherance to strict, consistent laboratory procedures be observed in order for the data collected to be useable and representative.

CHAPTER VI

CONCLUSIONS AND RECOMMENDATIONS

VI - 1 Conclusions

The conclusions of this investigation are as follows:

1. With rigorous control and consistency of laboratory procedures, using strain controlled testing and electronic data printout, the tests and data resulting from the direct shear and vane shear procedure described herein are both reliable and reproducible from one researcher to the next.
2. With similar results on tests of clay samples from the Pacific Ocean, Gulf of Mexico, and the Atlantic Ocean, the "combined" theory for "Total Failure Envelope" is a general theory that can be used (with slight modification) for any and all marine clays regardless of water content, deposition rate, geographic location, water depth, etc.
3. When using the "combined" theory, the slope of the portion of the direct shear failure envelope for $\sigma_n < P_c$ should be increased by approximately 2° - 3° (ϕ_f) to more closely approximate the failure envelope in this region (see figure 28).
4. For each sample there is a constant difference between C_d and C_v in the range $\sigma_n = 0$ to P_c. This difference appears to be a function of the differences between failure mechanisms for the direct and vane shear tests and present theory used to calculate shear stress in each case. The ratio of C_v/C_d varies from 0.66 to 0.76 indicating a consistent underestimation of shear strength by the vane shear test.
5. Acceptance of the "combined" shear testing procedure will

significantly reduce the number and size of sample specimens required and the number of laboratory tests required to determine the geotechnical properties of marine clays.

6. The values of "C" and "ϕ" obtained from this "combined" analysis can be easily and readily used in the present empirical formulas being utilized to determine the strength of the ocean floor for the design of foundations for ocean structures.

VI - 2 Recommendations

1. A procedure could be arranged to measure pore pressure during the direct and vane shear tests allowing analysis of shear strength in terms of effective normal stresses rather than total normal stresses.

2. By using larger diameter samples and a special pressure plate it may be possible to run the vane shear test under a normal stress rather than removing the normal stress during the vane test. This should give much better correlation between the direct and vane shear test results.

3. Great potential lies in the area of standardizing the vane shear test, i.e., diameter of vane, depth of vane, depth vane is pushed into sample and rate of rotation of vane, etc.

4. A correlation between the "combined" shear strength analysis presented herein and the results of triaxial tests would be of great interest.

BIBLIOGRAPHY

1. American Society for Testing and Materials, Research Conference on Shear Strength of Cohesive Soil, Colorado, 1960.

2. Bishop, A.W., Henkel, D.J., The Measurement of Soil Properties in the Triaxial Test, London: Edward Arnold, Ltd., 1974.

3. Bhushan, K., "Resistance of Ocean Sediments to Sampler Penetration", Eighth Annual Offshore Technology Conference, Paper Number. OTC 2624, Texas, 1976.

4. Bouma, A.H., et. al., "Comparison of Geological and Engineering Properties of Marine Sediments", Fourth Annual Offshore Technology Conference, Paper No., OTC 1514, Texas 1972.

5. Eide, O., "Marine Soil Mechanics - Applications to North Sea Offshore Structures", Norwegian Geotechnical Institute, Publication Number 103.

6. Herrman, H.G., et.al., Interim Design Guidelines for Seafloor Footing Foundations, U.S. Navy Civil Engineering Laboratory, Technical Report R799, October, 1973.

7. Inderbitzen, A.L., et.al., Deep Sea Sediments, New York: Plenum Press, 1974.

8. Jumikis, A.R., Soil Mechanics, New Jersey: D. Van Jostrand, Co., Inc., 1962.

9. Lambe, T.W., Soil Testing for Engineers, New York: Wiley and Sons, Inc., 1951.

10. Lambe, T.W., Whitman, R.V., Soil Mechanics, New York: Wiley and Sons, Inc., 1969.

11. McClellan, B., "Design of Deep Penetration Piles for Ocean Structures", Journal of the Geotechnical Engineering Division, Proceedings of the American Society of Civil Engineers, Volume 100, Number GT7, July, 1974.

12. Monney, N.T., Submarine Slope Stability, M.S. Thesis, Civil Engineering Department, University of Washington, Seattle, 1965.

13. Noorany, I., Gizienski, S.F., "Engineering Properties of Marine Soils: A State of the Art Review", Journal of the Soil Mechanics and Foundation Division, Proceedings of the American Society of Civil Engineers, Volume 96, Number 4-6, 1970.

14. Peck, R.B., Hanson, W.E., Thornburn, T.H., Foundation Engineering, New York: Wiley and Sons, Inc., 1974.

15. Richards, A.F., et.al., Marine Geotechnique, Illinois: University of Illinois Press, 1967.

16. Scott, R.F., Principles of Soil Mechanics, Massachusetts: Addison - Wesley Publishing Co., Inc., 1963.

17. Sherif, M.A., et. al., Proceedings: The International Symposium on the Engineering Properties of Sea Floor Soils and Their Geophysical Identification, UNESCO, National Science Foundation, University of Washington, Seattle, 1971.

18. Terzaghi, K., Peck, R.W., Soil Mechanics in Engineering Practice, New York: Wiley and Sons, Inc., 1967.

19. Tschebotarioff, G.P., Foundations, Retaining and Earth Structures, 2nd Ed., New York: McGraw - Hill Book Company, 1973.

20. U.S. Naval Civil Engineering Laboratory, "Geotechnical Properties of the Deep Sea Floor, Northeast Pacific", addendum to Marine Geology of a Region on the Northwest Pacific, California, 1974.

21. Webb, M.S., Combined Vane and Direct Shear Strength Analysis of Naturally Occurring Marine Soils, M.S. Thesis, Civil Engineering Department, University of Washington, Seattle, 1976.

22. Wu, Ming-Jiun, Dynamic Properties of Overconsolidated Seattle Clays, Ph.D. Dissertation, Civil Engineering Department, University of Washington, Seattle, 1972.

Description	Sensitivity	Percentage of Strength Lost on Remolding
Insensitive	Less than 1	0
Slightly sensitive	1 - 2	0 - 50
Medium sensitive	2 - 4	50 - 75
Very sensitive	4 - 8	75 - 87.5
Slightly quick	8 - 16	87.5 - 93.8
Medium quick	16 - 32	93.8 - 96.9
Very quick	Greater than 32	Greater than 96.9

Table 1 Classification of sensitivity(After Buchan, et al, reference 15 pg. 72).

Depth in Core (cm)	Shear Strength (PSF)	Void Ratio	Bulk Density (GM/CM^3)	Water Content (% dry wt.)	Specific Gravity
20	45	3.92	1.361	141	2.77
40	57	3.58	1.375	132	2.72
60	53	3.21	1.407	118	2.71
80	55	3.32	1.390	124	2.68
100	43	3.11	1.411	116	2.69
120	77	3.29	1.392	123	2.68
140	53	3.20	1.409	118	2.71
160	70	3.18	1.400	119	2.67
180	75	3.03	1.418	113	2.68
200	93	2.82	1.442	105	2.69
220	113	3.02	1.410	114	2.65
240	120	2.83	1.428	107	2.64
260	143	2.98	1.434	109	2.72
270	127	3.02	1.425	112	2.71
310	130	2.76	1.456	102	2.71
320	125	2.80	1.444	104	2.68
340	133	2.85	1.462	103	2.77
360	110	2.81	1.466	101	2.77
375	135	2.77	1.458	102	2.73
400	143	2.73	1.466	100	2.73
420	157	2.60	1.479	95	2.72
440	157	2.54	1.488	93	2.73
480	175	2.57	1.500	92	2.78
500	180	2.55	1.495	93	2.76
520	197	2.61	1.479	97	2.70
540	195	2.53	1.494	92	2.74
560	230	2.47	1.495	91	2.72
600	225	2.42	1.510	88	2.74
620	220	2.30	1.526	84	2.73
640	240	2.36	1.526	85	2.76
660	217	2.31	1.523	85	2.73
680	253	2.38	1.525	86	2.77
720	240	2.29	1.523	84	2.74
740	267	2.26	1.534	82	2.74
760	247	2.20	1.540	81	2.73
800	273	2.31	1.523	85	2.73
860	277	2.38	1.506	88	2.71

Table 2 Geotechnical properties of a typical core from deeper portions of the Gulf of Mexico(After Bouma, reference 4 pg. 32).

Location	Sample number	Depth, in feet	p_o', in kilograms per square centimeter	Estimated p_c, in kilograms per square centimeter	C_u/p_o'	C_c	C_v, in square centimeters per second
(1)	(2)	(3)	(4)	(5)	(6)	(7)	(8)
Mediterranean	A-31	3.1	0.06	0.07	1.2	0.41	4×10^{-4}
Mediterranean	B-83	0.9	0.02	0.04	2.8	0.34	2×10^{-4}
Mediterranean	B-87	1.6	0.03	0.15	2	0.34	1.5×10^{-3}
North Atlantic	C-16	2.1	0.045	0.15	1.5	0.36	1.5×10^{-3}
North Atlantic	C-18	2.1	0.04	0.16	1	0.56	6×10^{-4}
North Atlantic	C-20	1.1	0.02	0.2	2	0.59	—
West Atlantic	D-1b	6	0.10	0.2	1	0.75	—
West Atlantic	F-6	5.1	0.10	0.15	0.4	0.63	1×10^{-3}
West Atlantic	F-11	4.8	0.06	0.2	0.7	0.83	8×10^{-4}
West Atlantic	G-6	2.5	0.03	0.05	1.2	1.4	8×10^{-4}
East Pacific	I-NAGA	0.5	0.005	0.09	—	0.77	—
East Pacific	J-29	—	0.005	0.08	—	0.9	—

Term p_o' = the effective overburden pressure; p_c = the estimated preconsolidation pressure based on Casagrande method; C_u = the undrained shear strength, in kilograms per square centimeter; C_c = compression index; and C_v = coefficient of consolidation.

Table 3 Properties of near surface samples from the sea floor(After Noorany, reference 13 pg. 1745).

Sub-Bottom Depth (ft)	Vane Strength (psi)	Remolded Strength (psi)	Sensitivity	Liquid Limit %	Plastic Limit %	Plasticity Index %
.8	1.41	.36	3.9	159.9	66.7	93.2
4.1	1.97	1.09	1.8	228.6	101.1	127.5
6.5	1.78	.92	1.9	225.3	96.6	128.7
9.3	1.97	.86	2.3	214.8	95.6	119.2
14.1	1.38	.65	2.1	185.3	89.7	95.6
18.4	1.39	.33	4.1	213.5	97.0	116.5
21.5	1.80	.65	2.8	255.8	124.3	131.5
25.5	2.13	.91	2.3	260.0	102.5	157.5
29.5	2.13	.81	2.6	289.7	107.5	182.2
33.5	2.13	.67	3.2	235.8	109.8	126.0

TABLE 4 Soil properties vs. depth - Sample KK076 (after ref. 20)

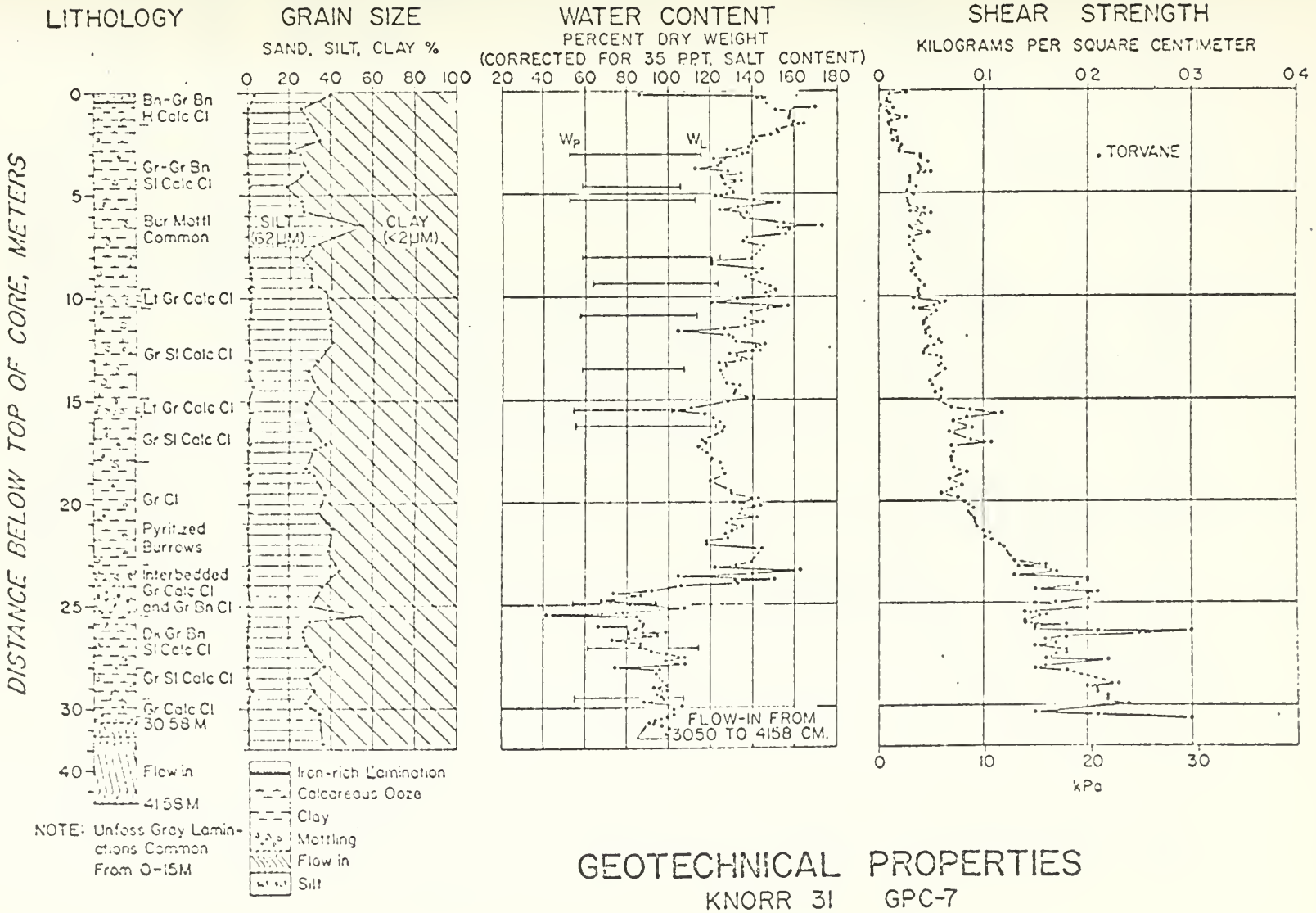

GEOTECHNICAL PROPERTIES
KNORR 31 GPC-7

TABLE 5 SOIL PROPERTIES VS. DEPTH - SAMPLE ATL

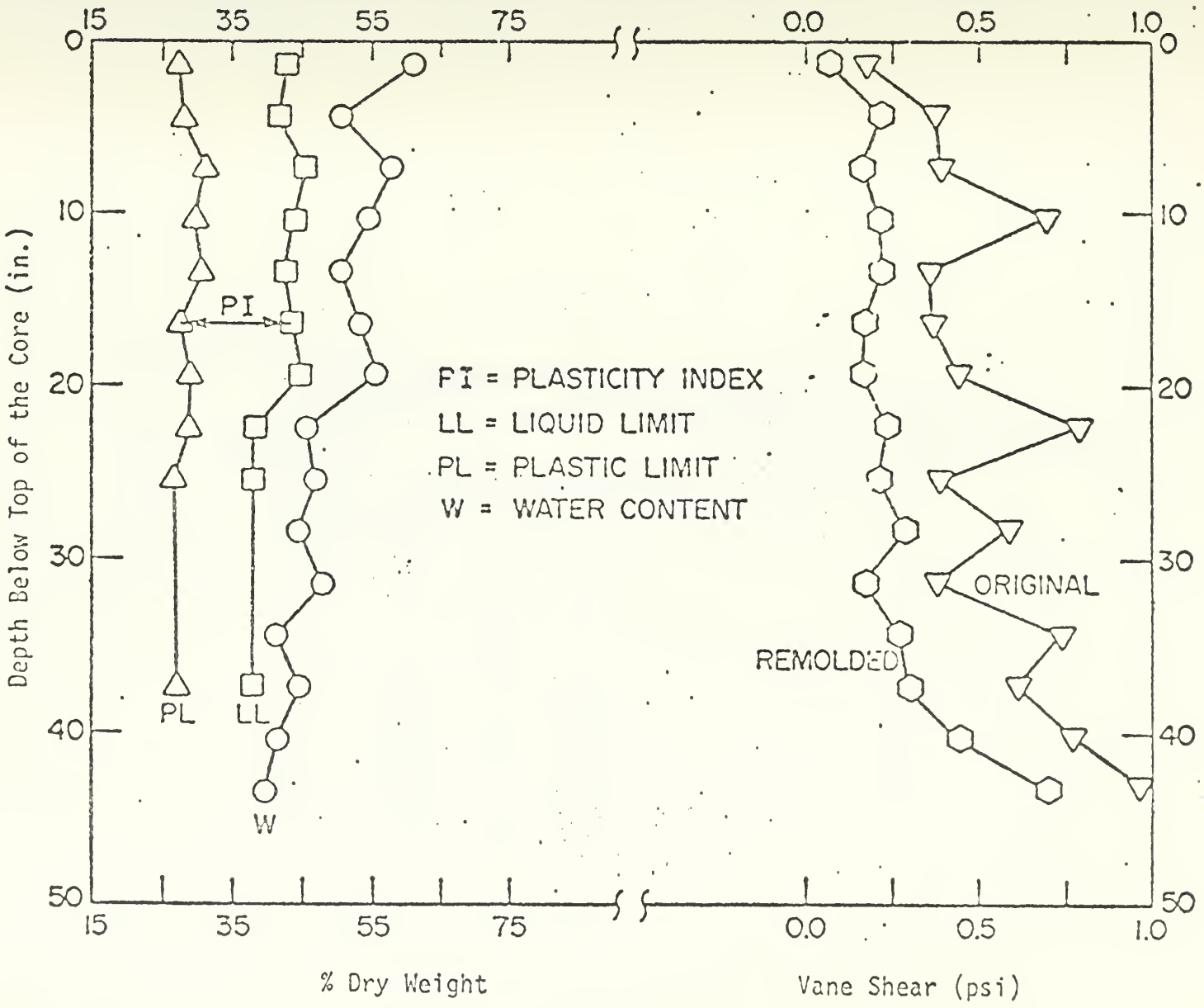

Figure 1 Soil paramters vs. Depth (After Sherif, reference 17, pg. 65)

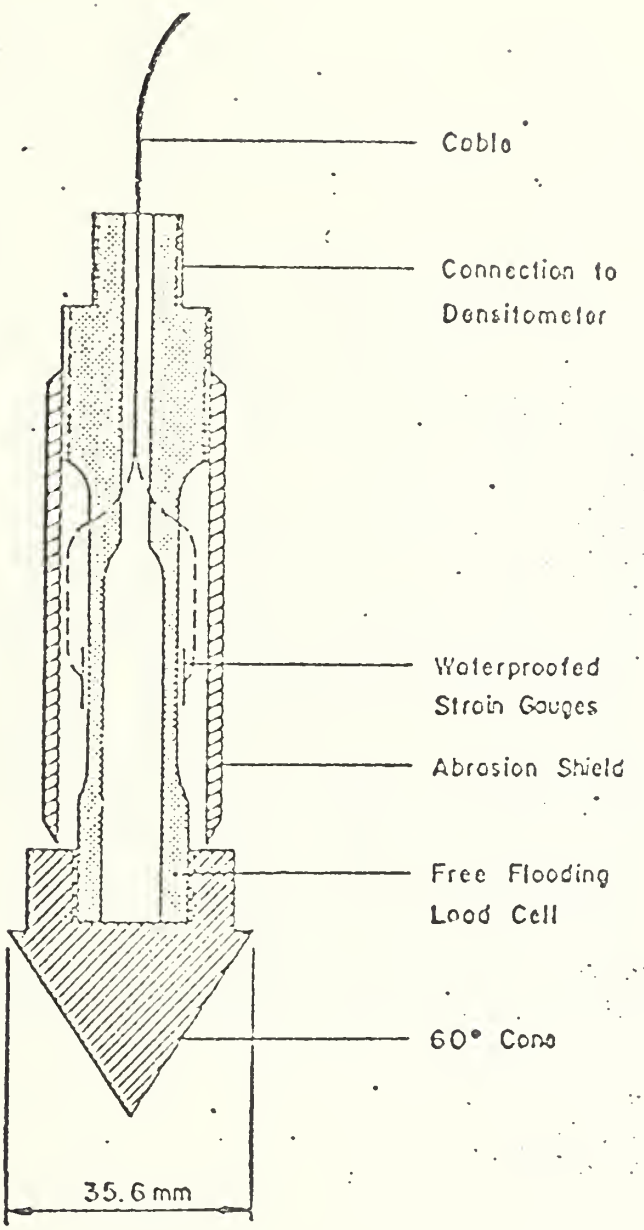

Figure 2 Cone penetrometer

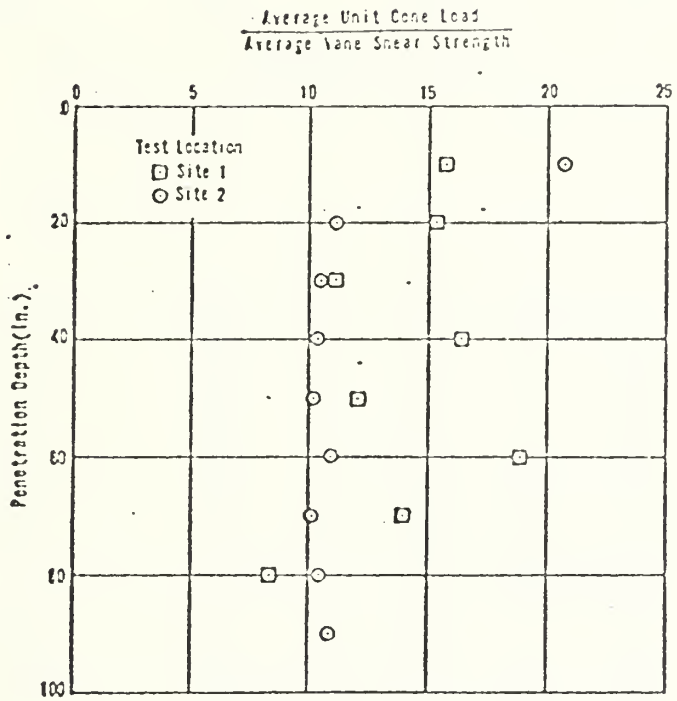

Figure 3 Cone penetration data compared to vane shear data

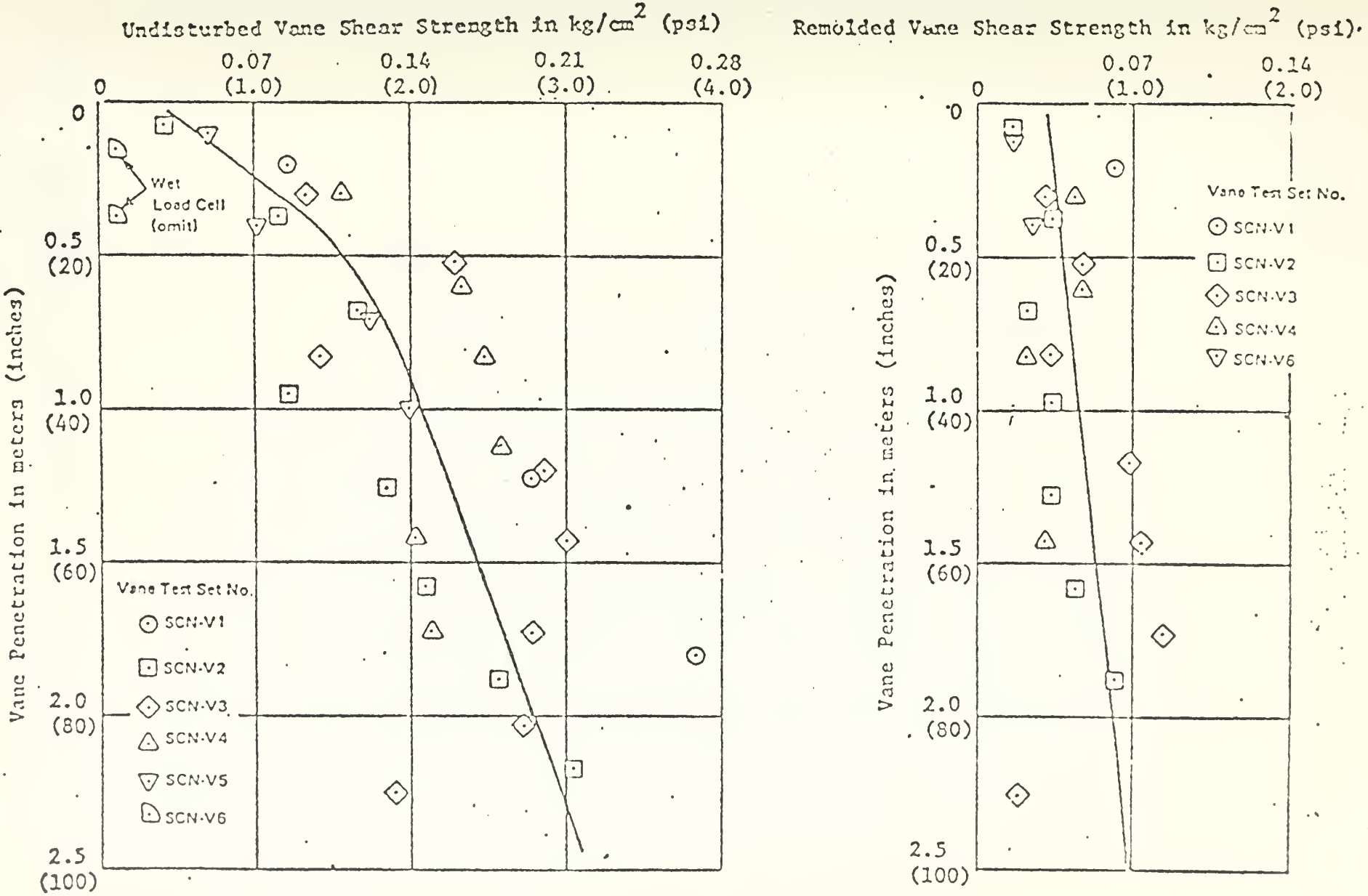

Figure 4 In-situ vane shear strength vs. vane penetration (After True, reference 17 pg. 18)

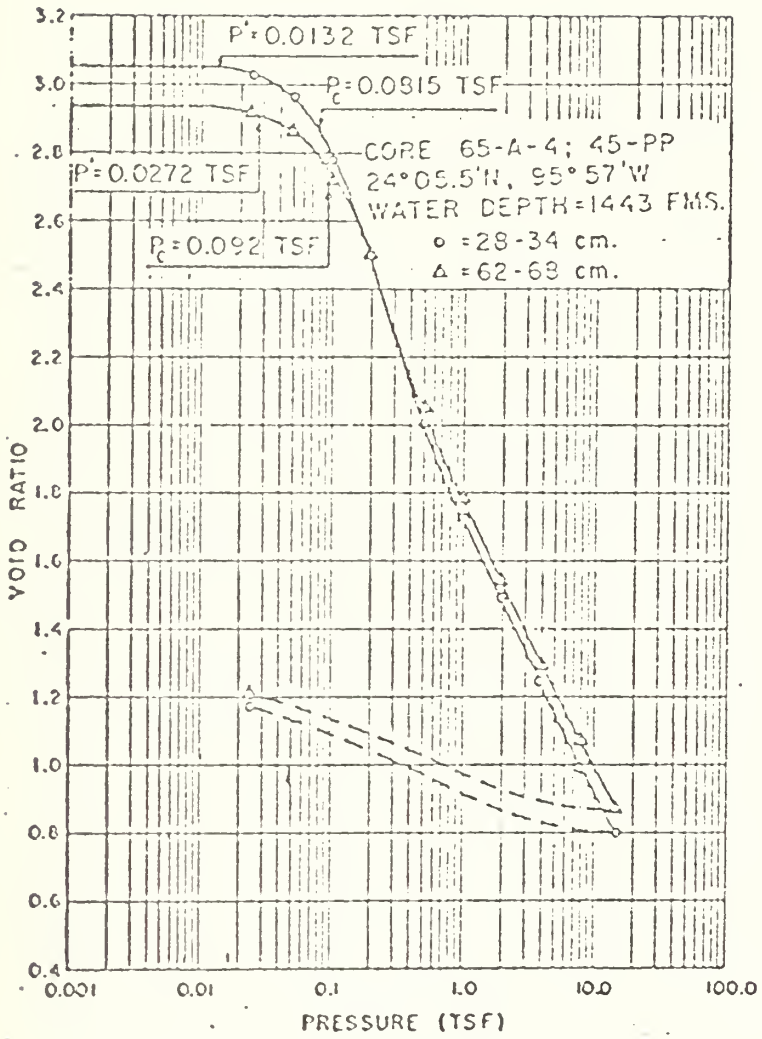

Figre 5 Void ratio vs. log of pressure(After Bryant, et al, reference 15 pg. 61)

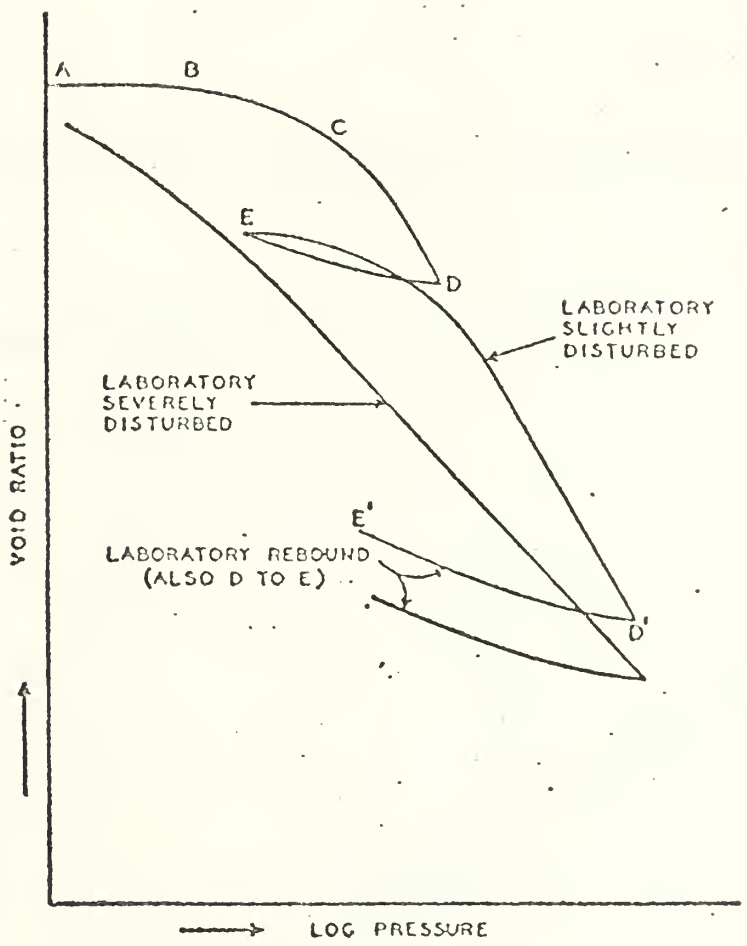

Figure 6 Generalized e-log P diagram(After Richards, reference 15, pg. 104).

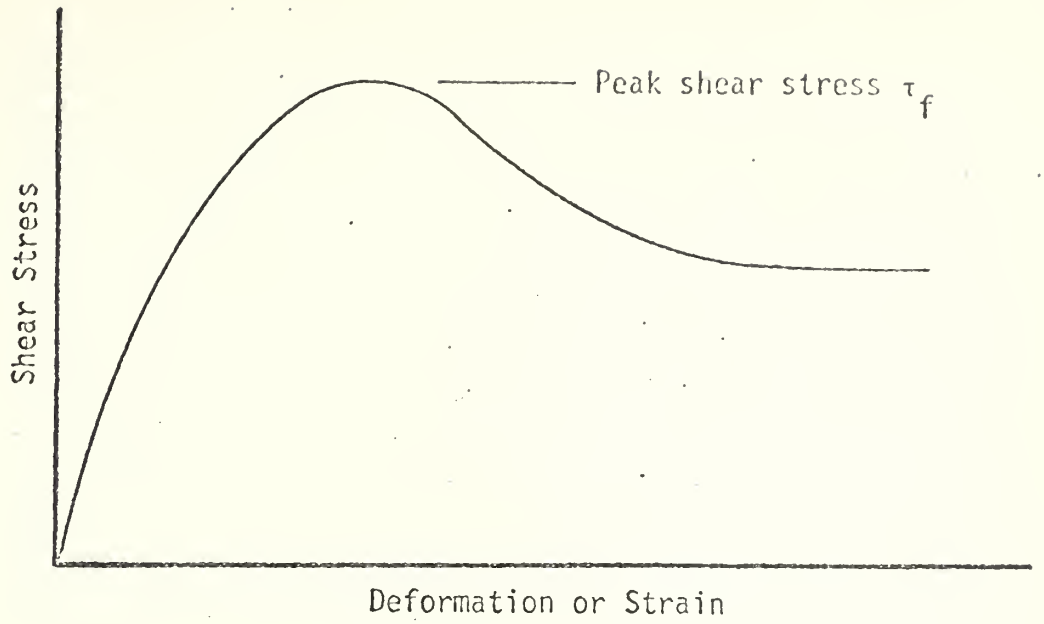

Figure 7 Shear strength - deformation diagram.

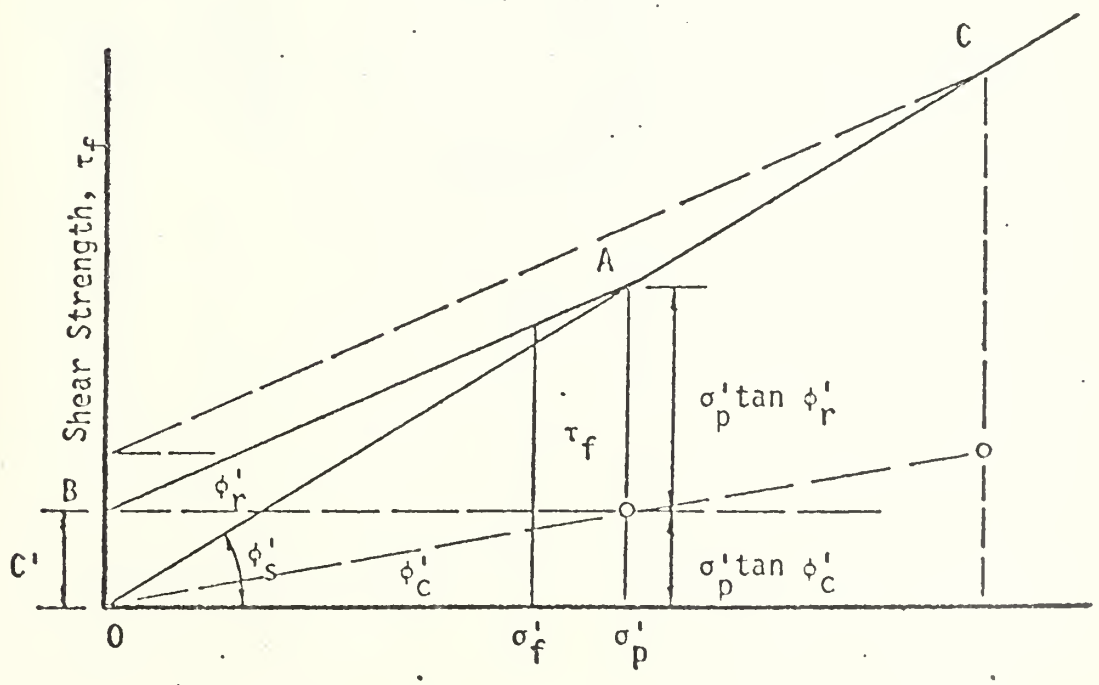

Figure 8 Shear strength diagram(After Hvorslev, reference 1, pg. 175).

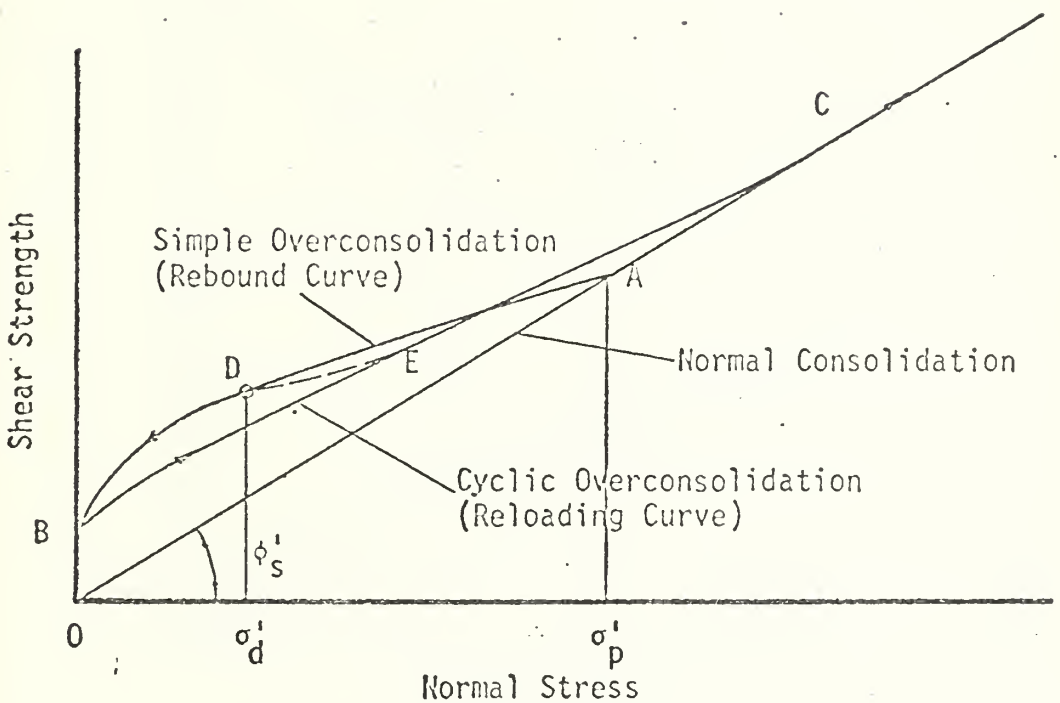

Figure 9 Shear strength hysteresis loop(After Hvorslev, reference 1 pg. 175)

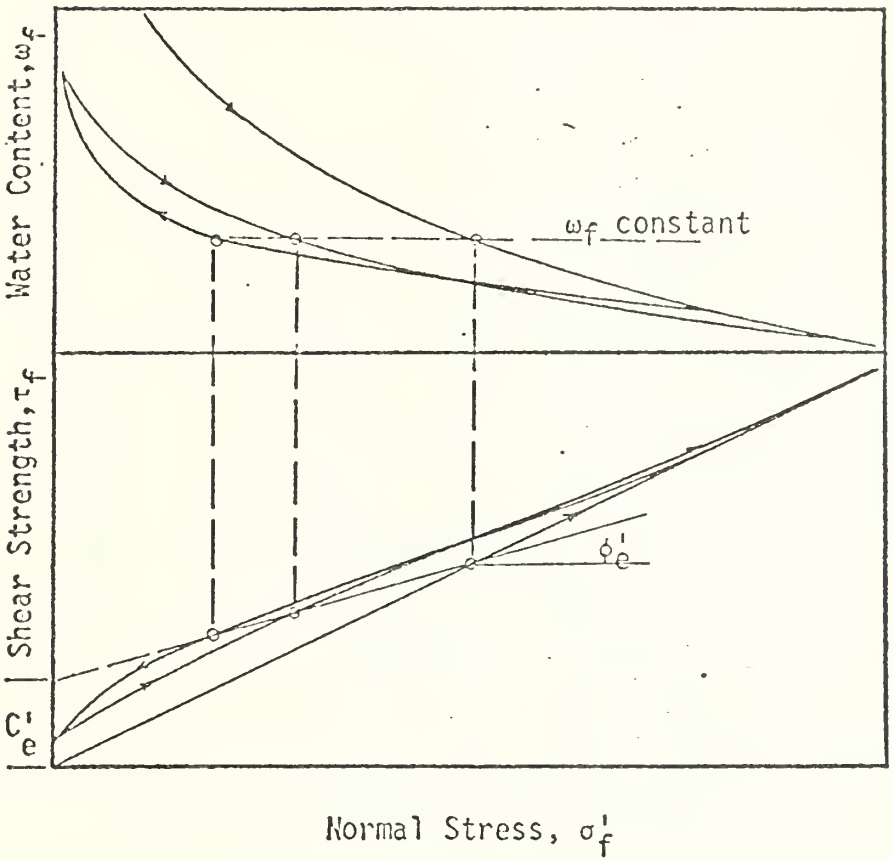

Figure 10 Determination of the cohesion and friction components, C'_e and ϕ'_e (After Hvorslev, reference 1 pg. 203).

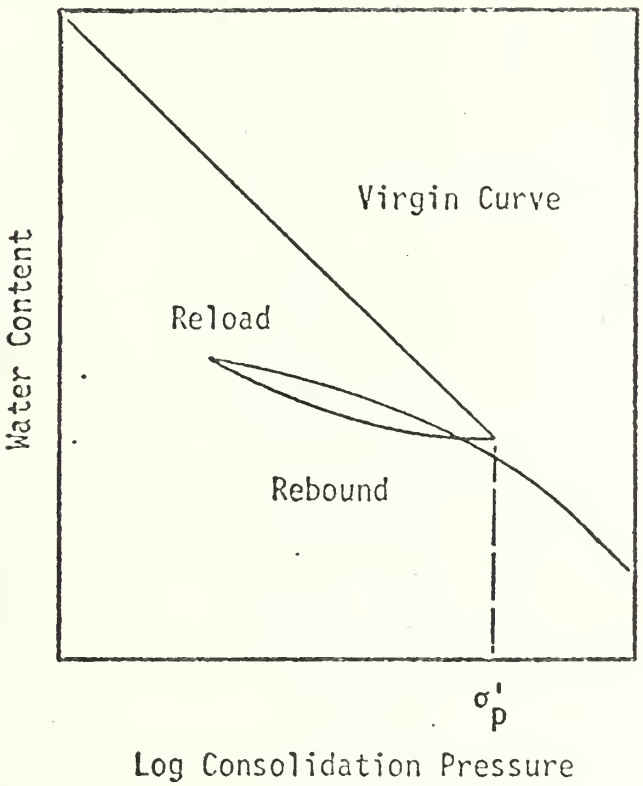

Figure 11 Water Content vs. log consolidation pressure(After Hvorslev, reference 1, pg. 196).

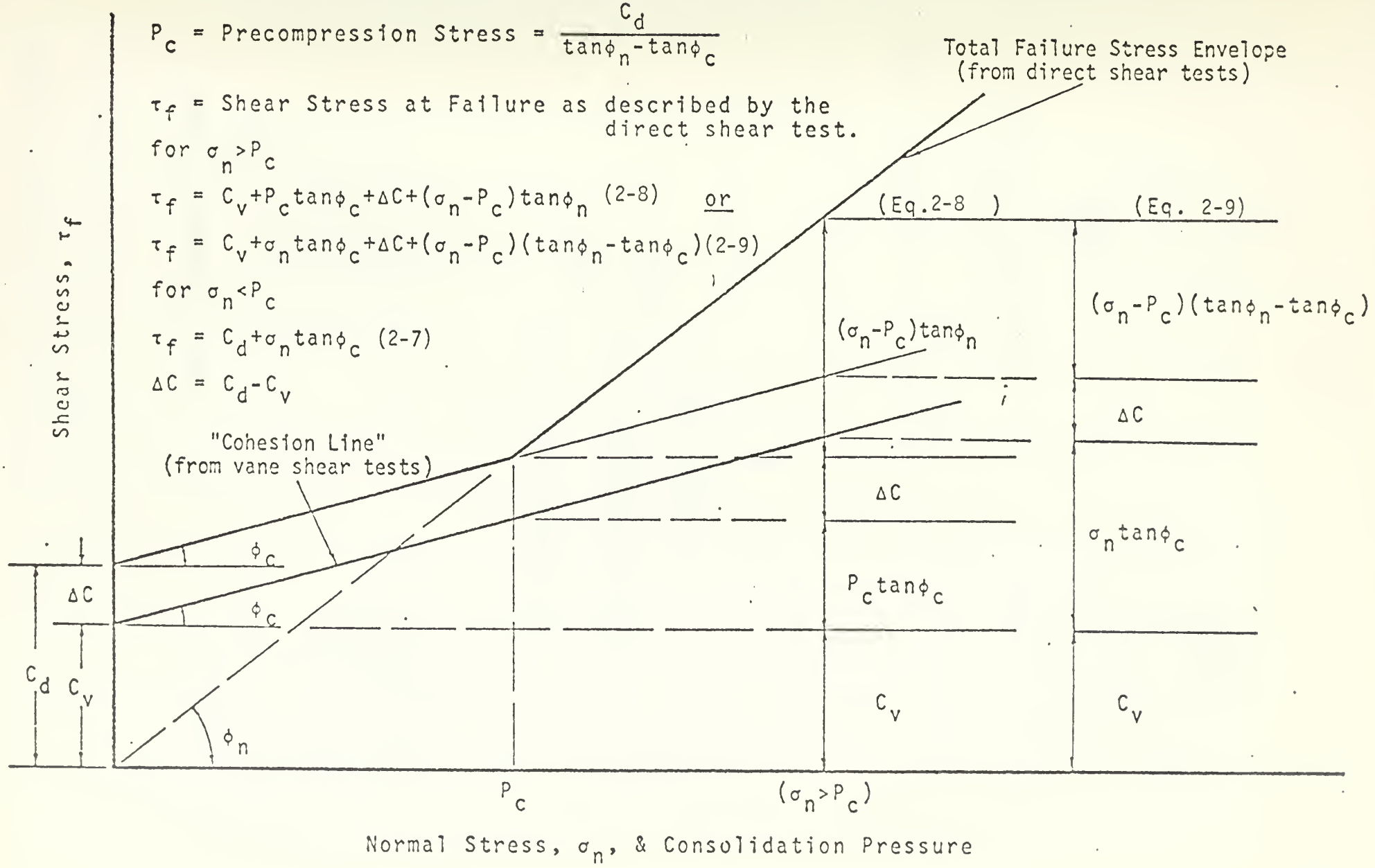

Figure 12 Illustration and definition of terms for "combined" vane and direct shear test strength analysis. (After Webb, reference 21, Figure 41).

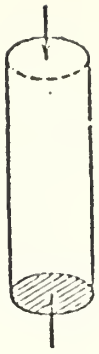

Cylindrical Compression
"Triaxial Shear"

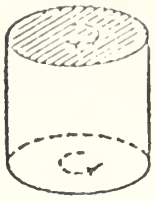

Torsional Shear

Figure 13 Types of soil shear tests.

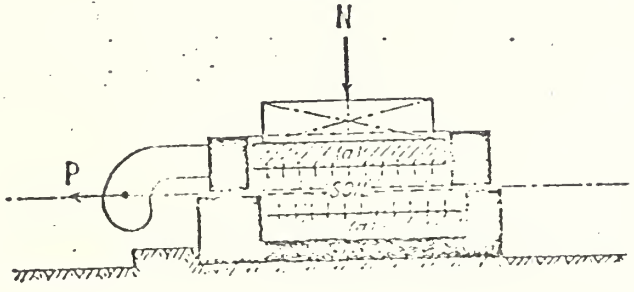

Two-piece Single Shear Box

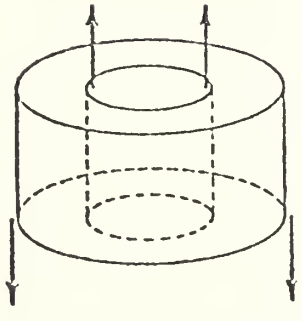

Annular or "Punching" Shear

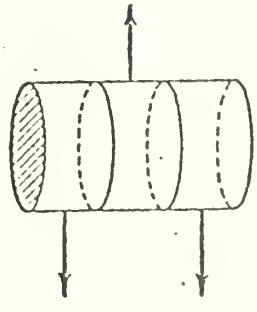

Ring Shear

Figure 14 Types of direct shear tests.

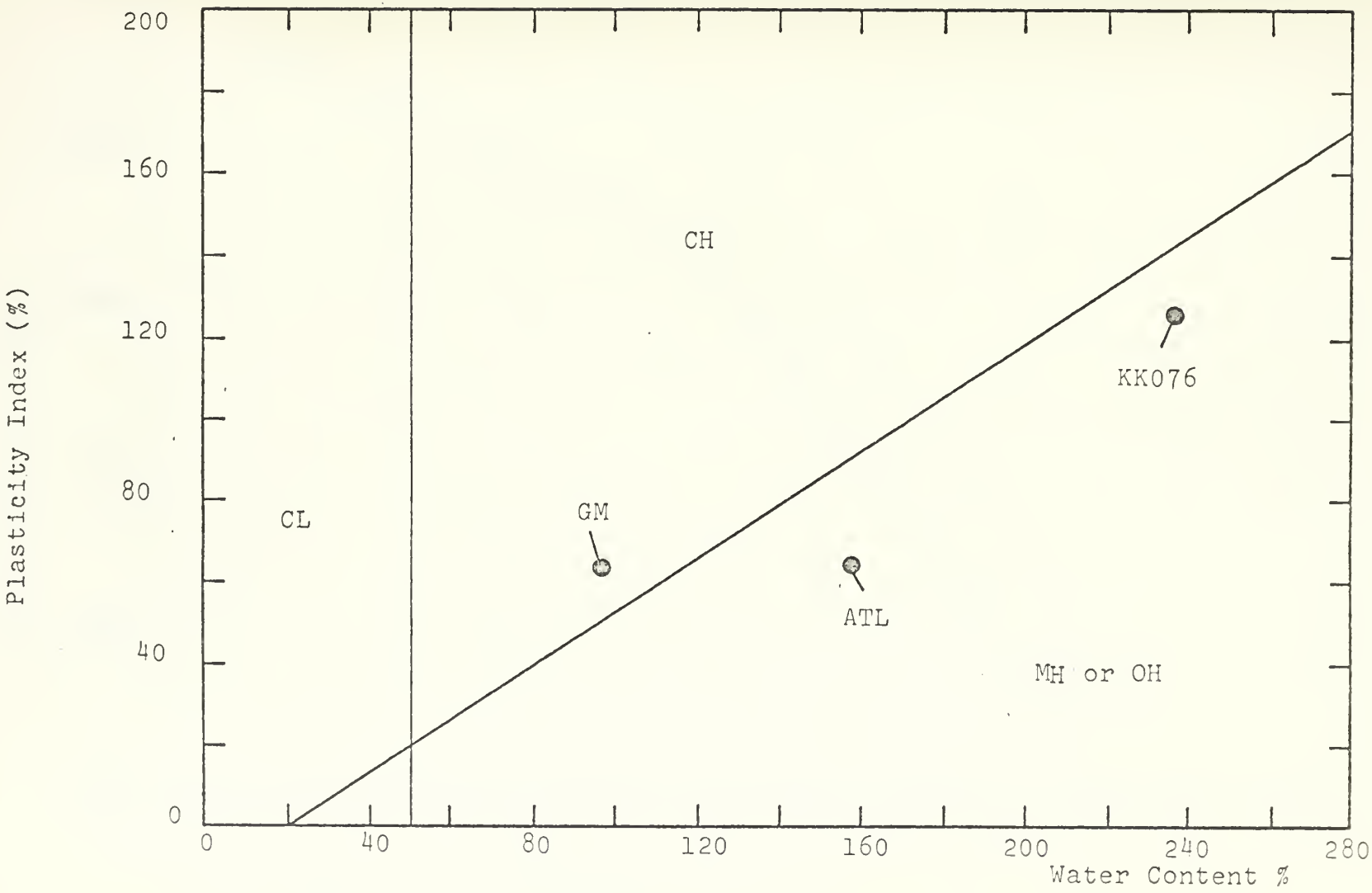

Figure 15 Atterberg Limits of Test Samples

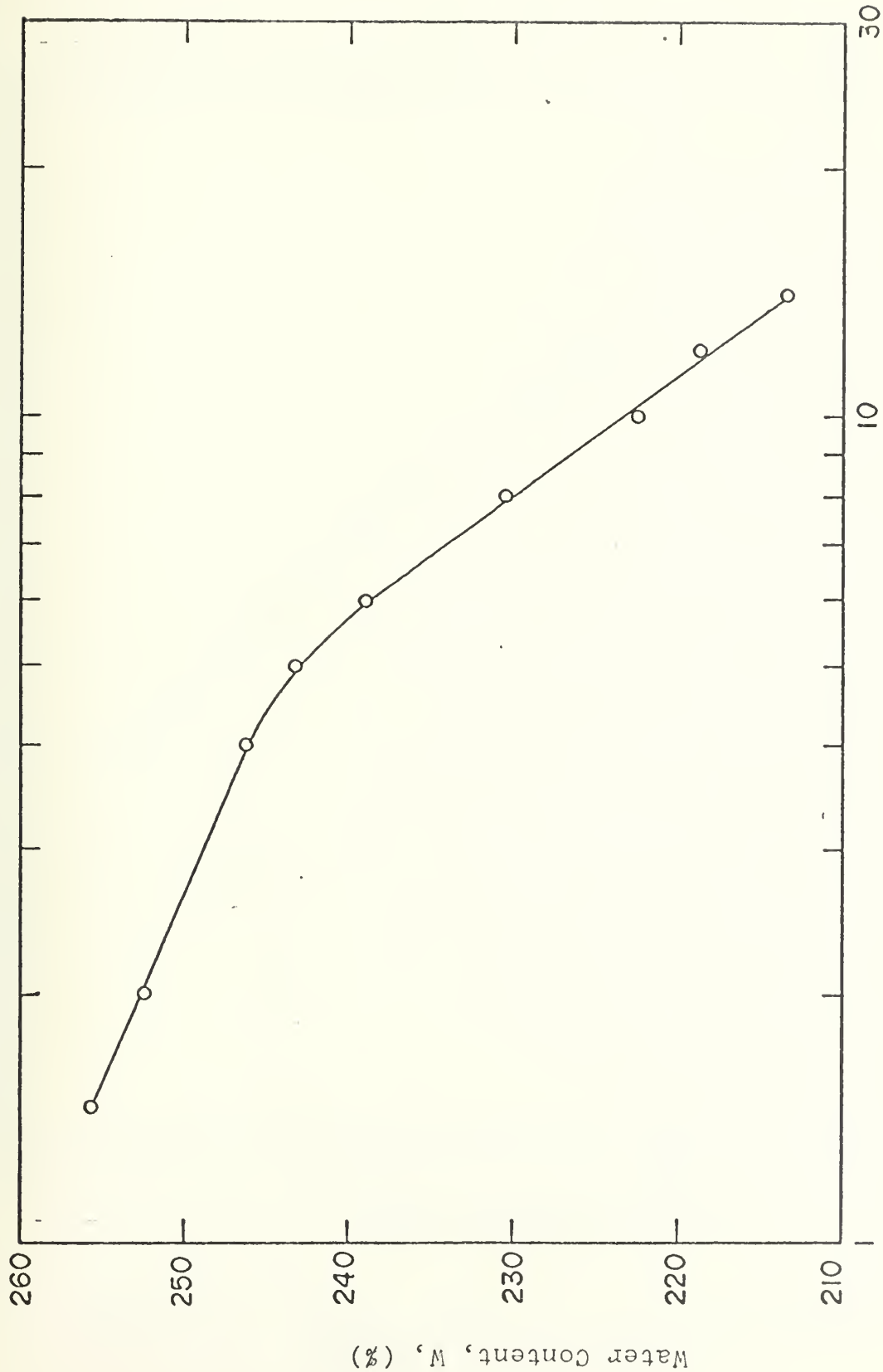

Figure 16 Water Content vs. log consolidation pressure - Sample KK076

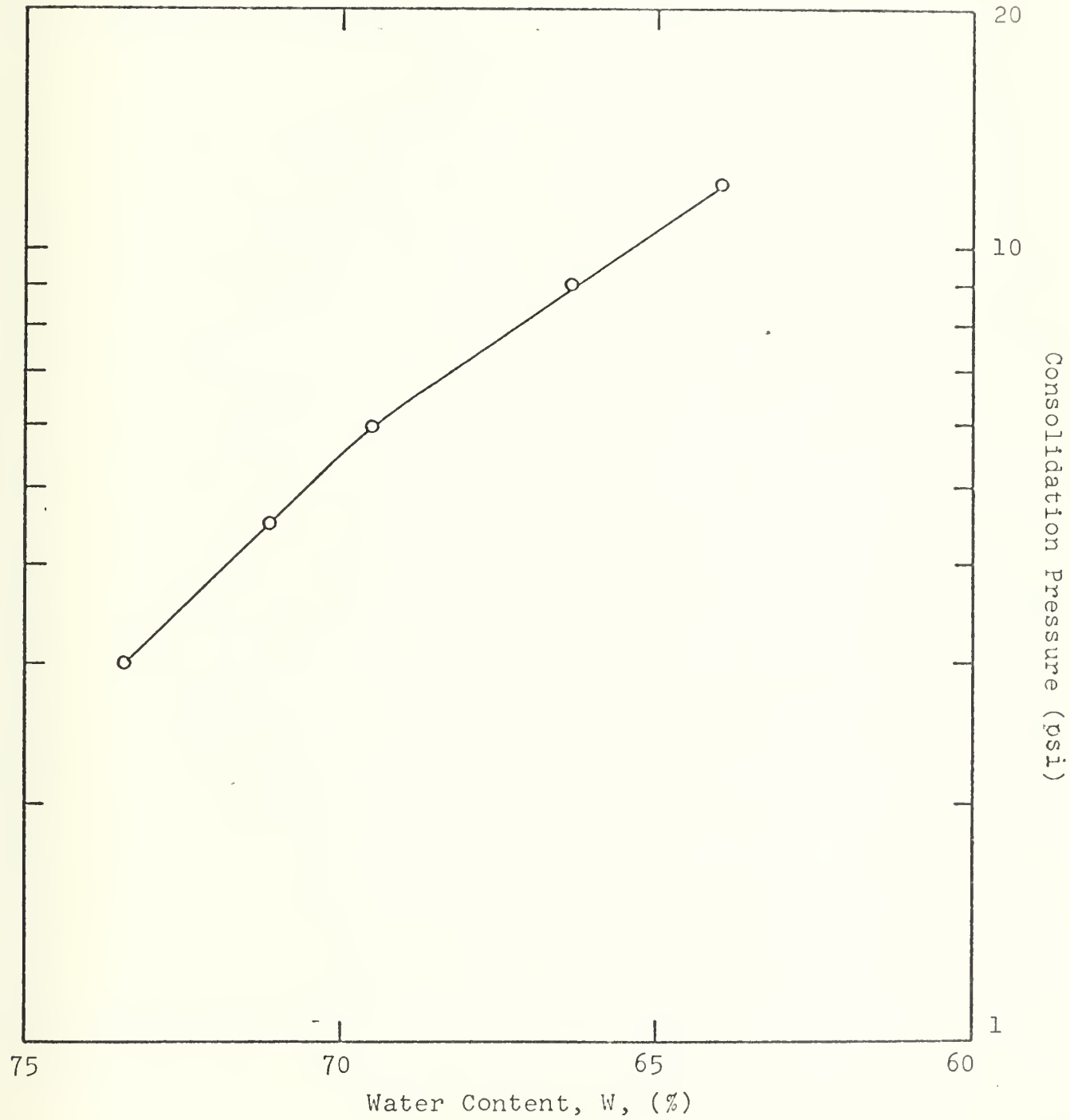

Figure 17 Water content vs. log consolidation pressure - Sample GM

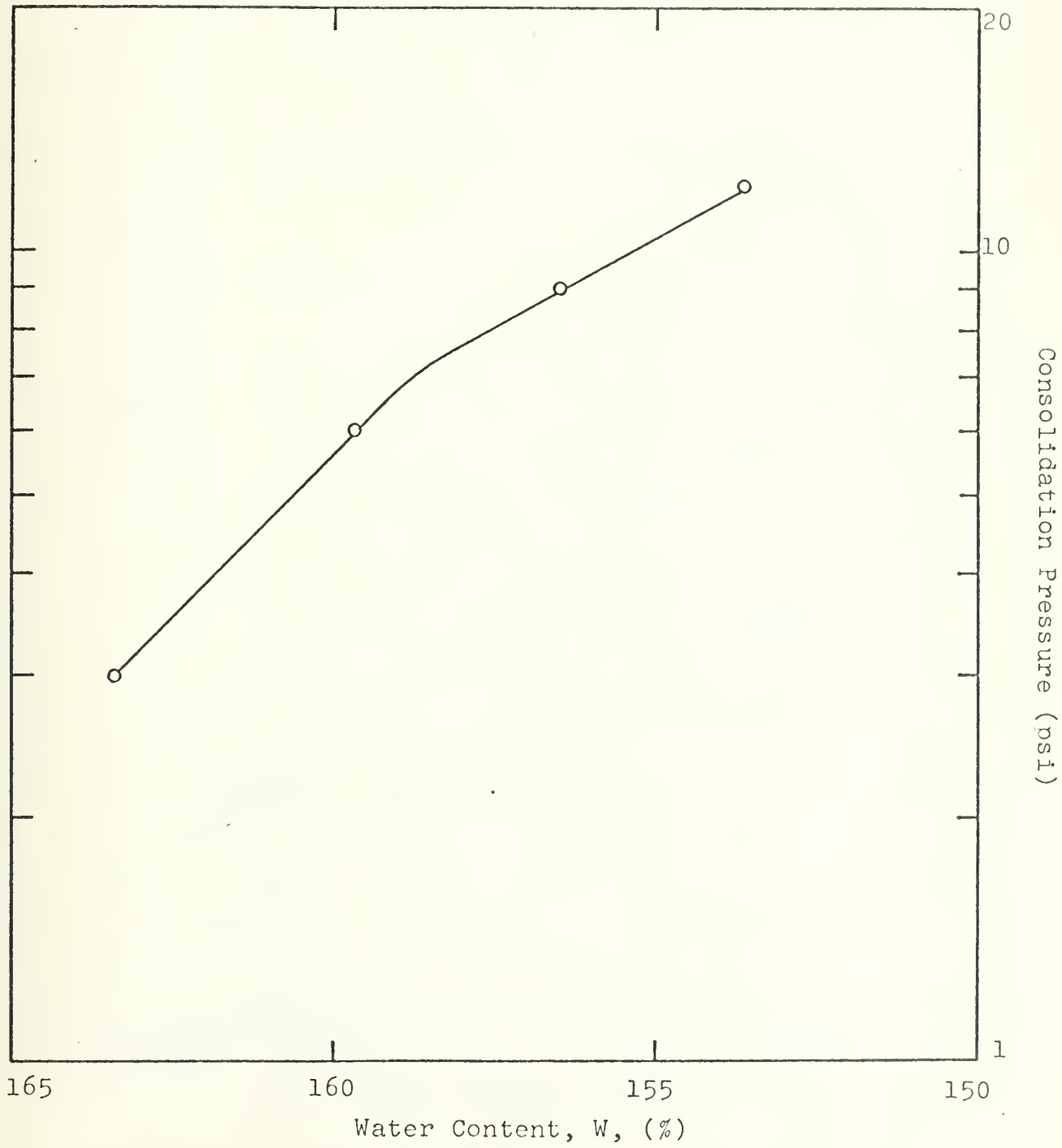

Figure 18 Water content vs. log consolidation pressure - Sample ATL

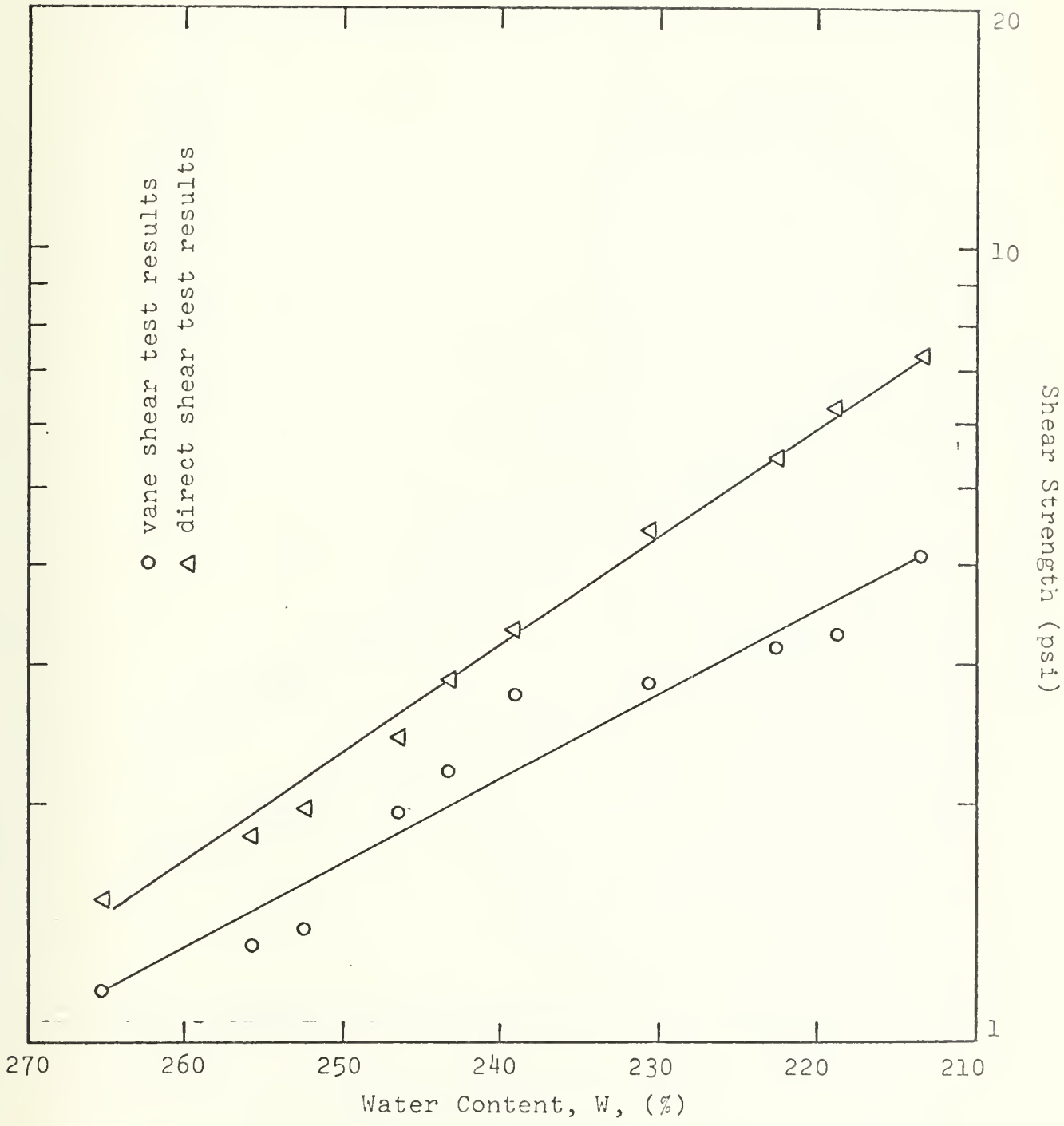

Figure 19 Water content vs. log shear strength - Sample KK076

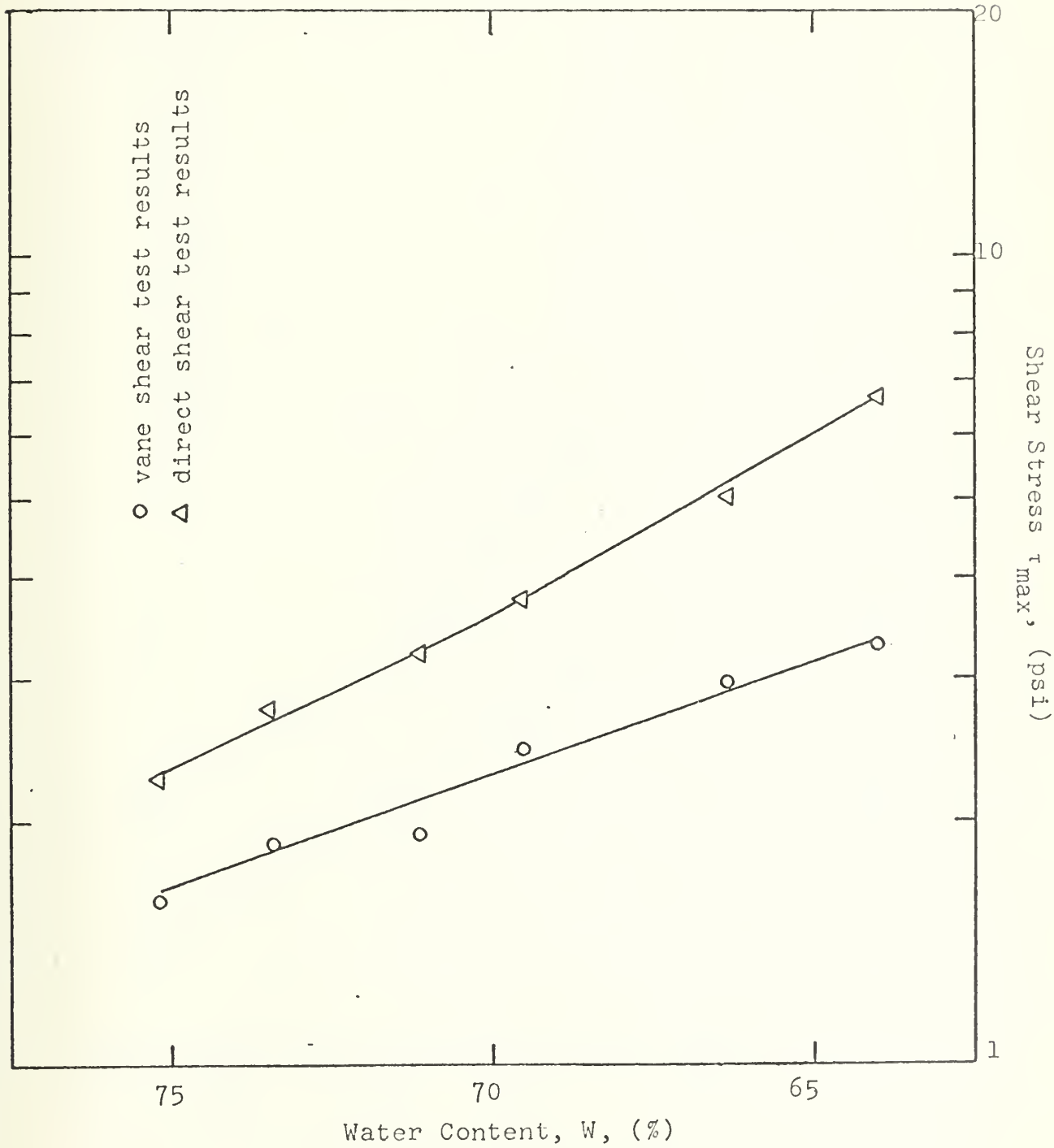

Figure 20 Water content vs. log shear strength - Sample GM

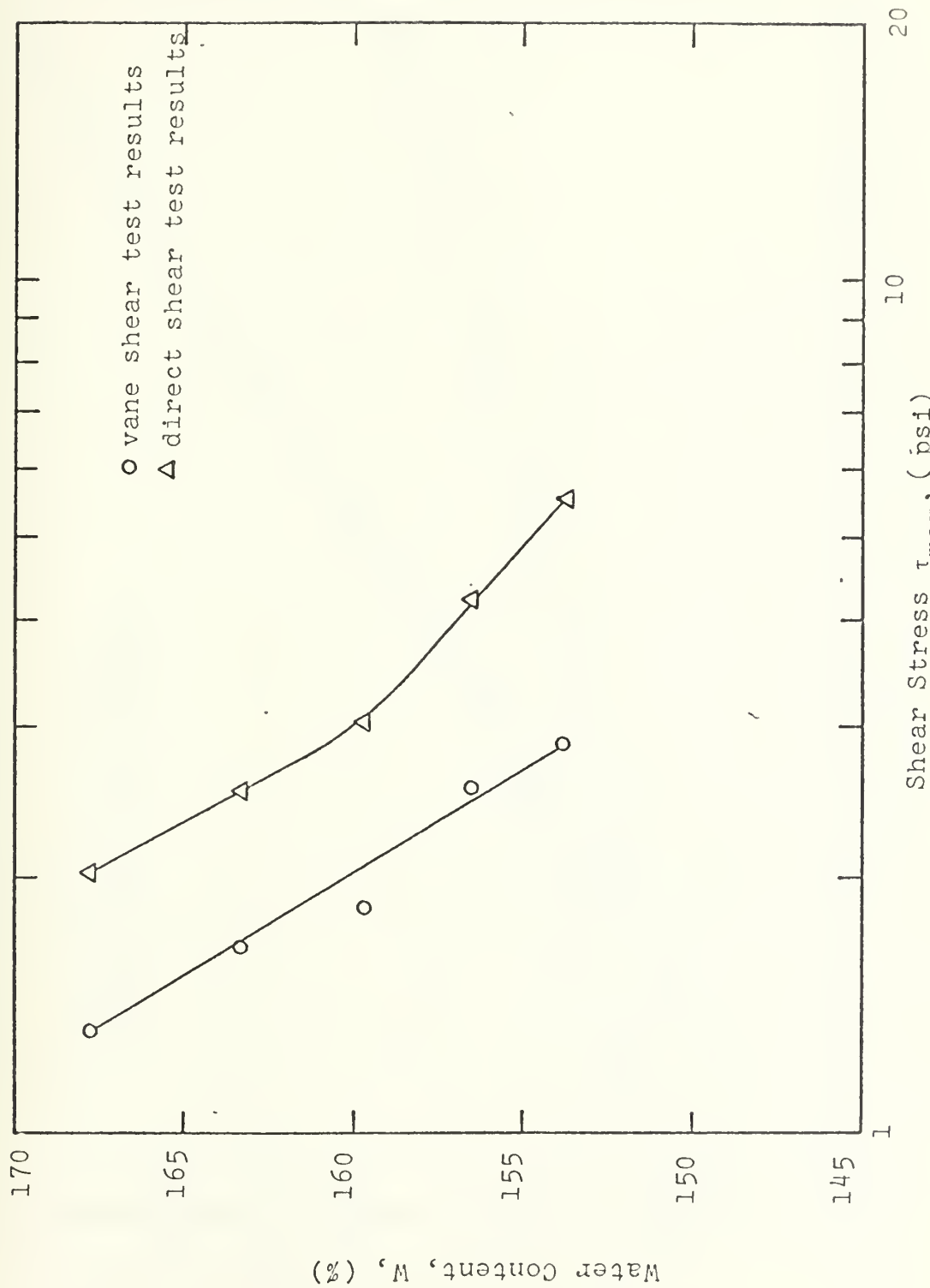

Figure 21 Water content vs. log shear strength - Sample ATL

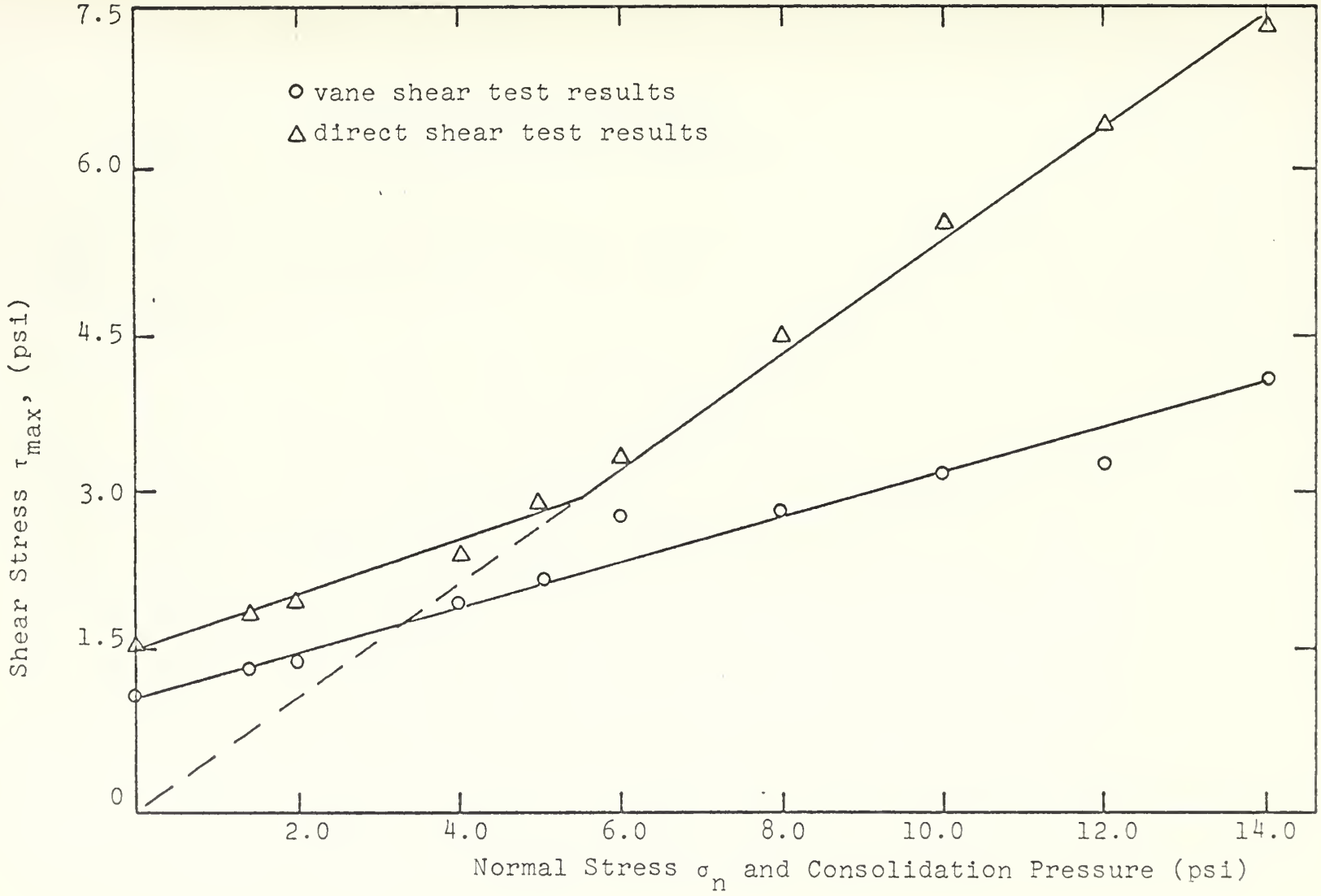

Figure 22 Shear Strength vs. normal stress and consolidation pressure - Sample KK076

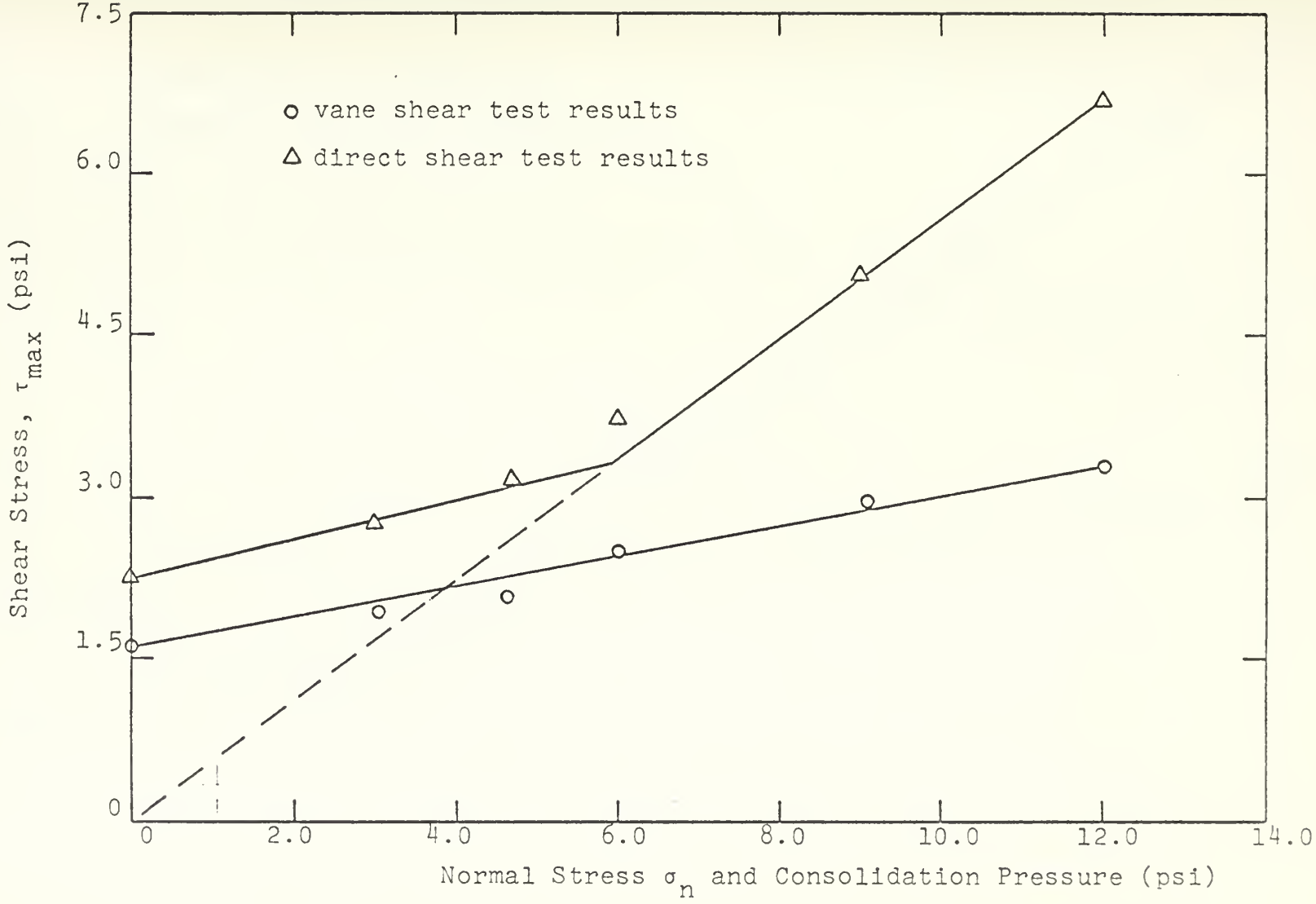

Figure 23 Shear Strength vs. normal stress and consolidation pressure - Sample GM

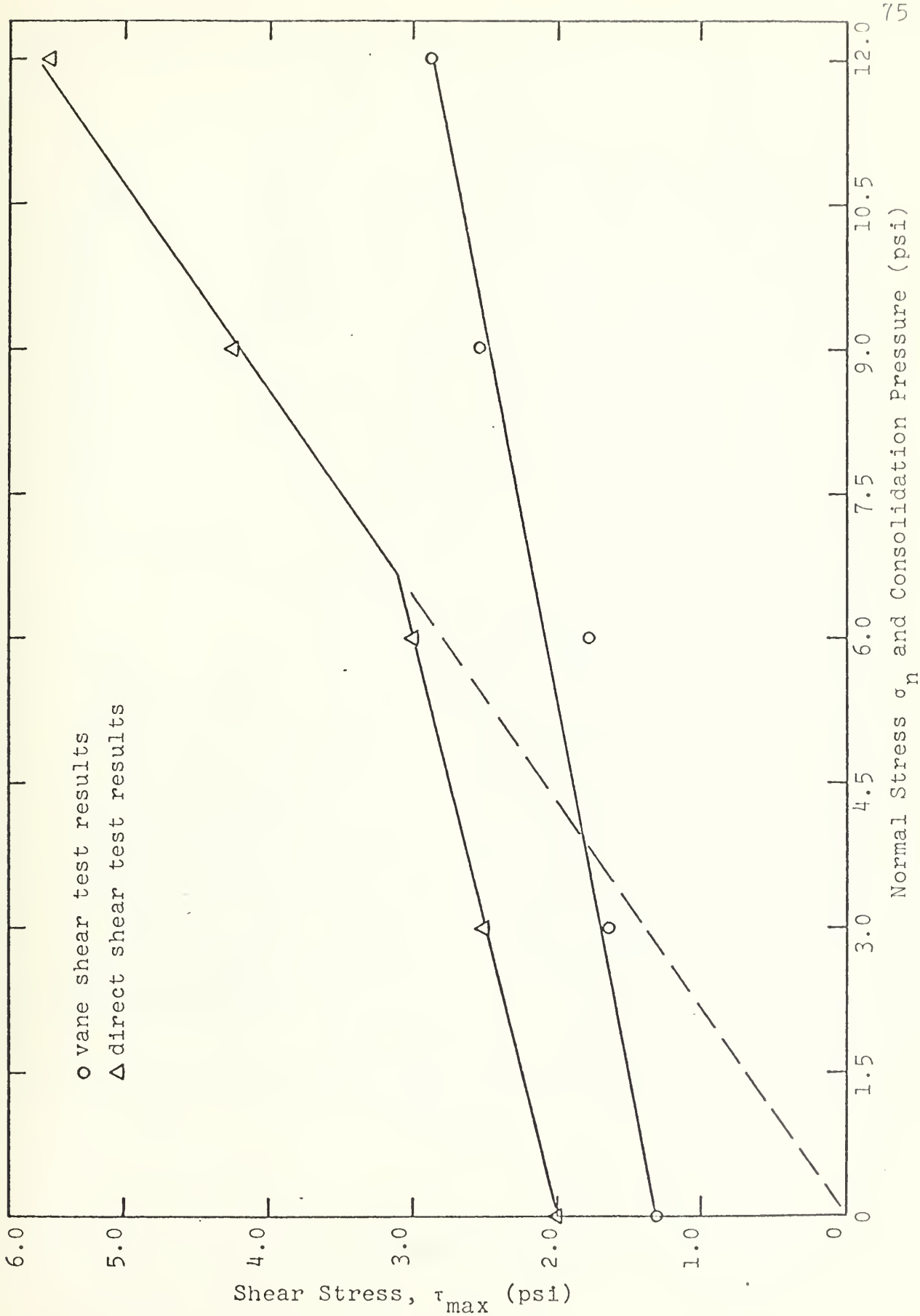

Figure 24 Shear Strength vs. normal stress and consolidation pressure - Sample ATL

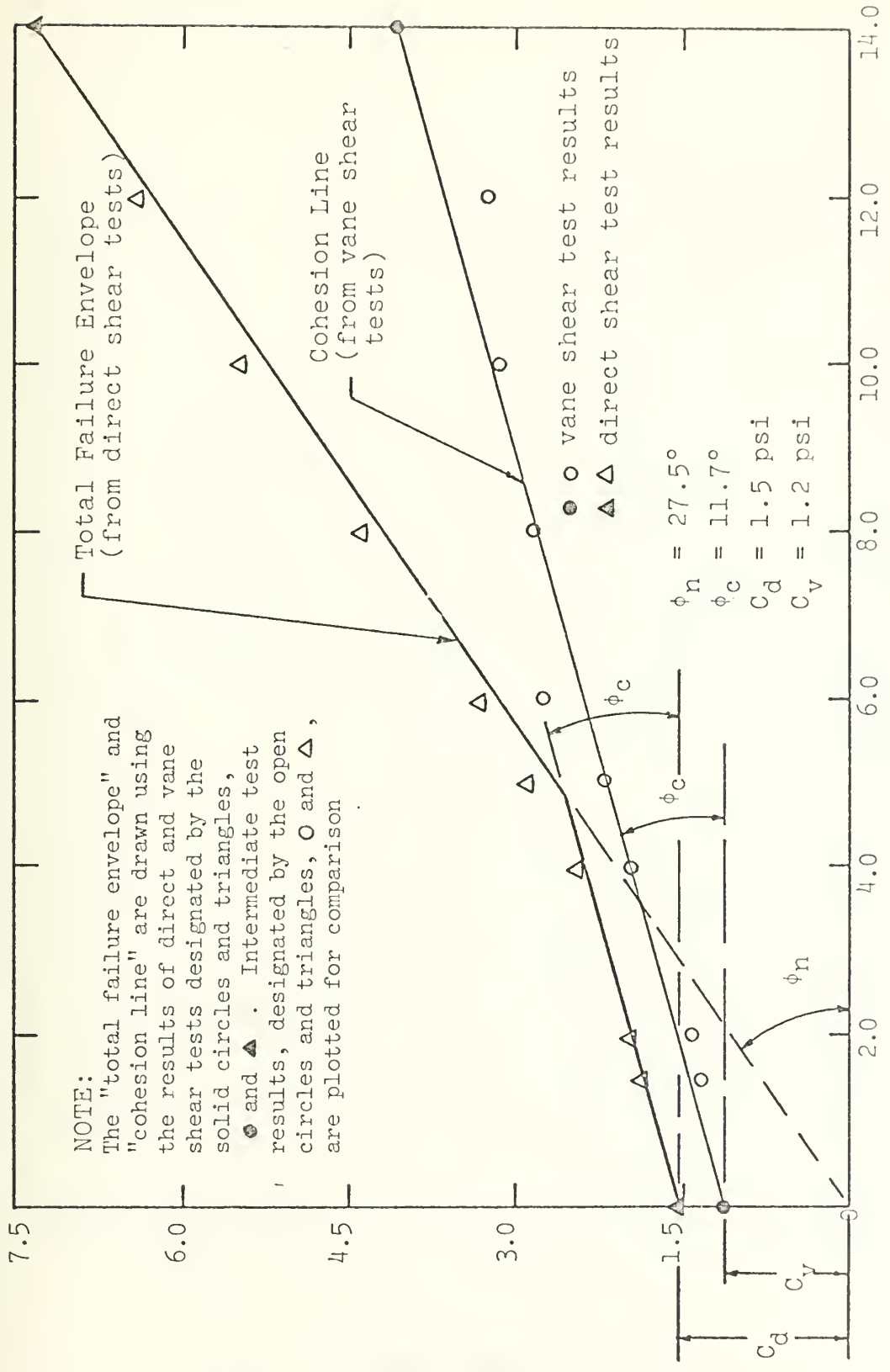

Figure 25 "Combined" shear strength analysis - shear strength vs. normal stress and consolidation pressure - Sample KK076

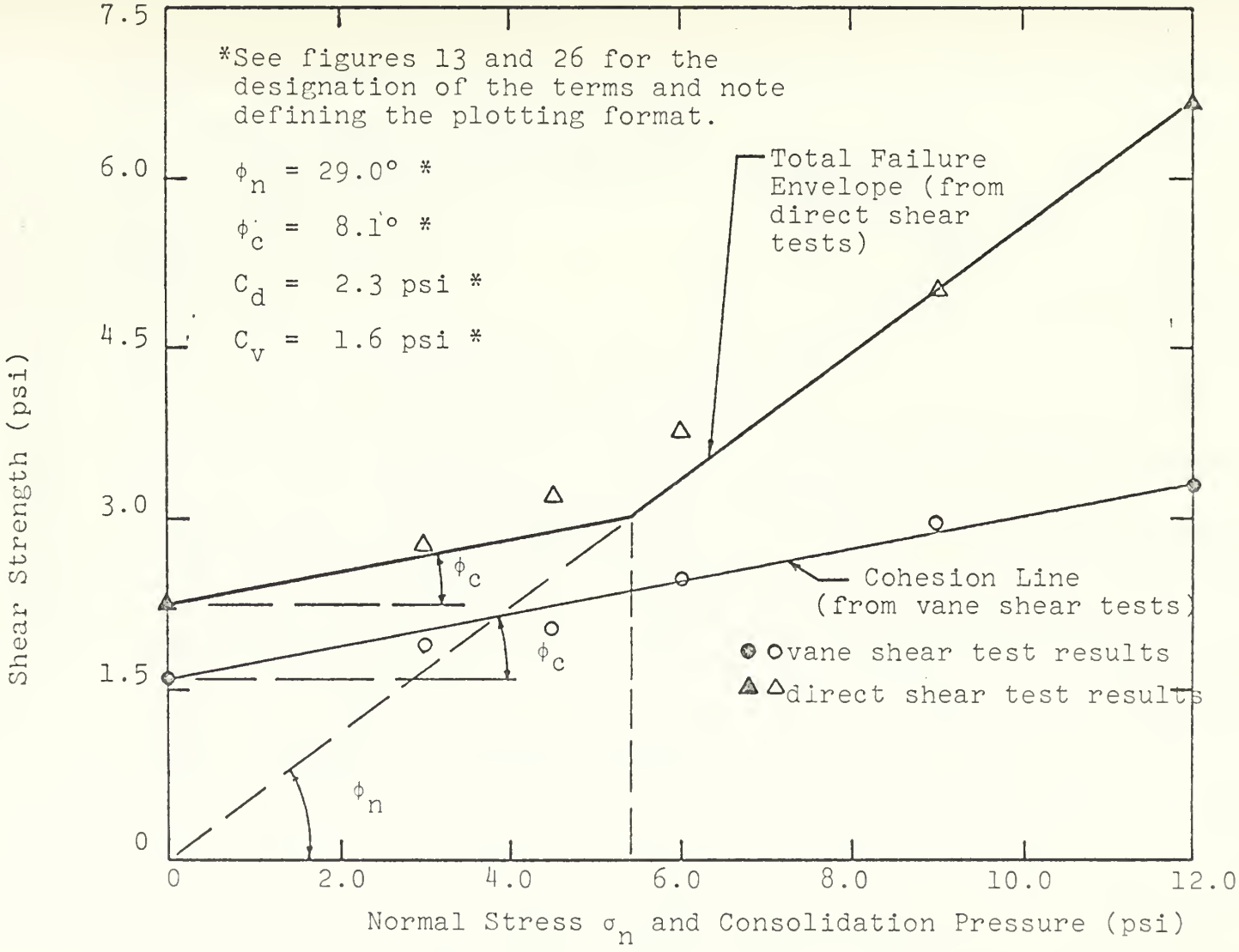

Figure 26 "Combined" shear strength analysis - shear strength vs. normal stress and consolidation pressure - Sample GM

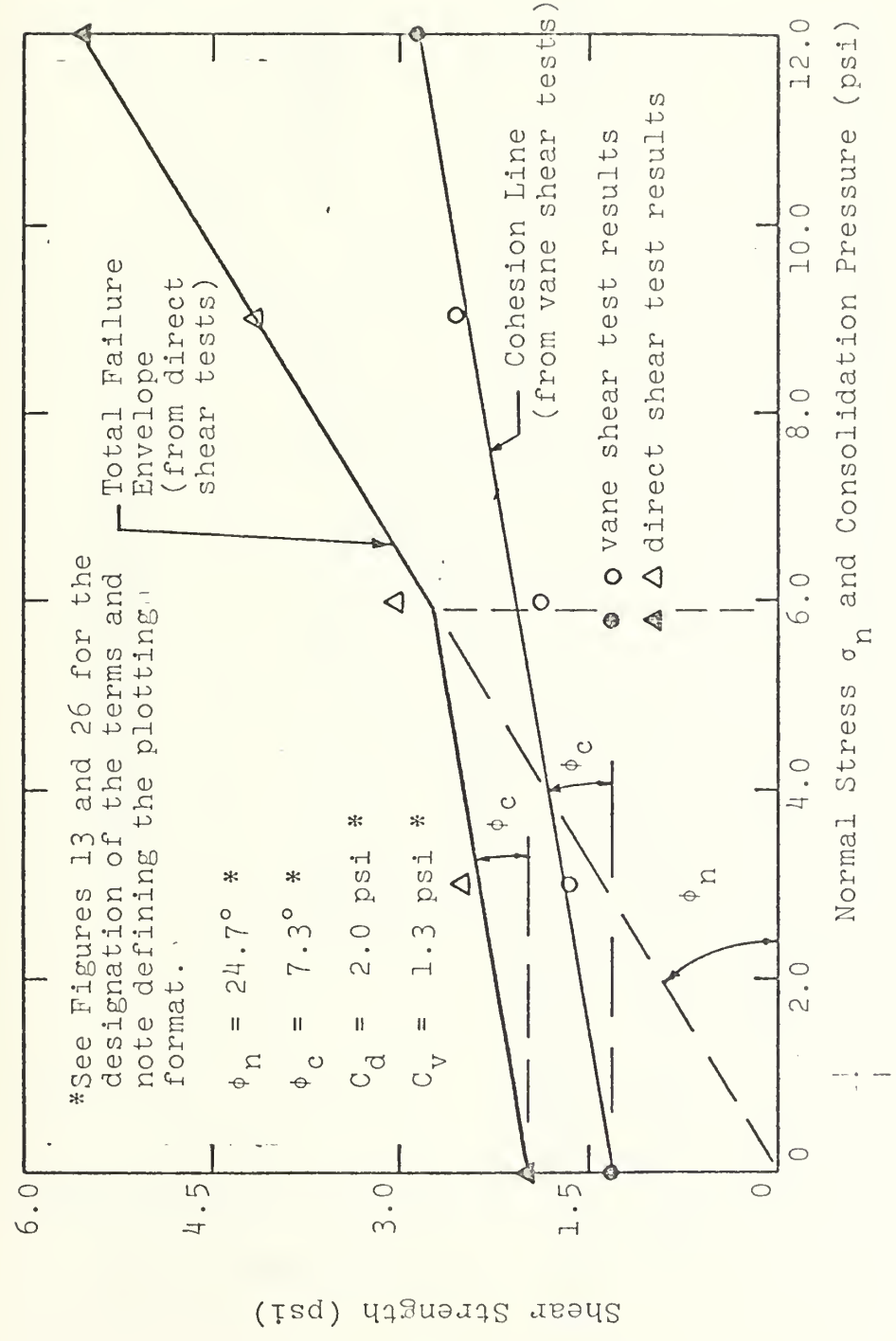

Figure 27 "Combined" shear strength analysis - shear strength vs. normal stress and consolidation pressure - Sample ATL

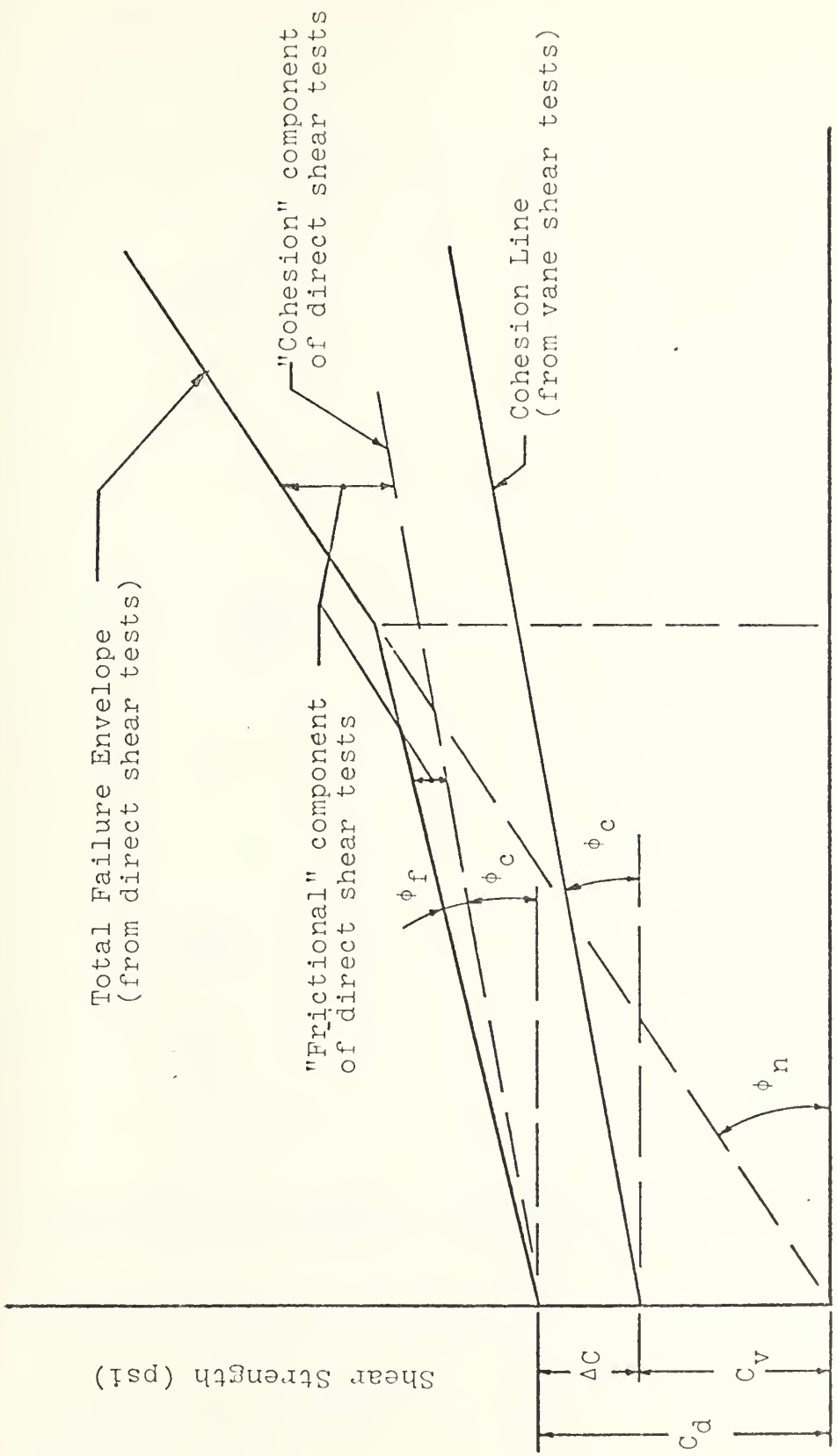

Figure 28 Illustration of "friction" component of direct shear tests

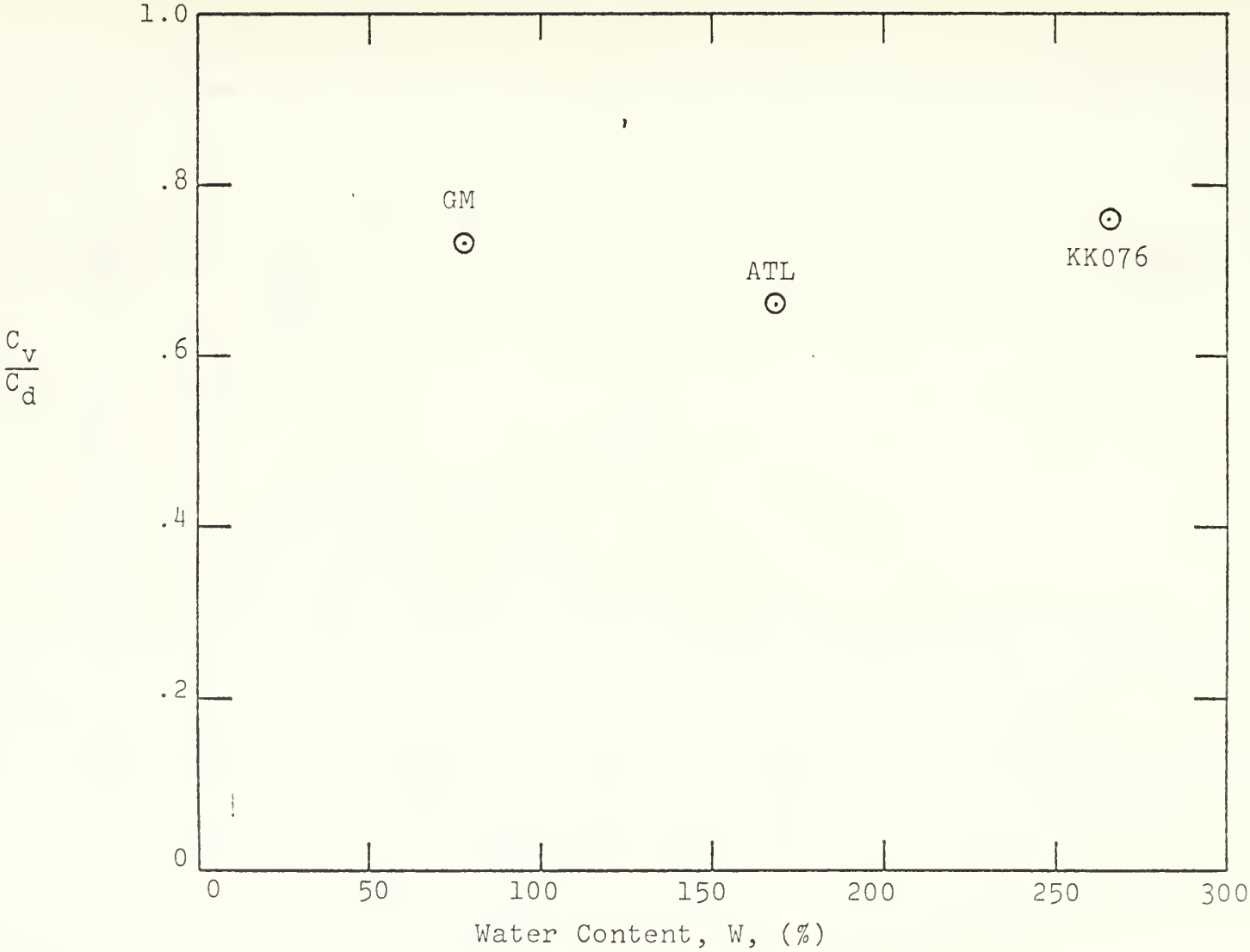

Figure 29 Water content vs. ratio C_v/C_d for $\sigma_n = 0$

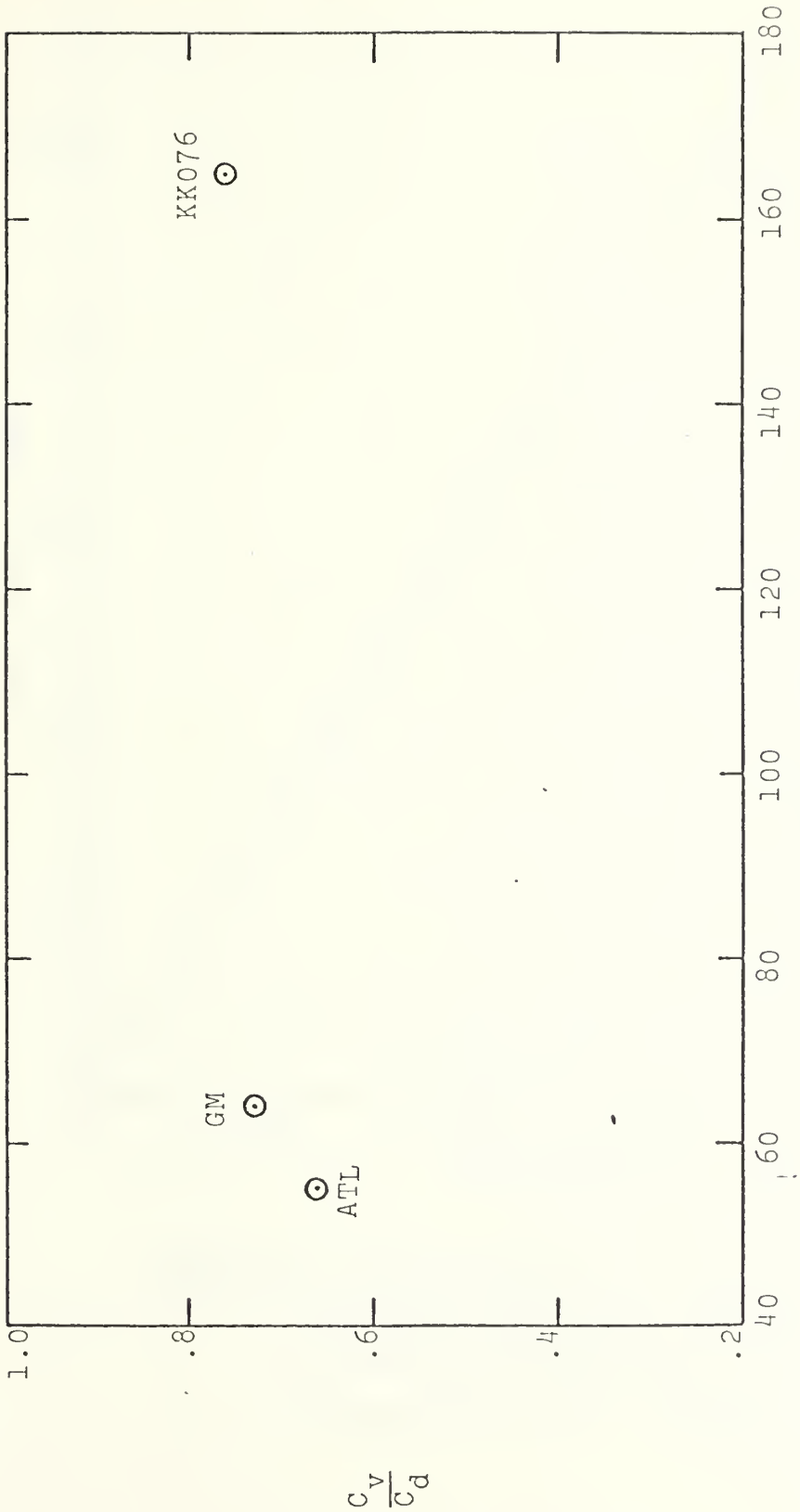

Figure 30 Plasticity Index vs. ratio C_c/C_d for $\sigma_n = 0$

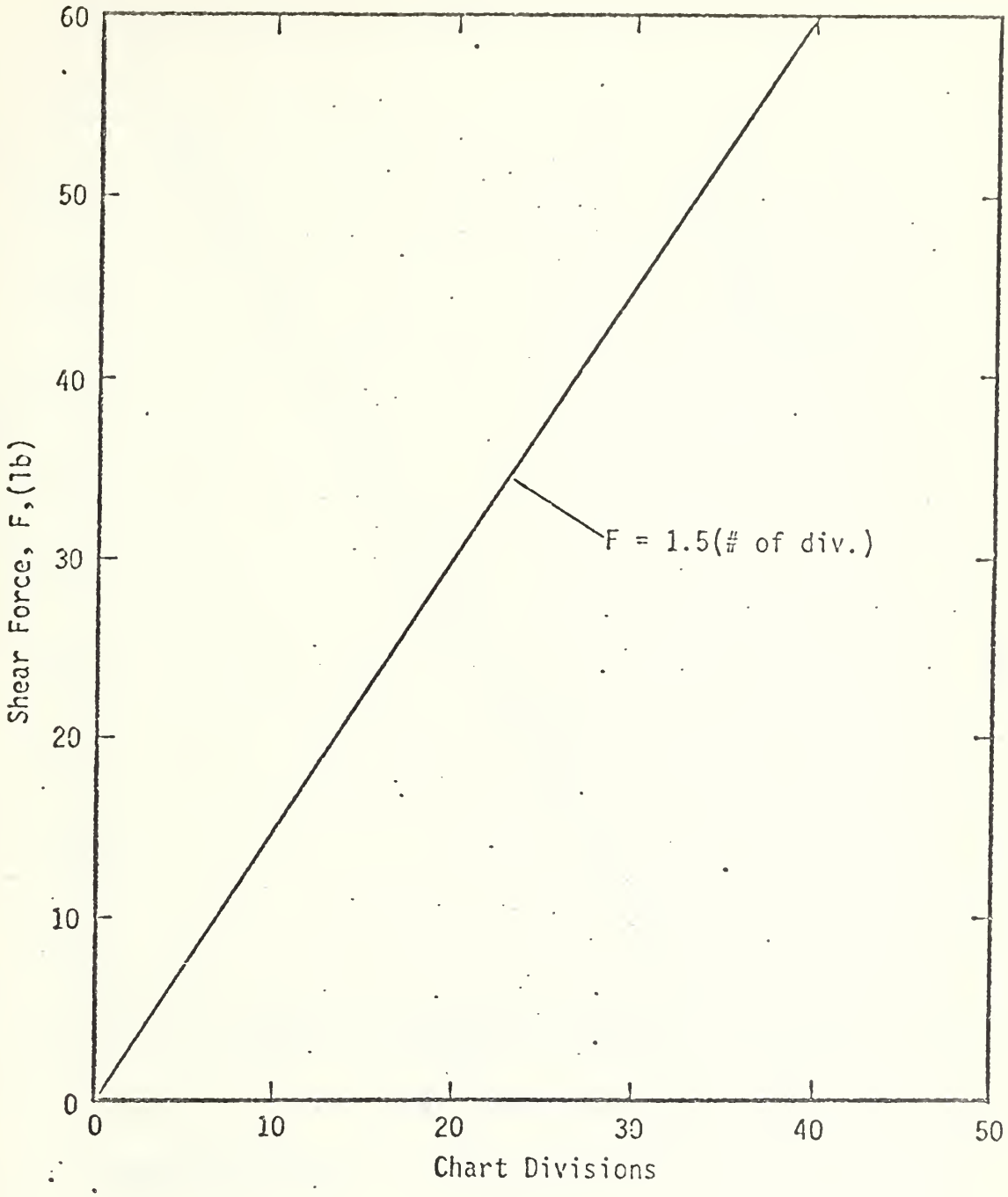

Calibration determined for:

1. BLH Electronics, Inc. Load Cell, Type U3G1
2. Strain Gage Conditioner = 20 volts
3. Chart Sensitivity = 10 mv/division

Figure A-1. Recording chart calibration for direct shear test.

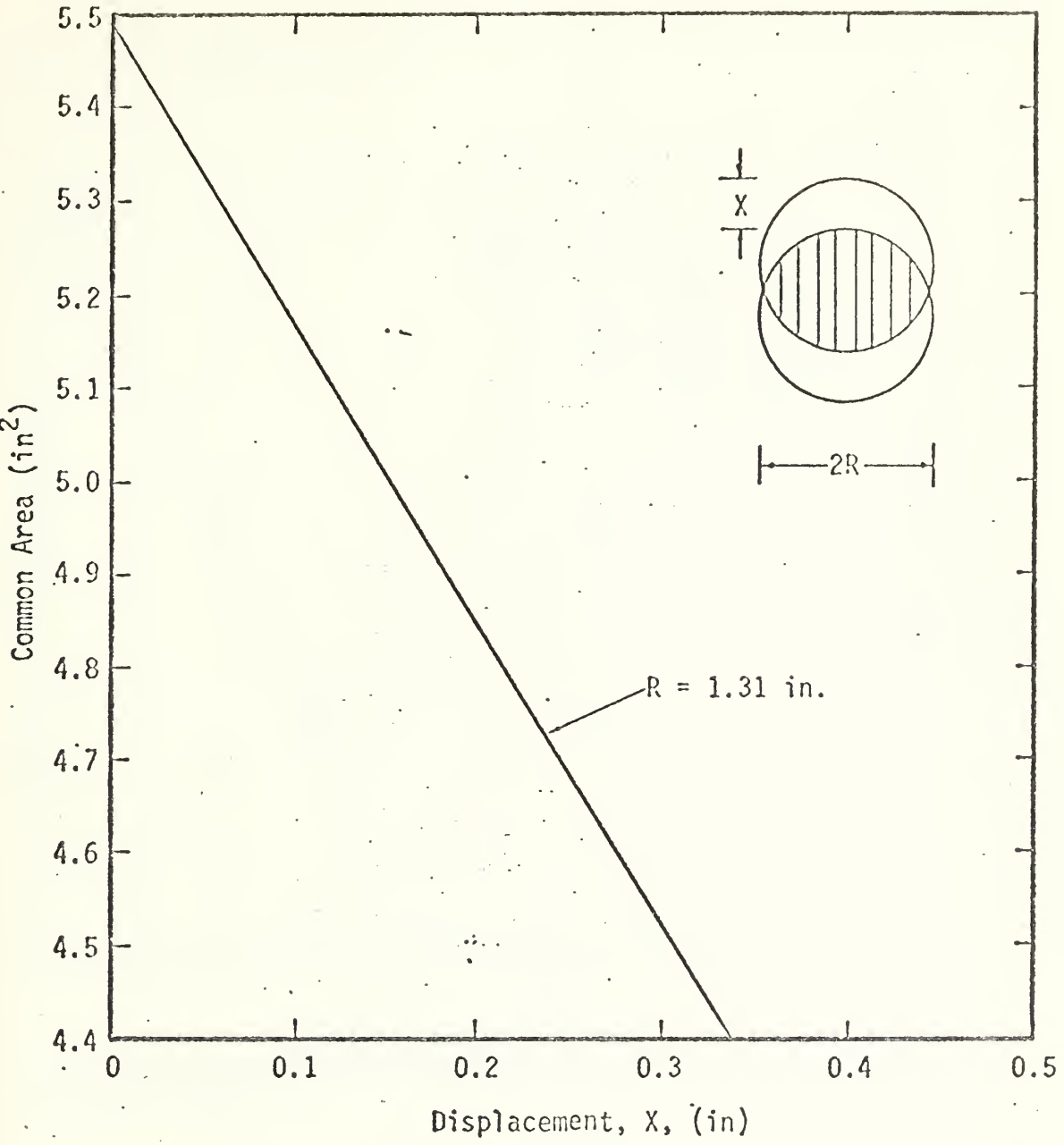

General Equation:

$$\text{Common Area} = R^2 \left\{ \frac{\pi \cos^{-1}\left(\frac{X}{2R}\right)}{90^o} - \sin\left[2\cos^{-1}\left(\frac{X}{2R}\right)\right] \right\}$$

Figure A-2. Common area vs. displacement for direct shear test.

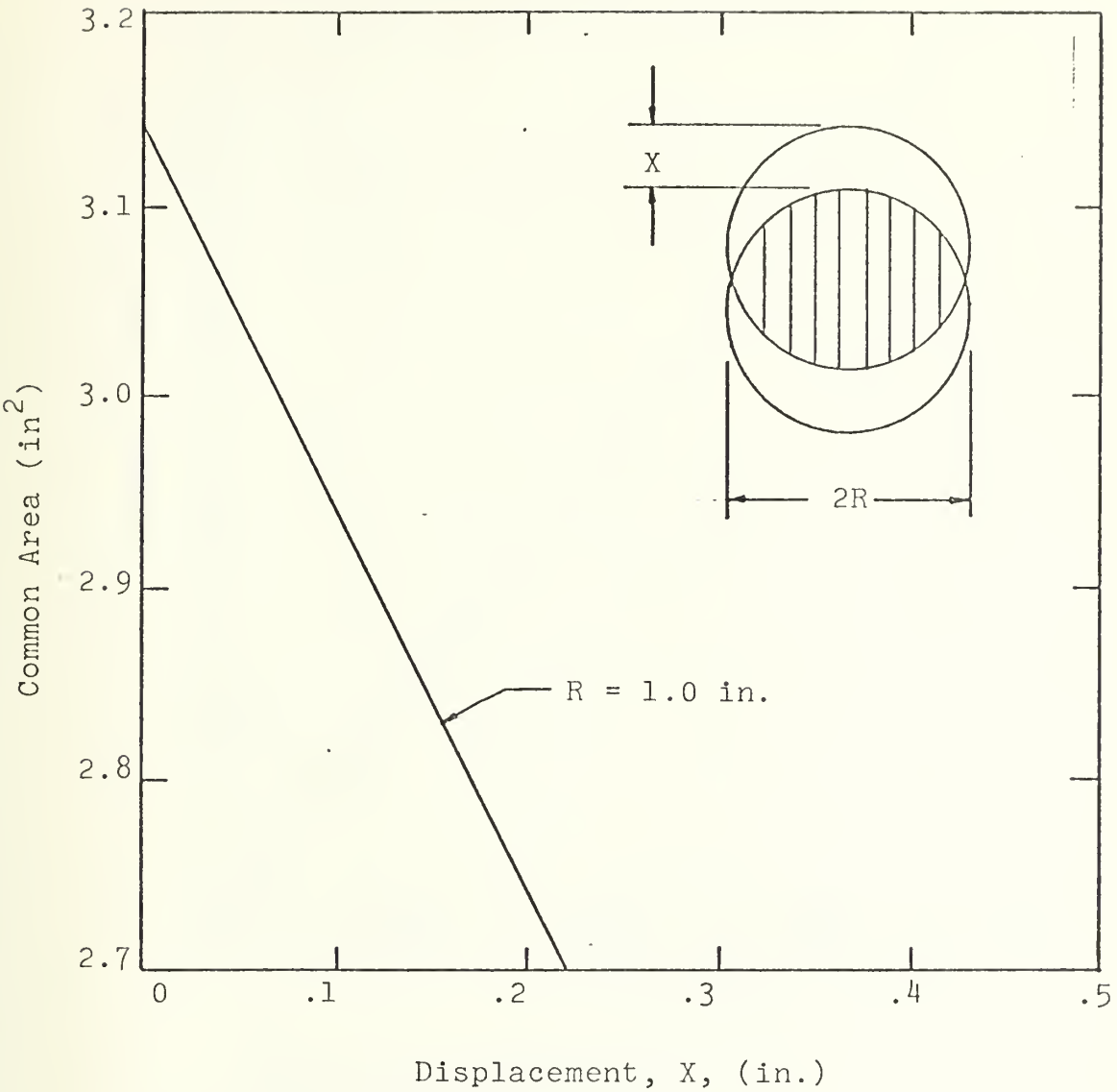

General Equation:

$$\text{Common Area} = R^2 \left\{ \frac{\pi \cos^{-1}\left(\frac{X}{2R}\right)}{90^\circ} - \sin\left[2 \cos^{-1}\left(\frac{X}{2R}\right)\right] \right\}$$

Figure A-3 Common Area vs. displacement for direct shear test (R = 1.0 in.)

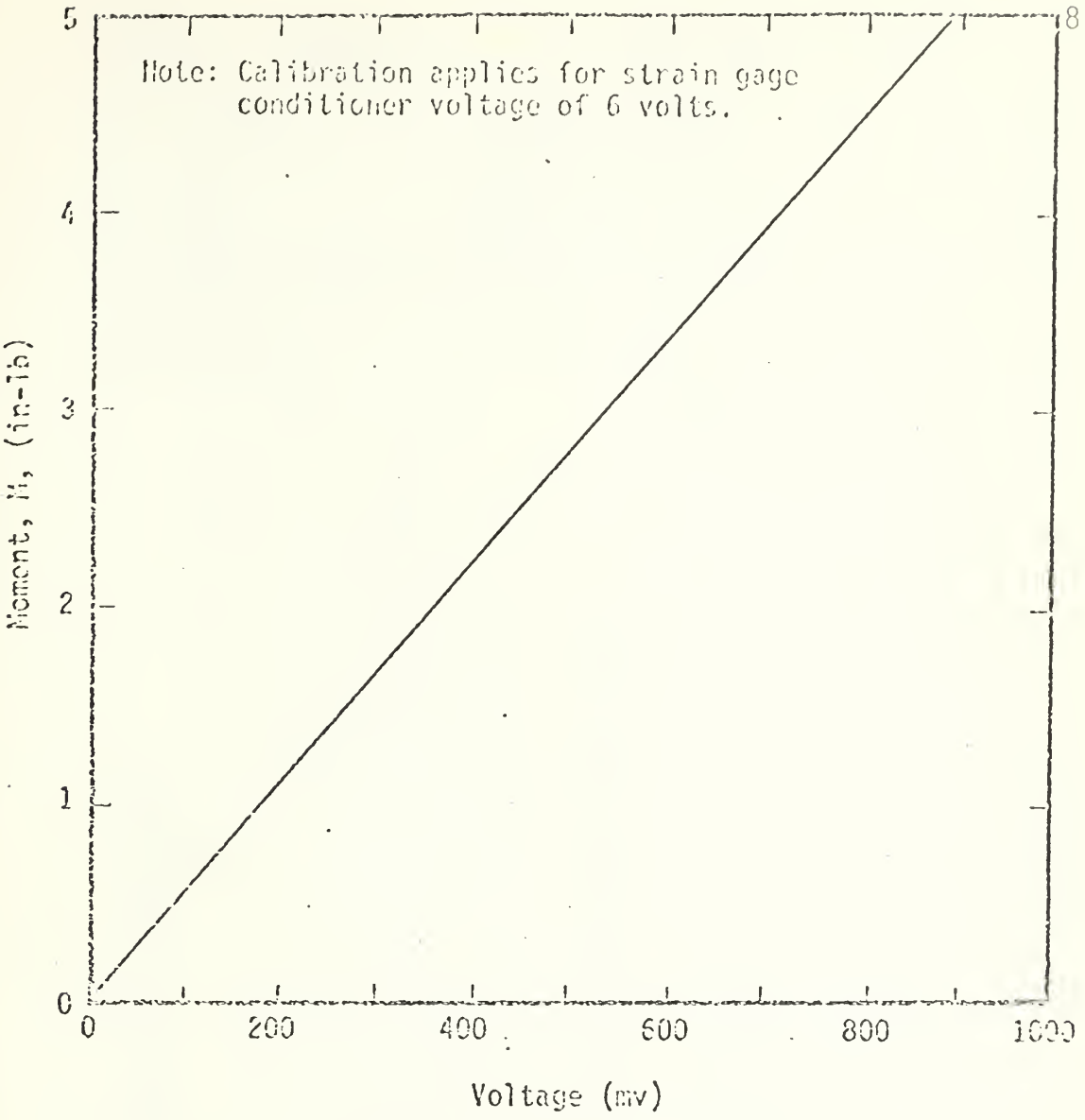

for top of vane not in soil;

$$\tau = \frac{M}{\pi}\left(\frac{12}{6D^2H + D^3}\right)$$

for top of vane in soil;

$$\tau = \frac{M}{\pi}\left(\frac{6}{3D^2H + D^3}\right)$$

τ = Shear Stress (psi) M = Moment on Vane Shaft (in-lb)

H = Vane Height (in) D = Vane Diameter (in)

Figure A- 4 Recording chart calibration for vane shear test.

Date: 10/5/76		Tested by: J. Foster	
Sample #: KK076	Water depth: 5000+m	Sample depth: ± 36'	
25 mm/min	Chart speed	25 mm/min	
20 v	Signal Conditioner	6 v	
10 mv	Sensitivity	20 mv	
0.0 psi	Normal Stress, Consolidation Pressure	0.0 psi	
1.57 psi	τ_{max}	1.16 psi	

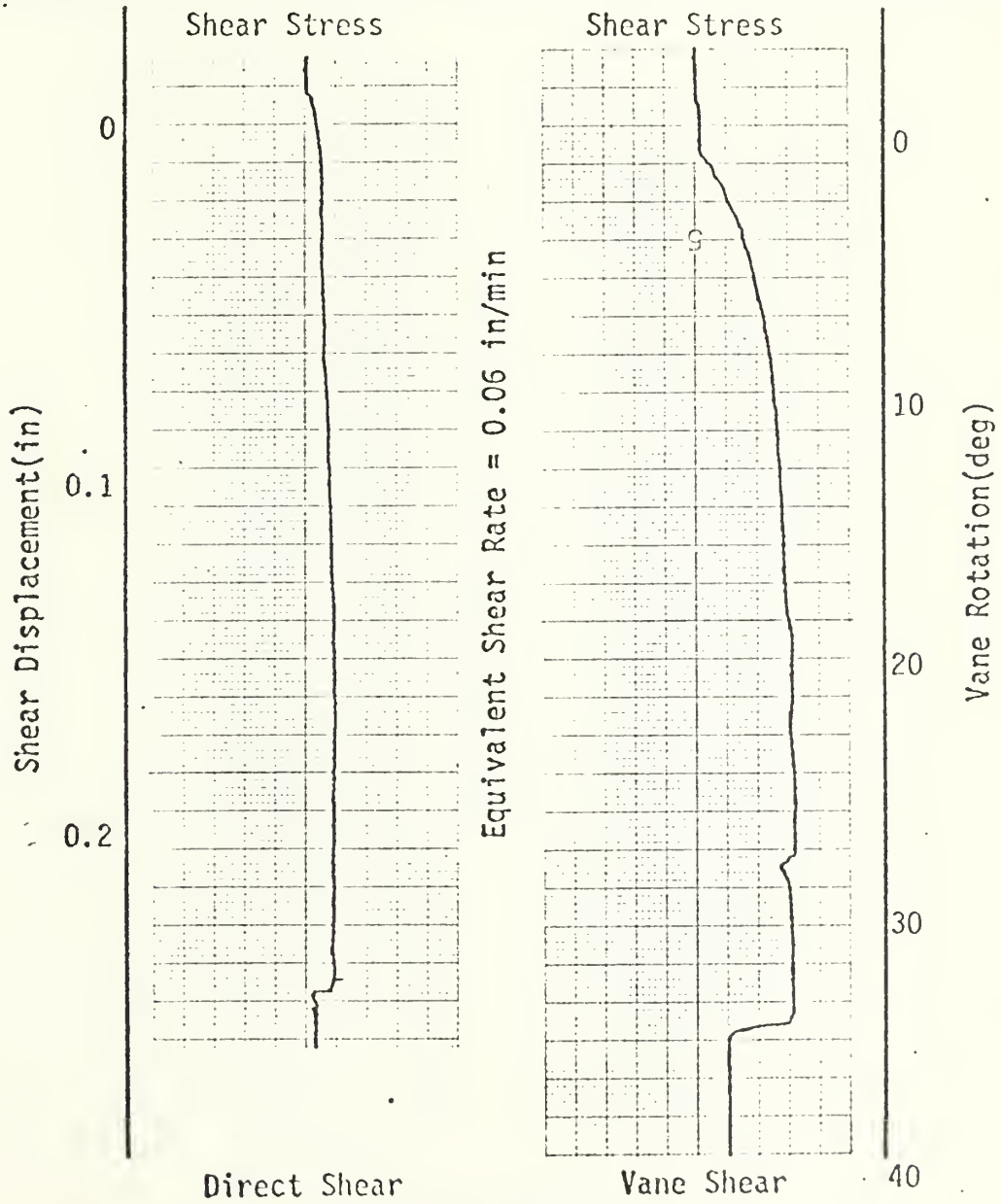

Water Content (%): 265.1

1 mm = 1.5 lb. 1 mm = .11 psi

Figure A- 5 Test Results - Sample KK076

Date: 10/6/76		Tested by: J. Foster	
Sample #: KK076	Water depth: 5000+m	Sample depth: ± 36'	
25 mm/min	Chart speed	25 mm/min	
20 v	Signal Conditioner	6 v	
10 mv	Sensitivity	20 mv	
1.46 psi	Normal Stress, Consolidation Pressure	1.46psi	
1.82 psi	τ_{max}	1.33 psi	

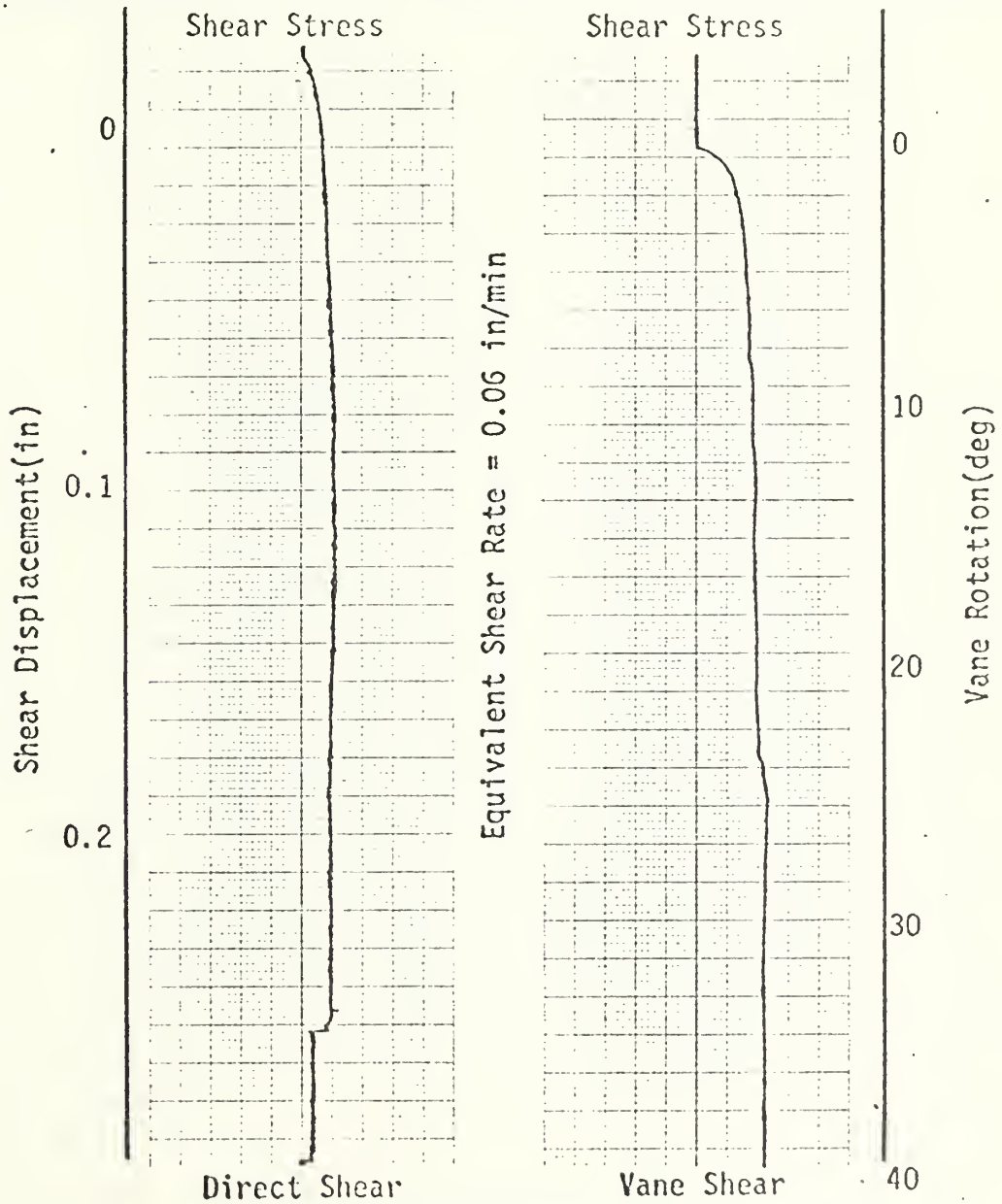

Figure A- 6 Test Results - Sample KK076

Date: 10/7/76		Tested by: J. Foster	
Sample #: KK076	Water depth: 5000+ m	Sample depth: ± 36'	
25 mm/min	Chart speed	25 mm/min	
20 v	Signal Conditioner	6 v	
10 mv	Sensitivity	20 mv	
2.0 psi	Normal Stress, Consolidation Pressure	2.0 psi	
1.97 psi	τ_{max}	1.39 psi	

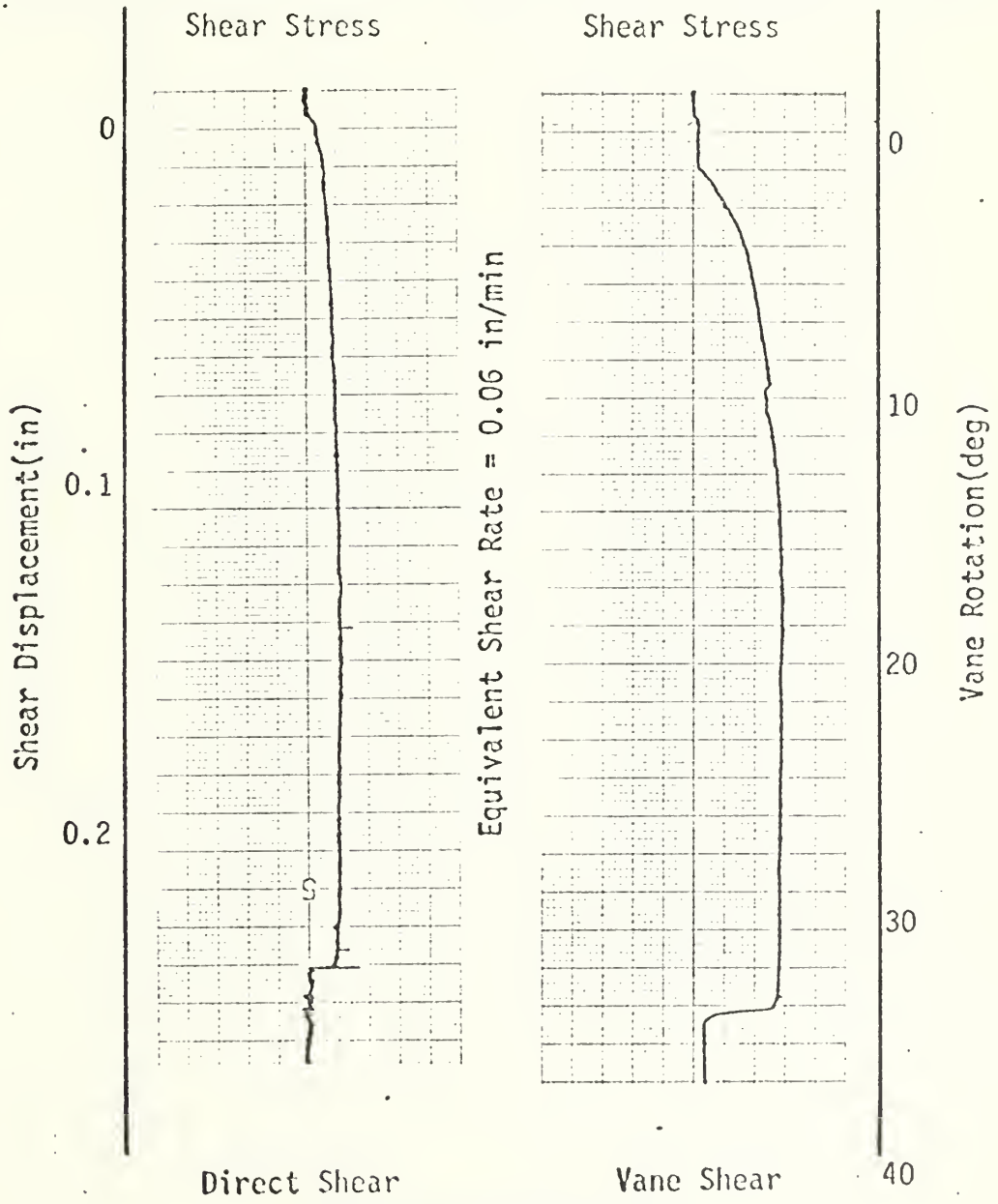

Water Content (%): 252.5

1 mm = 1.5 lb. 1 mm = .11 psi

Figure A- 7 Test Results - Sample KK076

Date: 10/8/76		Tested by: J. Foster	
Sample #: KK076	Water depth: 5000+m	Sample depth: ± 36'	
25 mm/min	Chart speed	25 mm/min	
20 v	Signal Conditioner	6 v	
10 mv	Sensitivity	20 mv	
4.0 psi	Normal Stress, Consolidation Pressure	4.0 psi	
2.42 psi	τ_{max}	1.95 psi	

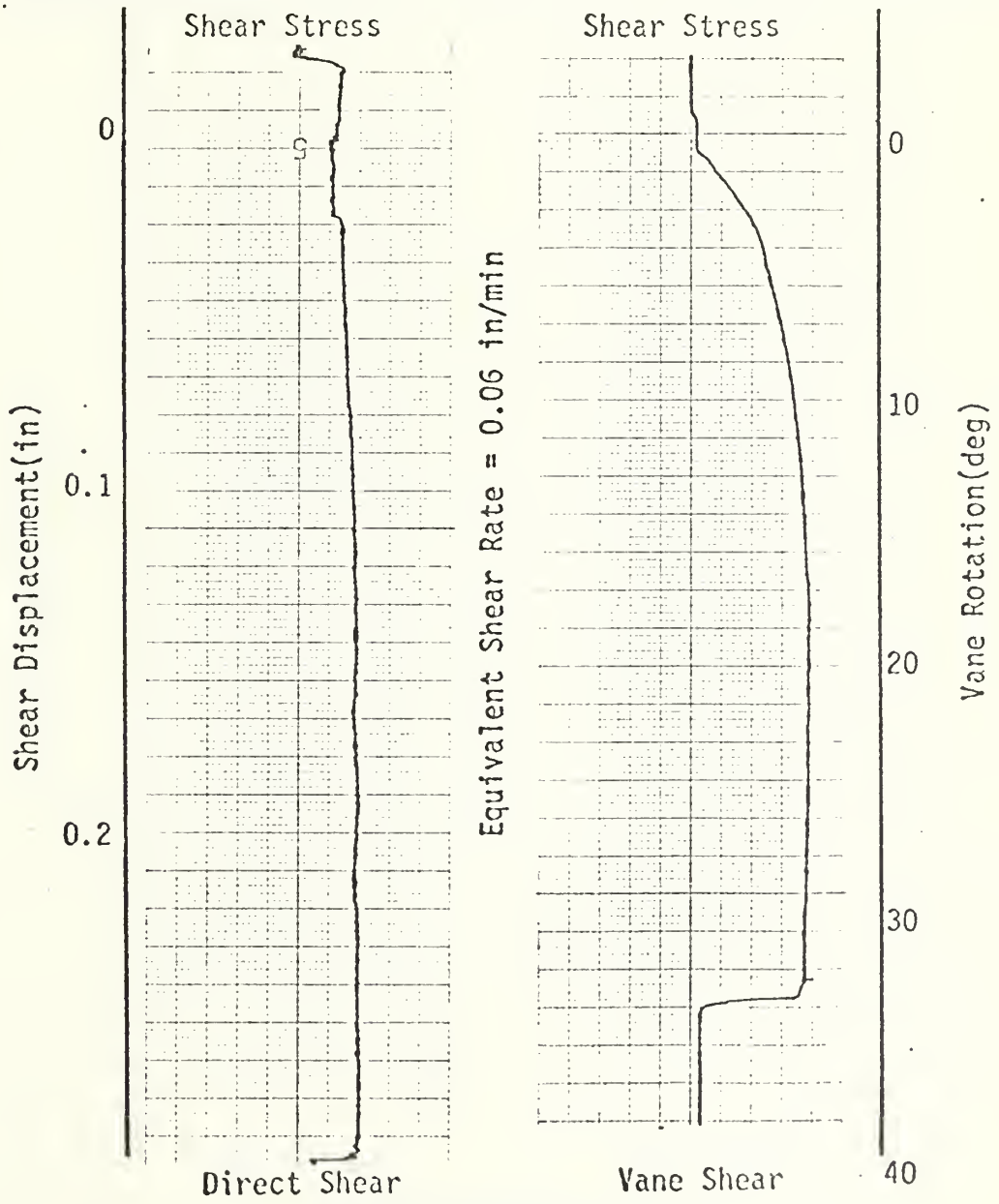

Water Content (%): 246.2

1 mm = 1.5 lb. 1 mm = .11 psi

Figure A- 8 Test Results - Sample KK076

Date: 10/9/76		Tested by: J. Foster	
Sample #: KK076	Water depth: 5000+m	Sample depth: ± 36'	
25 mm/min	Chart speed	25 mm/min	
20 v	Signal Conditioner	6 v	
10 mv	Sensitivity	20 mv	
5.0 psi	Normal Stress, Consolidation Pressure	5.0 psi	
2.89 psi	τ_{max}	2.20 psi	

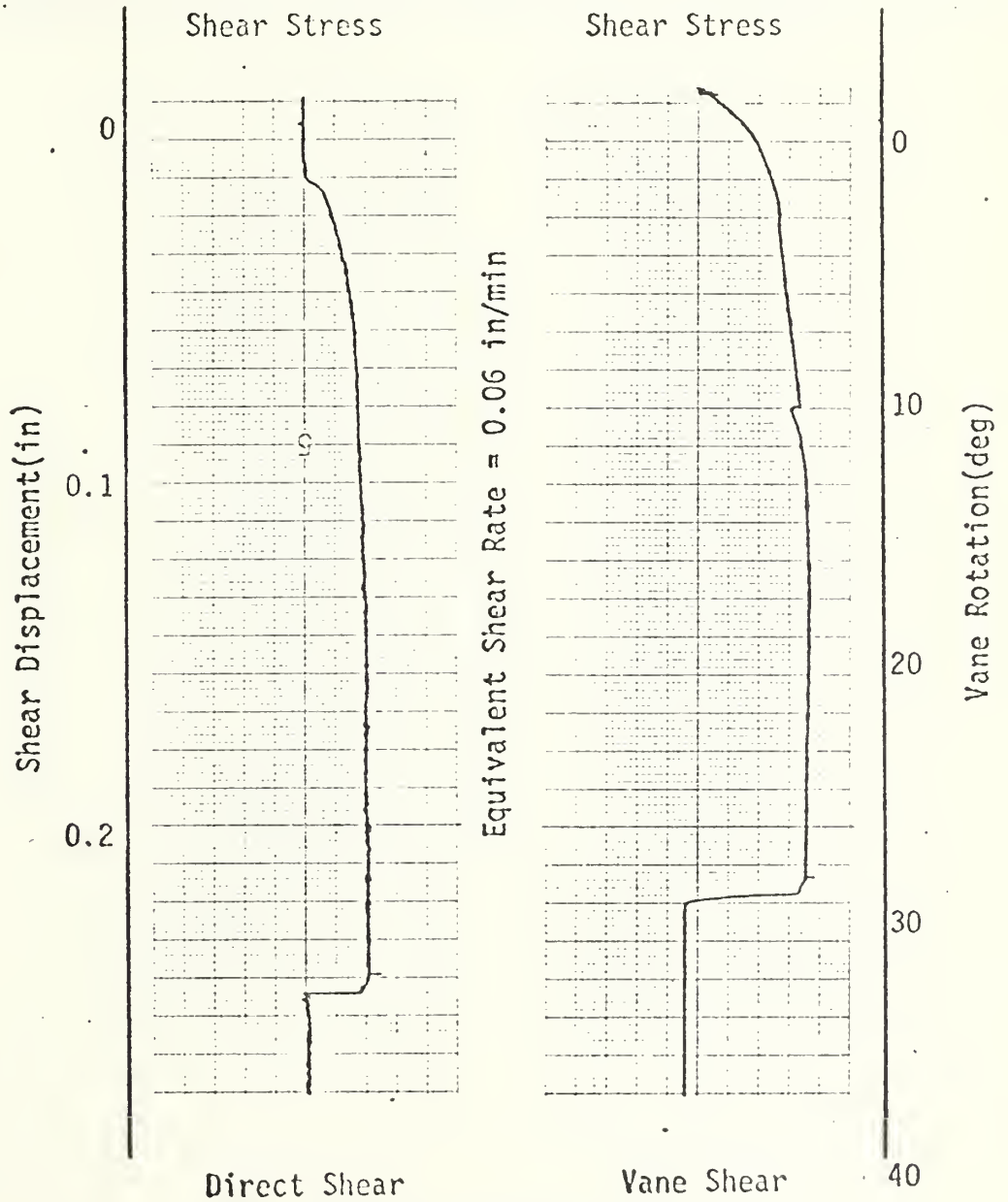

Water Content (%): 243.1

1 mm = 1.5 lb. 1 mm = .11 psi

Figure A- 9 Test Results - Sample KK076

Date: 10/11/76		Tested by: J. Foster	
Sample #: KK076	Water depth: 5000+m	Sample depth: ± 36'	
25 mm/min	Chart speed	25 mm/min	
20 v	Signal Conditioner	6 v	
10 mv	Sensitivity	20 mv	
6.0 psi	Normal Stress, Consolidation Pressure	6.0 psi	
3.31 psi	τ_{max}	2.75 psi	

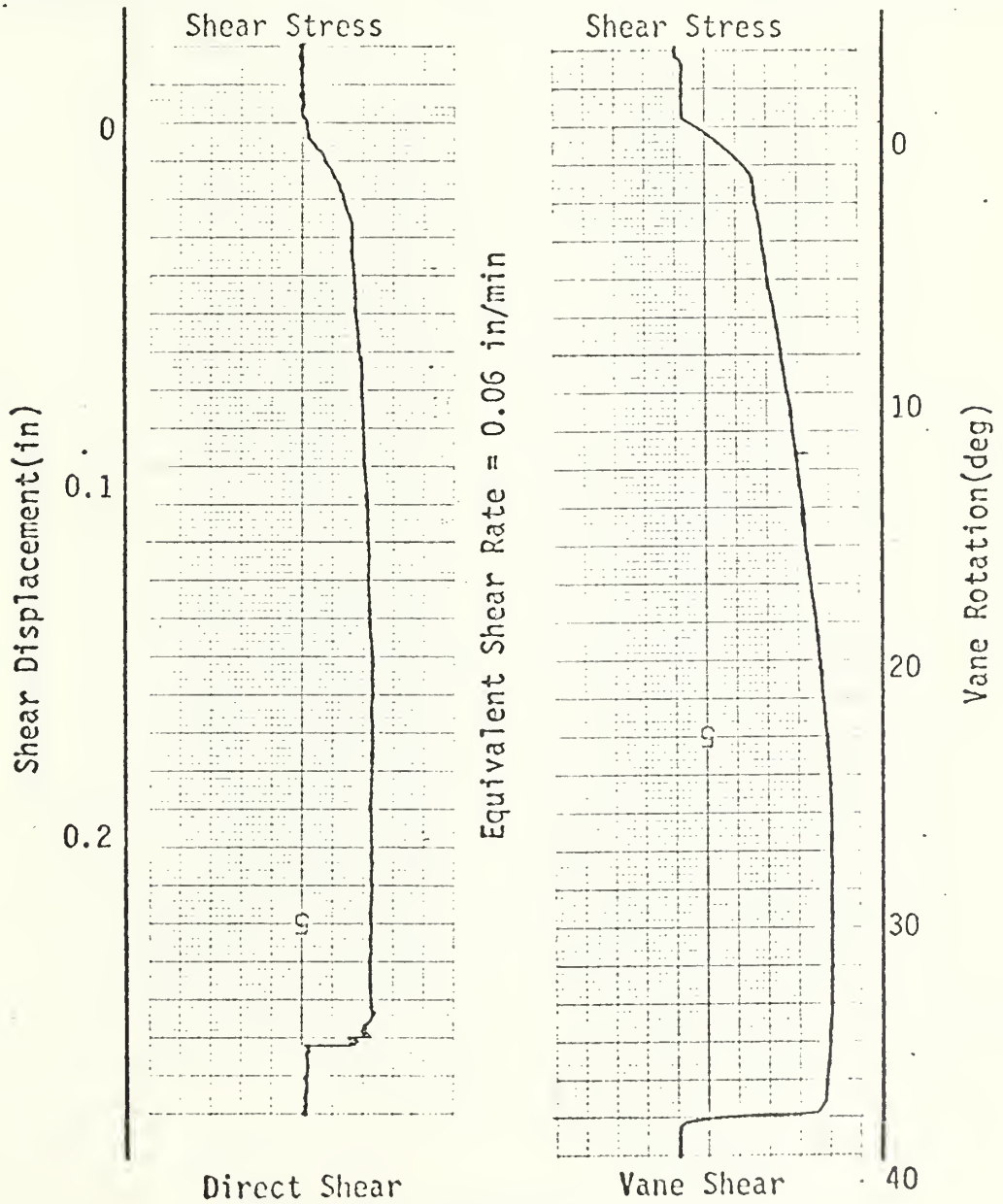

Water Content (%): 239.0

1 mm = 1.5 lb. 1 mm = .11 psi

Figure A- 10 Test Results - Sample KK076

Date: 10/12/76		Tested by: J. Foster	
Sample #: KK076	Water depth: 5000+m	Sample depth: ± 36'	
25 mm/min	Chart speed	25 mm/min	
20 v	Signal Conditioner	6 v	
10 mv	Sensitivity	20 mv	
8.0 psi	Normal Stress, Consolidation Pressure	psi	
4.41= psi	τ_{max}	2.81	psi

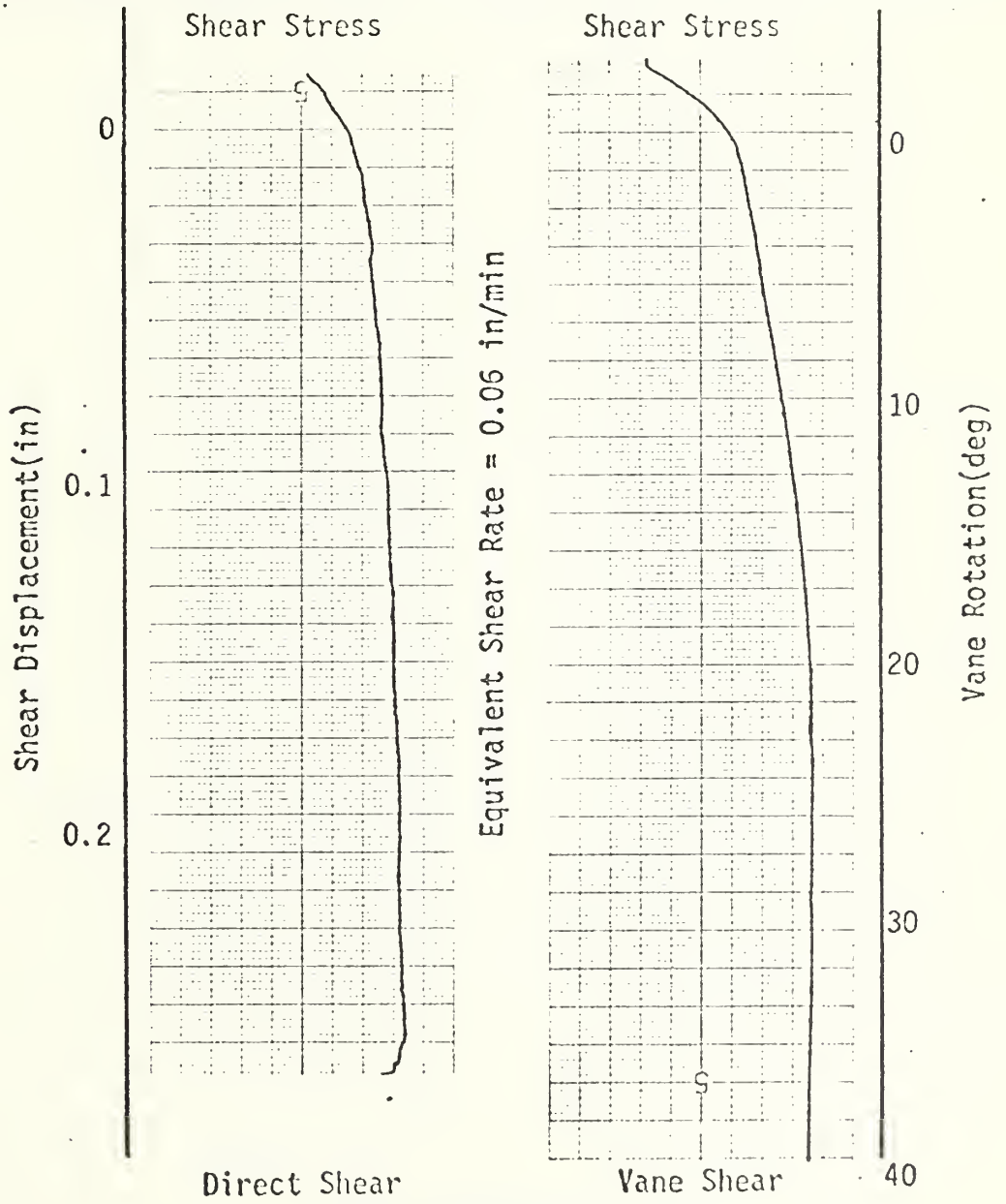

Water Content (%): 230.5

1 mm = 1.5 lb. 1 mm = .11 psi

Figure A- 11 Test Results - Sample KK076

Date: 10/13/76		Tested by: J. Foster	
Sample #: KK076	Water depth: 5000+m	Sample depth: ± 36'	
25 mm/min	Chart speed	25 mm/min	
20 v	Signal Conditioner	6 v	
10 mv	Sensitivity	20 mv	
10.0 psi	Normal Stress, Consolidation Pressure	10.0 psi	
5.48 psi	τ_{max}	3.14 psi	

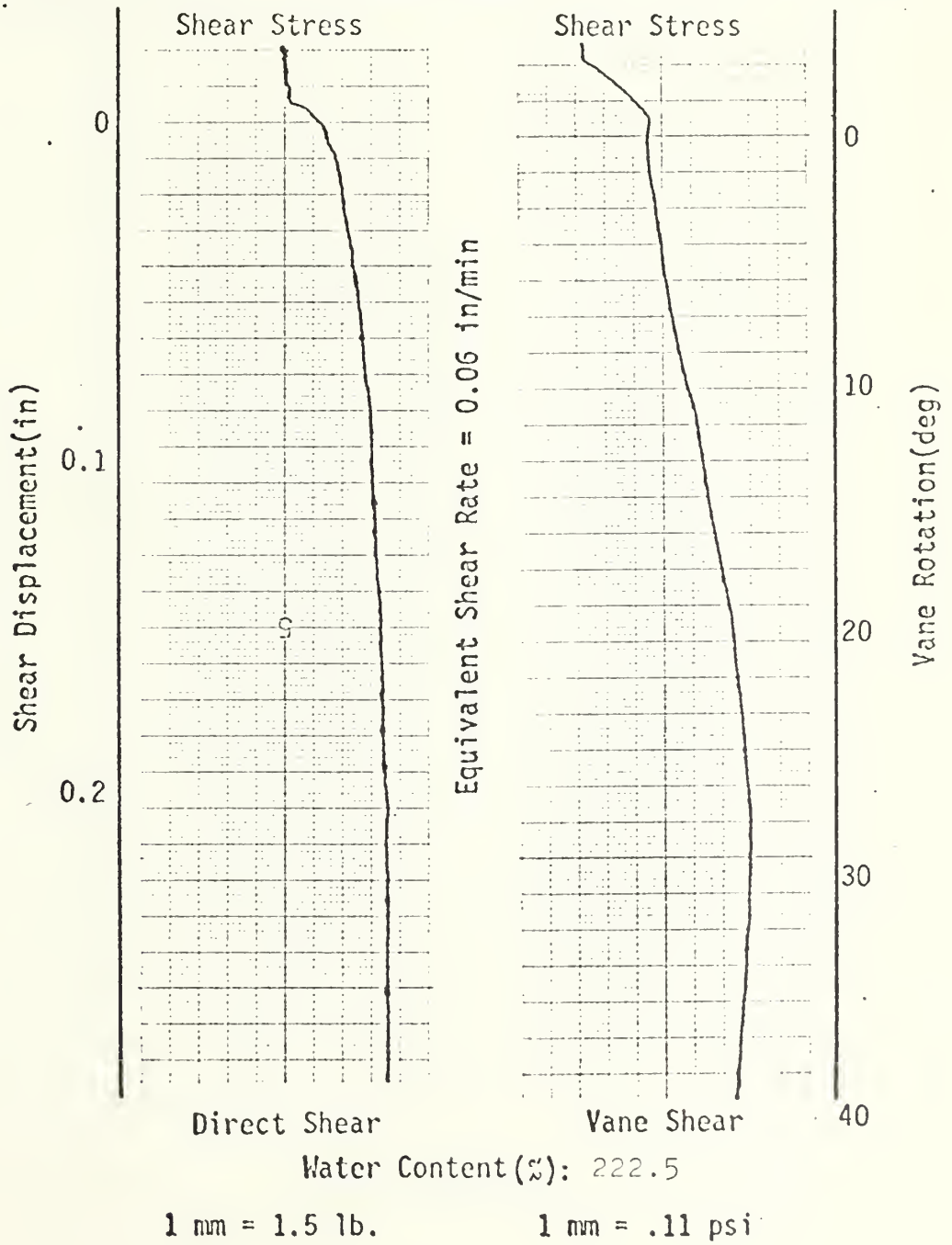

Figure A- 12 Test Results - Sample KK076

Date: 10/14/76		Tested by: J. Foster	
Sample #: KK076	Water depth: 5000+m	Sample depth: ± 36'	
25 mm/min	Chart speed	25 mm/min	
20 v	Signal Conditioner	6 v	
10 mv	Sensitivity	20 mv	
12.0 psi	Normal Stress, Consolidation Pressure	12.0 psi	
6.39 psi	τ_{max}	3.25 psi	

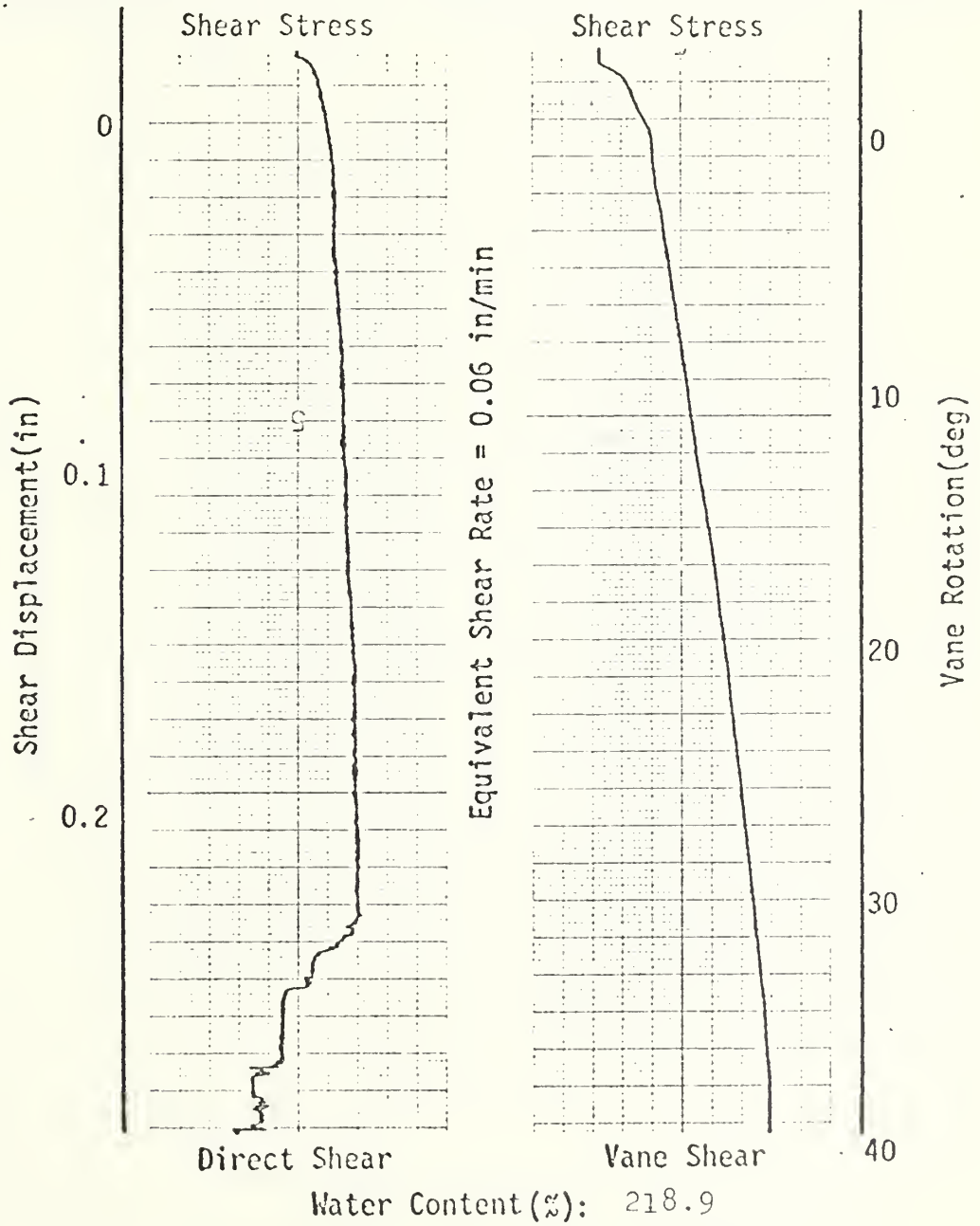

Figure A- 13 Test Results - Sample KK076

Date: 10/15/76		Tested by: J. Foster	
Sample #: KK076	Water depth: 5000+m	Sample depth: ± 36'	
25 mm/min	Chart speed	25 mm/min	
20 v	Signal Conditioner	6 v	
10 mv	Sensitivity	20 mv	
14.0 psi	Normal Stress, Consolidation Pressure	14.0 psi	
7.30 psi	τ_{max}	4.07 psi	

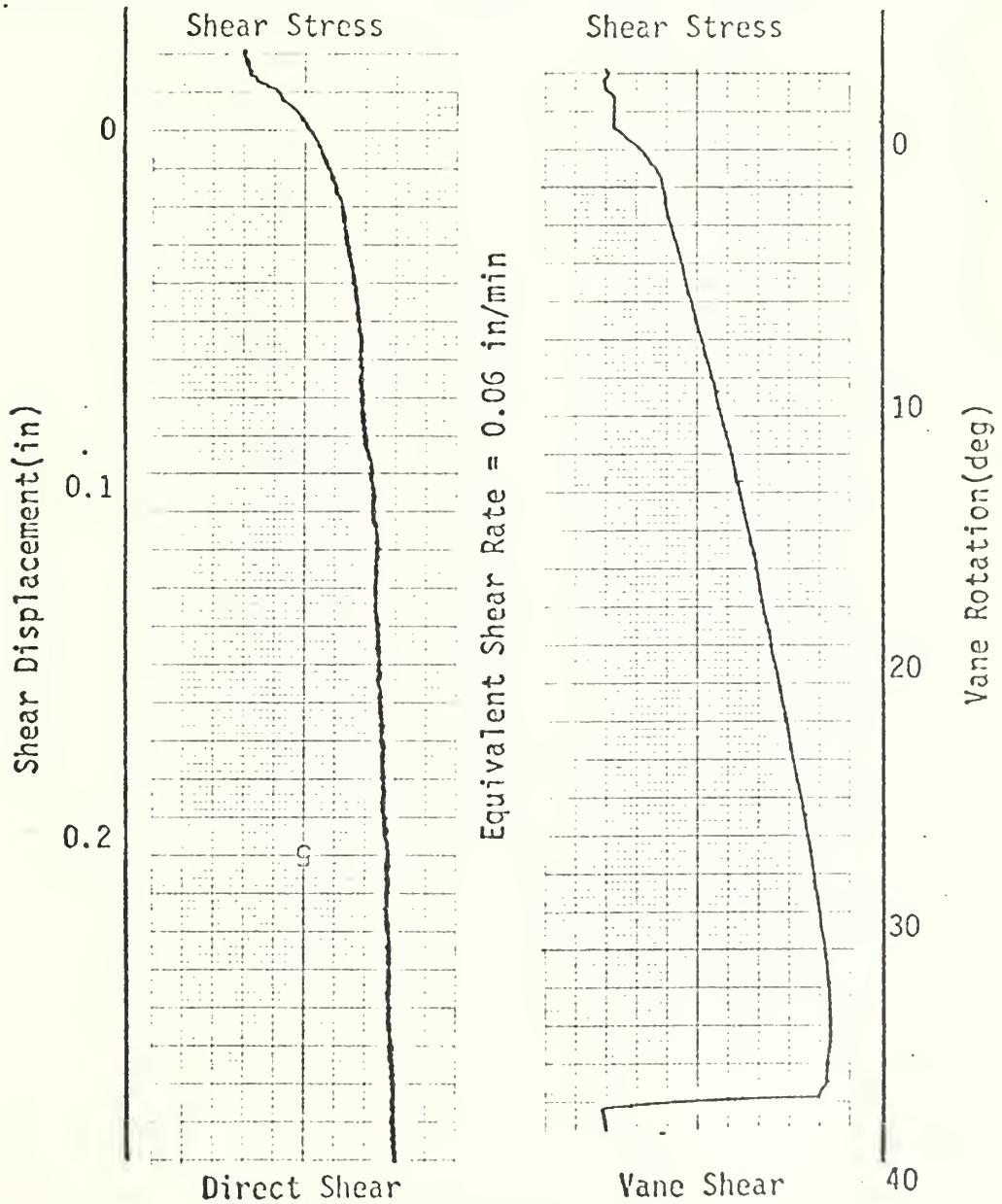

Figure A- 14 Test Results - Sample KK076

Date: 10/18/76		Tested by: J. Foster	
Sample #: GM	Water depth: 67'	Sample depth: ± 30'	
25 mm/min	Chart speed	25 mm/min	
20 v	Signal Conditioner	6 v	
10 mv	Sensitivity	20 mv	
0.0 psi	Normal Stress, Consolidation Pressure	0.0 psi	
2.26 psi	τ_{max}	1.60 psi	

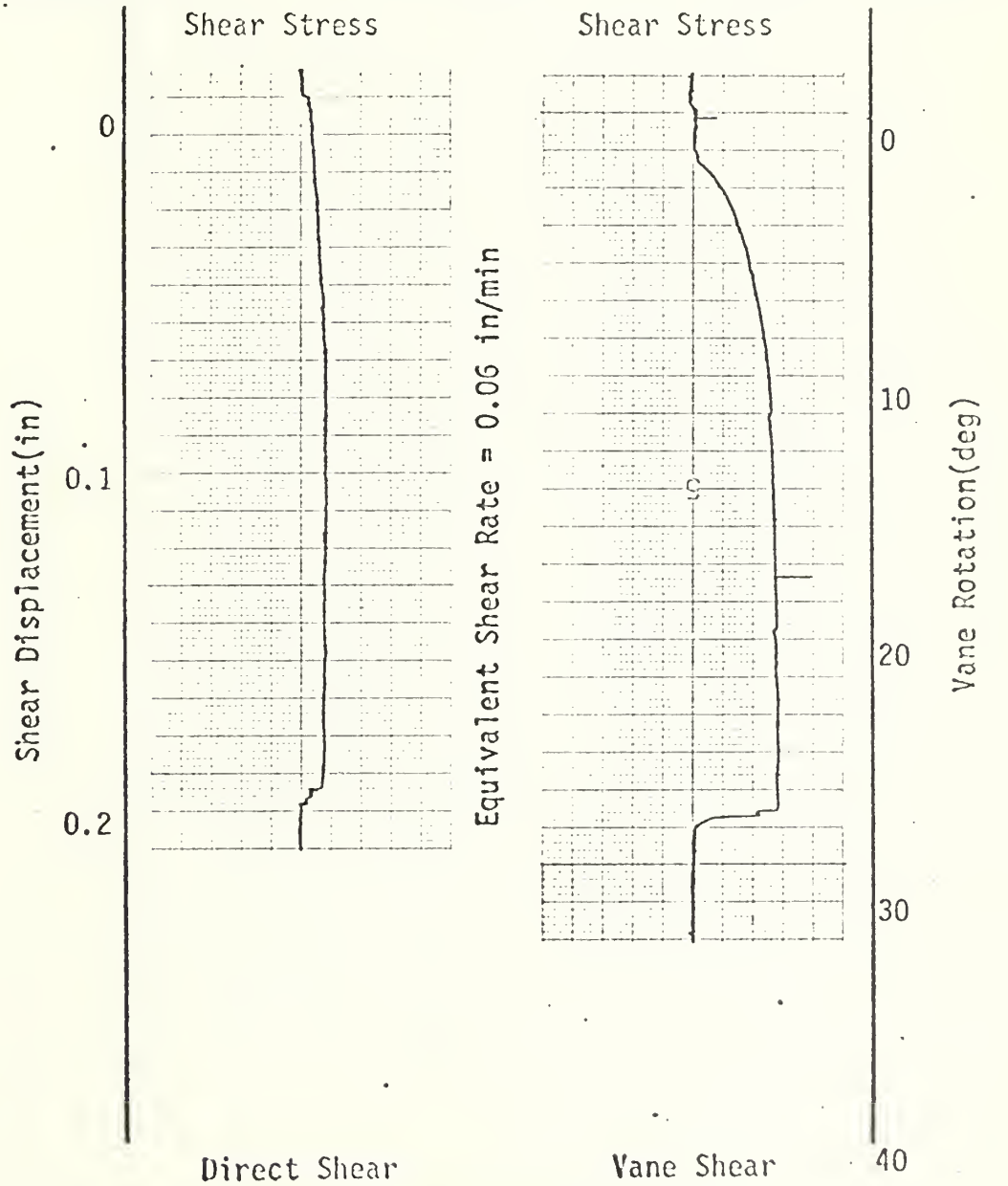

Water Content (%): 75.2

1 mm = 1.5 lb. 1 mm = .11 psi

Figure A-15 Test Results - Sample GM

Date: 10/19/76		Tested by: J. Foster	
Sample #: GM	Water depth: 1671'	Sample depth: ± 30'	
25 mm/min	Chart speed	25 mm/min	
20 v	Signal Conditioner	6 v	
10 mv	Sensitivity	20 mv	
3.0 psi	Normal Stress, Consolidation Pressure	3.0 psi	
2.76 psi	τ_{max}	1.87 psi	

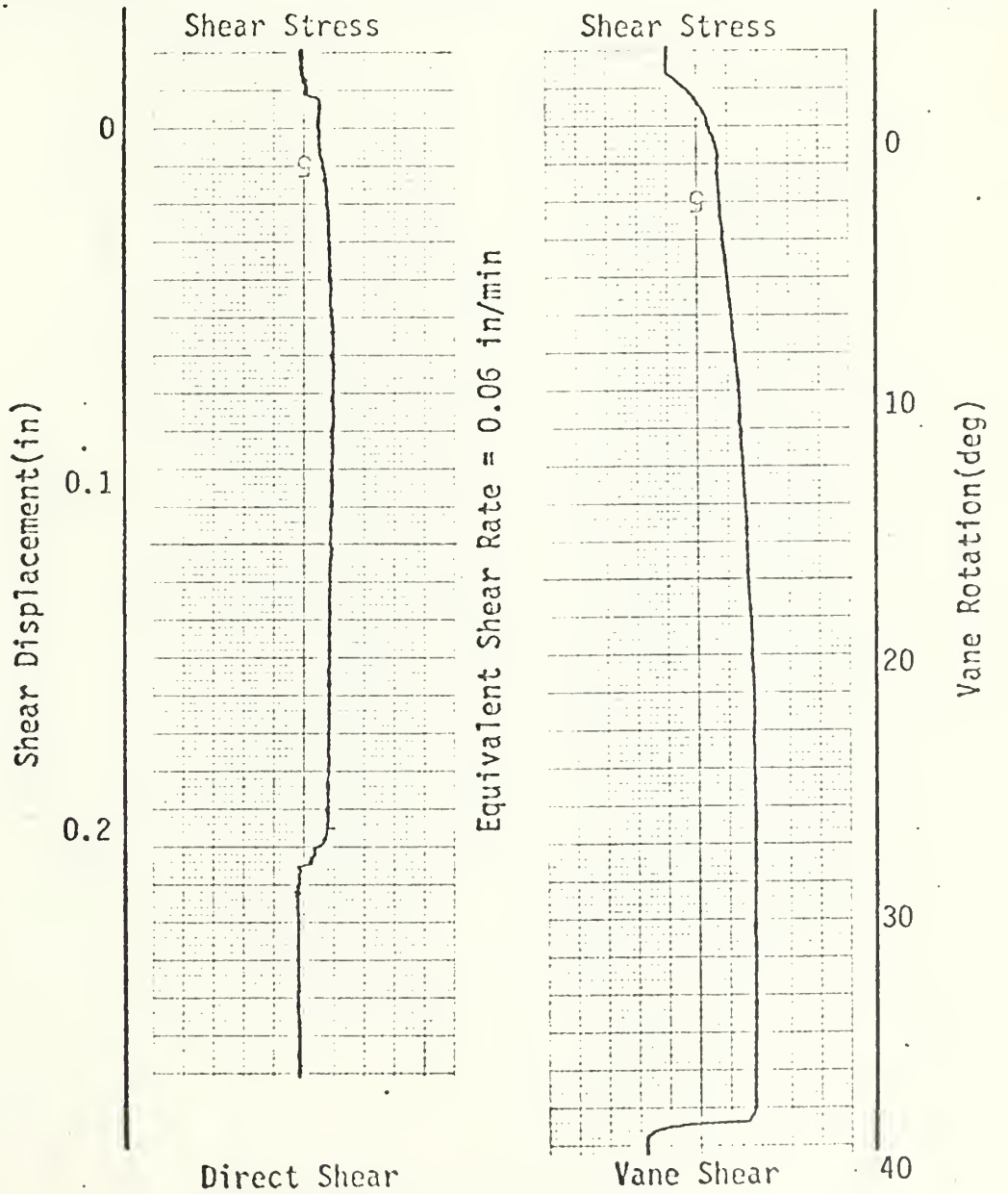

Figure A- 16 Test Results - Sample GM

Date: 10/21/76		Tested by: J. Foster	
Sample #: GM	Water depth: 167'	Sample depth: +30'	
25 mm/min	Chart speed	25 mm/min	
20 v	Signal Conditioner	6 v	
10 mv	Sensitivity	20 mv	
4.5 psi	Normal Stress, Consolidation Pressure	4.5 psi	
3.26 psi	τ_{max}	1.93 psi	

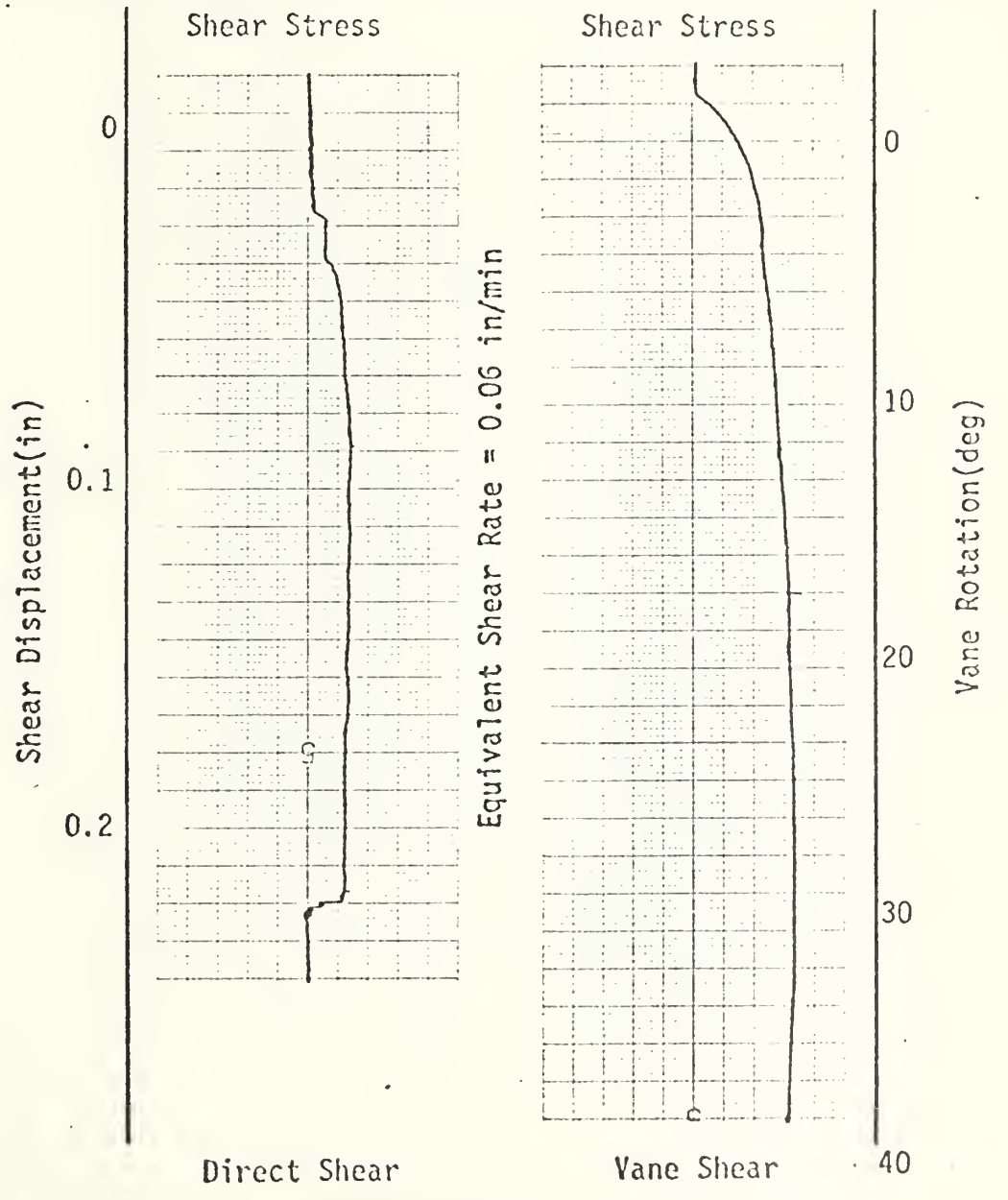

Water Content (%): 71.1

1 mm = 1.5 lb. 1 mm = .11 psi

Figure A- 17 Test Results - Sample GM

Date: 10/22/76		Tested by: J. Foster	
Sample #: GM	Water depth: 167'	Sample depth: ± 30'	
25 mm/min	Chart speed	25 mm/min	
20 v	Signal Conditioner	6 v	
10 mv	Sensitivity	20 mv	
6.0 psi	Normal Stress, Consolidation Pressure	6.0 psi	
3.76 psi	τ_{max}	2.48 psi	

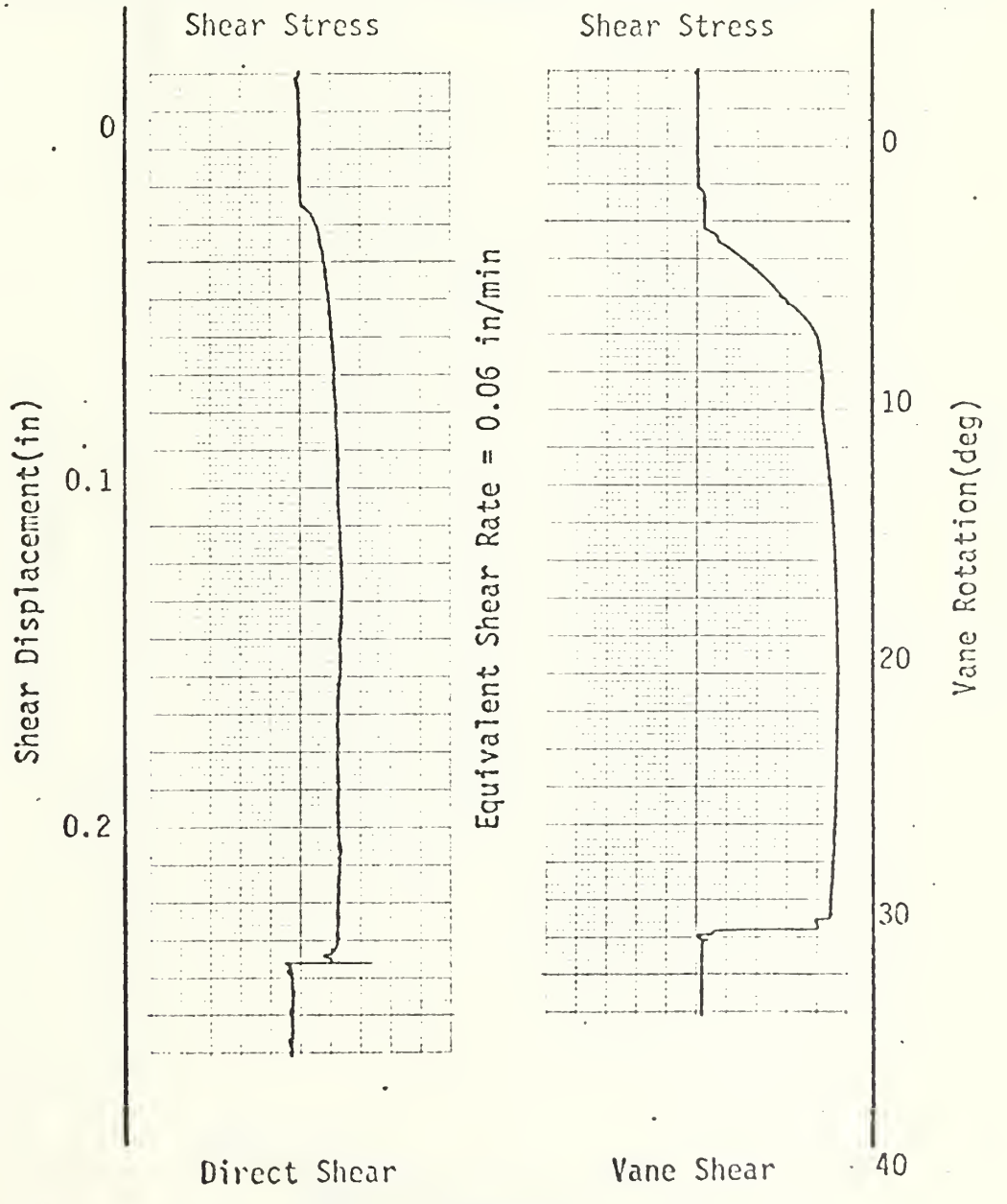

Figure A-18 Test Results - Sample GM

Date: 10/26/76		Tested by: J. Foster	
Sample #: GM	Water depth: 167'	Sample depth: ± 30'	
25 mm/min	Chart speed	25 mm/min	
20 v	Signal Conditioner	6 v	
10 mv	Sensitivity	20 mv	
9.0 psi	Normal Stress, Consolidation Pressure	9.0 psi	
5.02 psi	τ_{max}	2.98 psi	

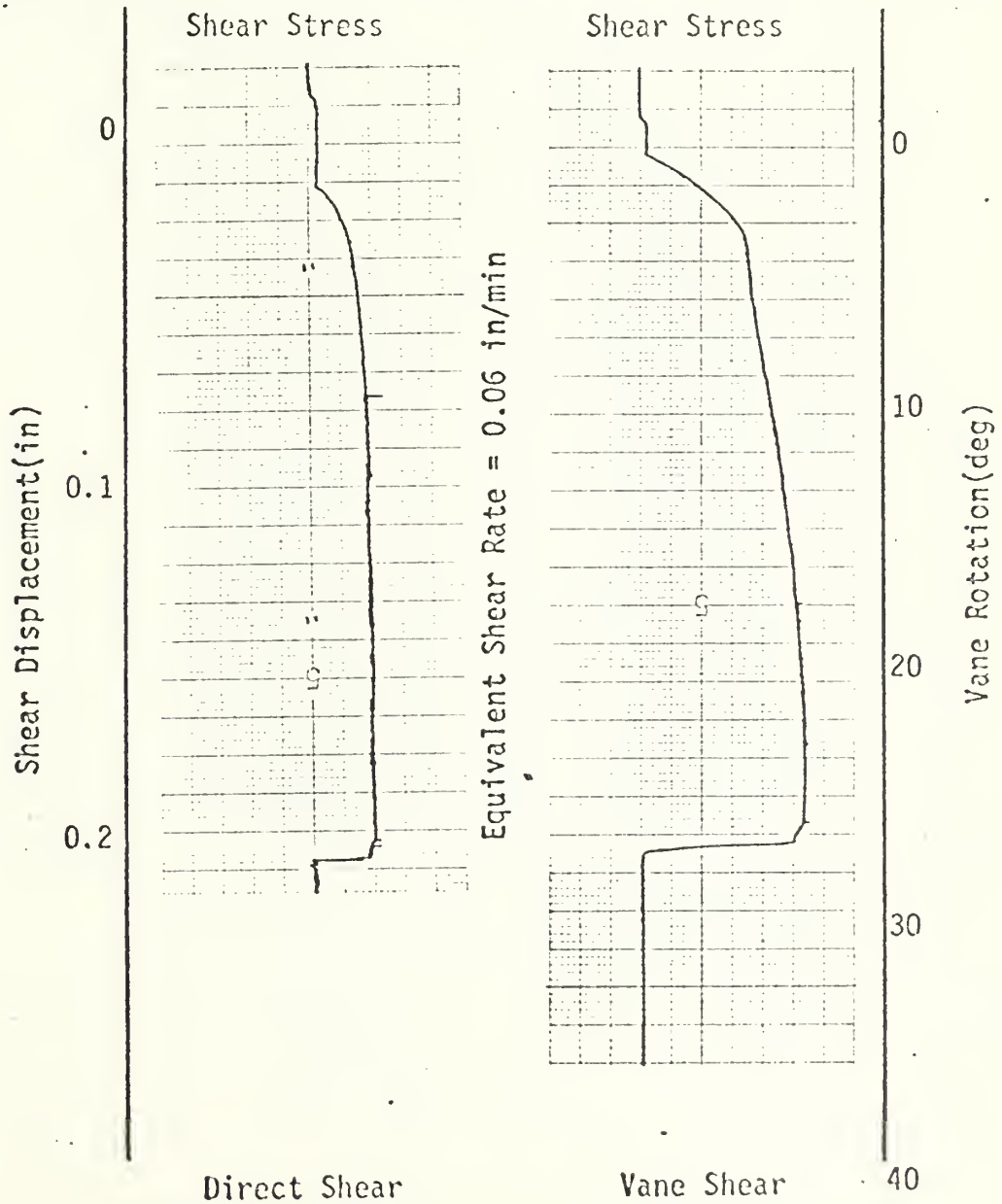

Water Content(%): 66.3

1 mm = 1.5 lb. 1 mm = .11 psi

Figure A-19 Test Results - Sample GM

Date: 10/20/76		Tested by: J. Foster	
Sample #: GM	Water depth: 167'	Sample depth: ± 30'	
25 mm/min	Chart speed	25 mm/min	
20 v	Signal Conditioner	6 v	
10 mv	Sensitivity	20 mv	
12.0 psi	Normal Stress, Consolidation Pressure	12.0 psi	
6.64 psi	τ_{max}	3.30 psi	

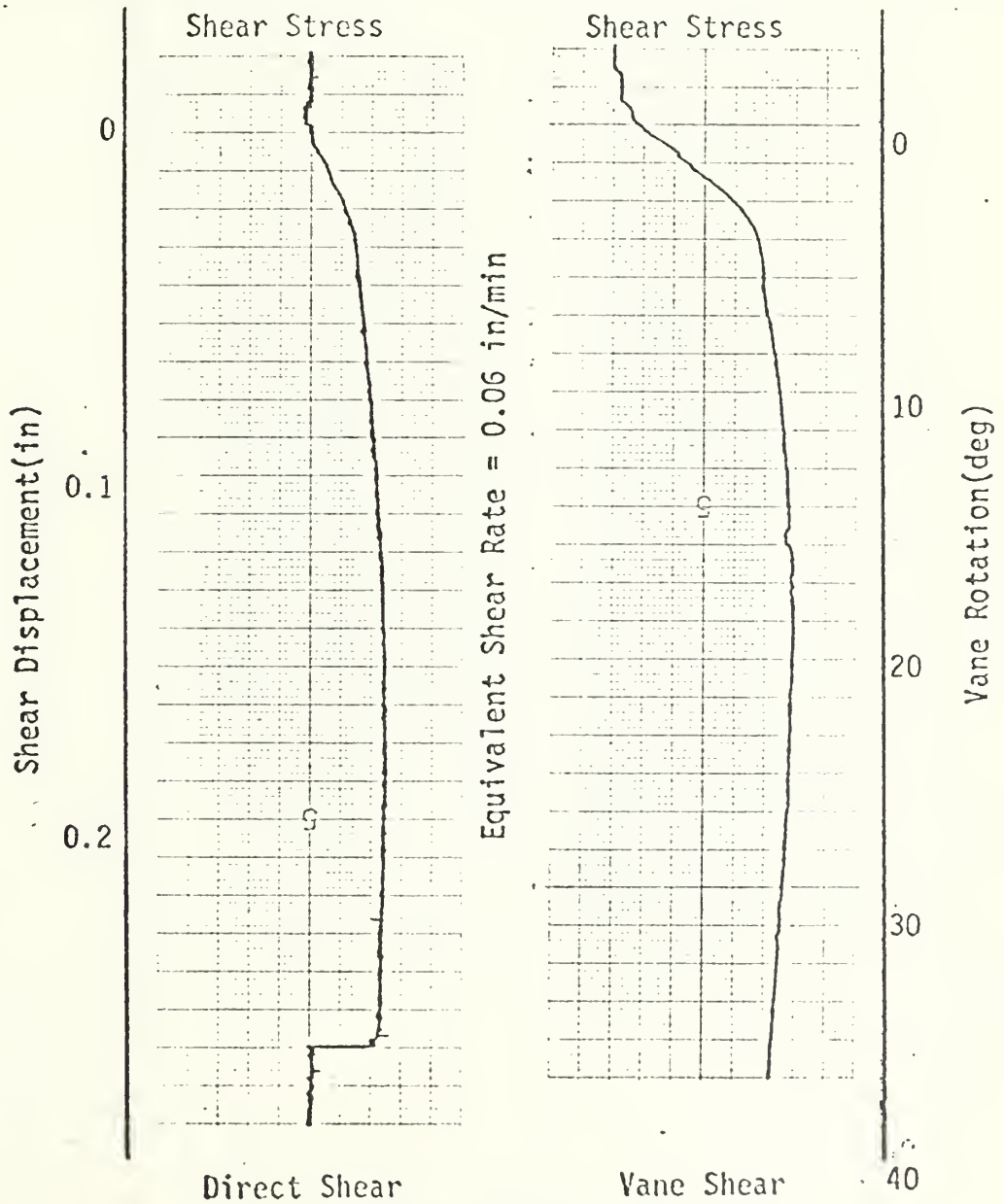

Water Content(%): 64.0

1 mm = 1.5 lb. 1 mm = .11 psi

Figure A-20 Test Results - Sample GM

Date: 11/15/76		Tested by: J. Foster	
Sample #: ATL	Water depth: 4935m	Sample depth: ± 11m	
25 mm/min	Chart speed	25 mm/min	
20 v	Signal Conditioner	6 v	
10 mv	Sensitivity	20 mv	
0.0 psi	Normal Stress, Consolidation Pressure	0.0 psi	
2.01 psi	τ_{max}	1.32 psi	

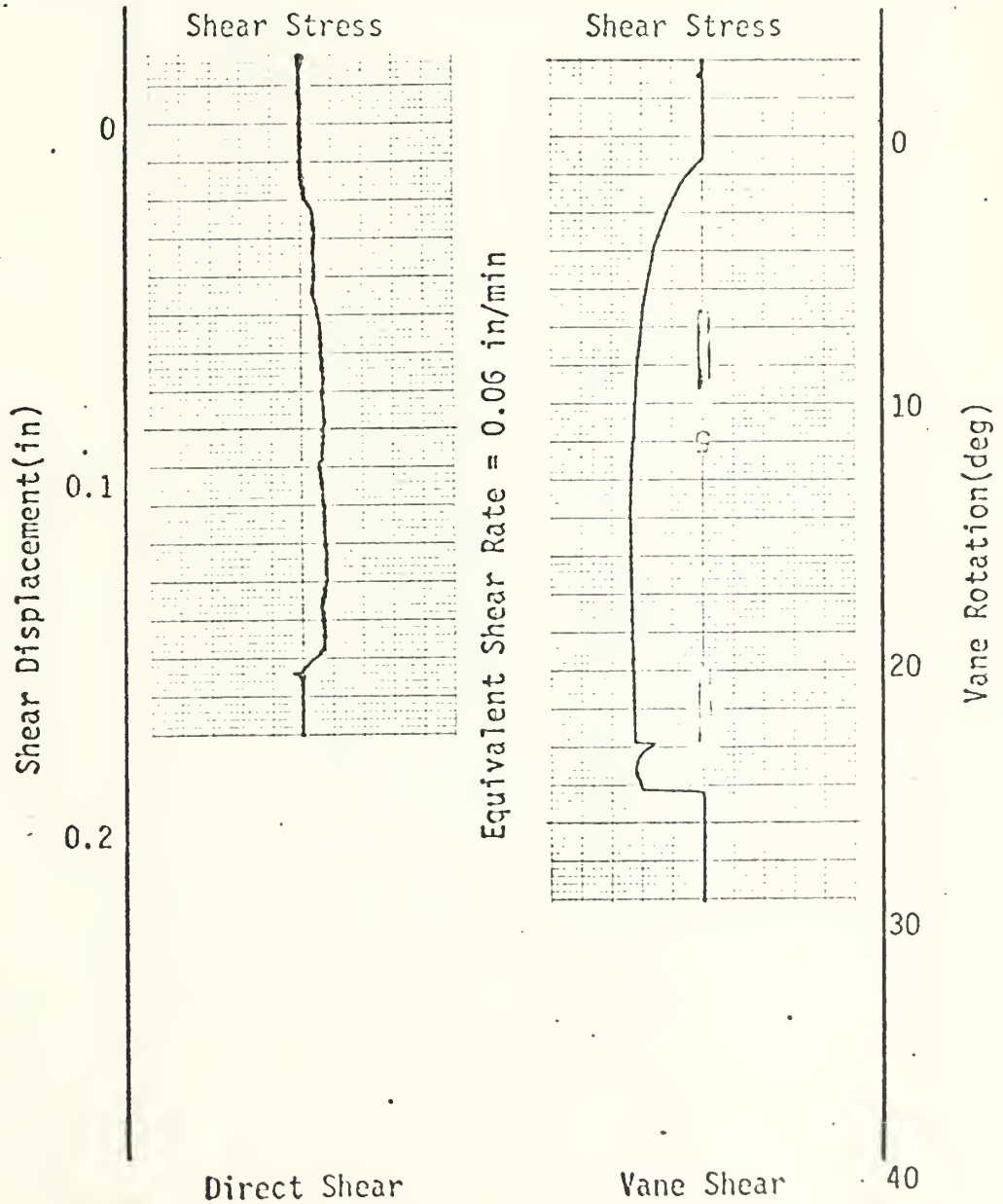

Figure A-21 Test Results - Sample ATL

Date: 11/18/76		Tested by: J. Foster	
Sample #: ATL	Water depth: 4935 m	Sample depth: ± 11m	
25 mm/min	Chart speed	25 mm/min	
20 v	Signal Conditioner	6 v	
10 mv	Sensitivity	20 mv	
3.0 psi	Normal Stress, Consolidation Pressure	3.0 psi	
2.51 psi	τ_{max}	1.65 psi	

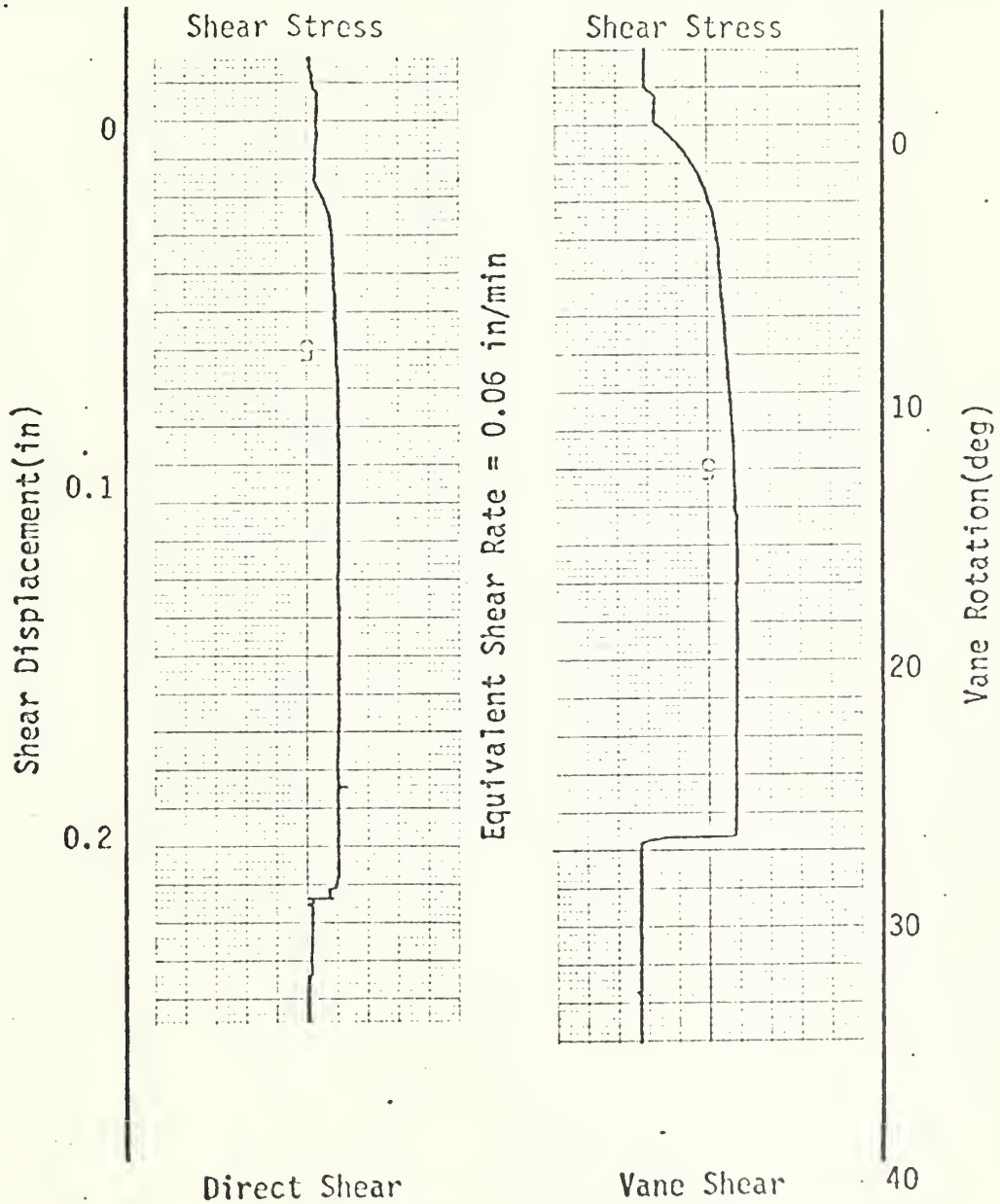

Water Content(%): 163.4

1 mm = 1.5 lb. 1 mm = .11 psi

Figure A- 22 Test Results - Sample ATL

Date: 11/16/76		Tested by: J. Foster	
Sample #: ATL	Water depth: 4935 m	Sample depth: ± 11 m	
25 mm/min	Chart speed	25 mm/min	
20 v	Signal Conditioner	6 v	
10 mv	Sensitivity	20 mv	
6.0 psi	Normal Stress, Consolidation Pressure	6.0 psi	
3.01 psi	τ_{max}	1.82 psi	

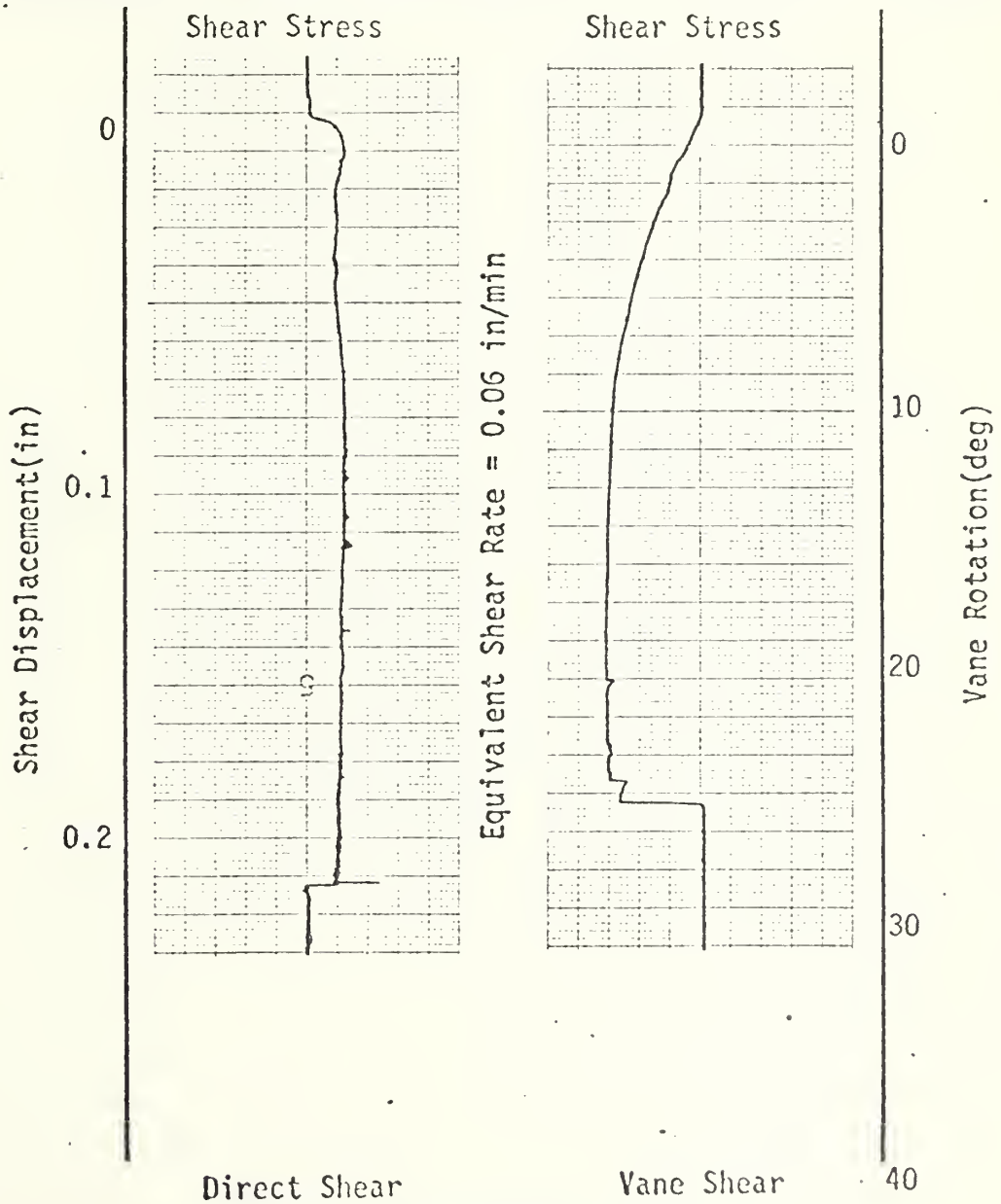

Water Content (%): 159.7

1 mm = 1.5 lb. 1 mm = .11 psi

Figure A- 23 Test Results - Sample ATL

Date: 11/19/76		Tested by: J. Foster	
Sample #: ATL	Water depth: 4.935 m	Sample depth: ± 11 m	
25 mm/min	Chart speed	25 mm/min	
20 v	Signal Conditioner	6 v	
10 mv	Sensitivity	20 mv	
9.0 psi	Normal Stress, Consolidation Pressure	9.0 psi	
4.26 psi	τ_{max}	2.53	psi

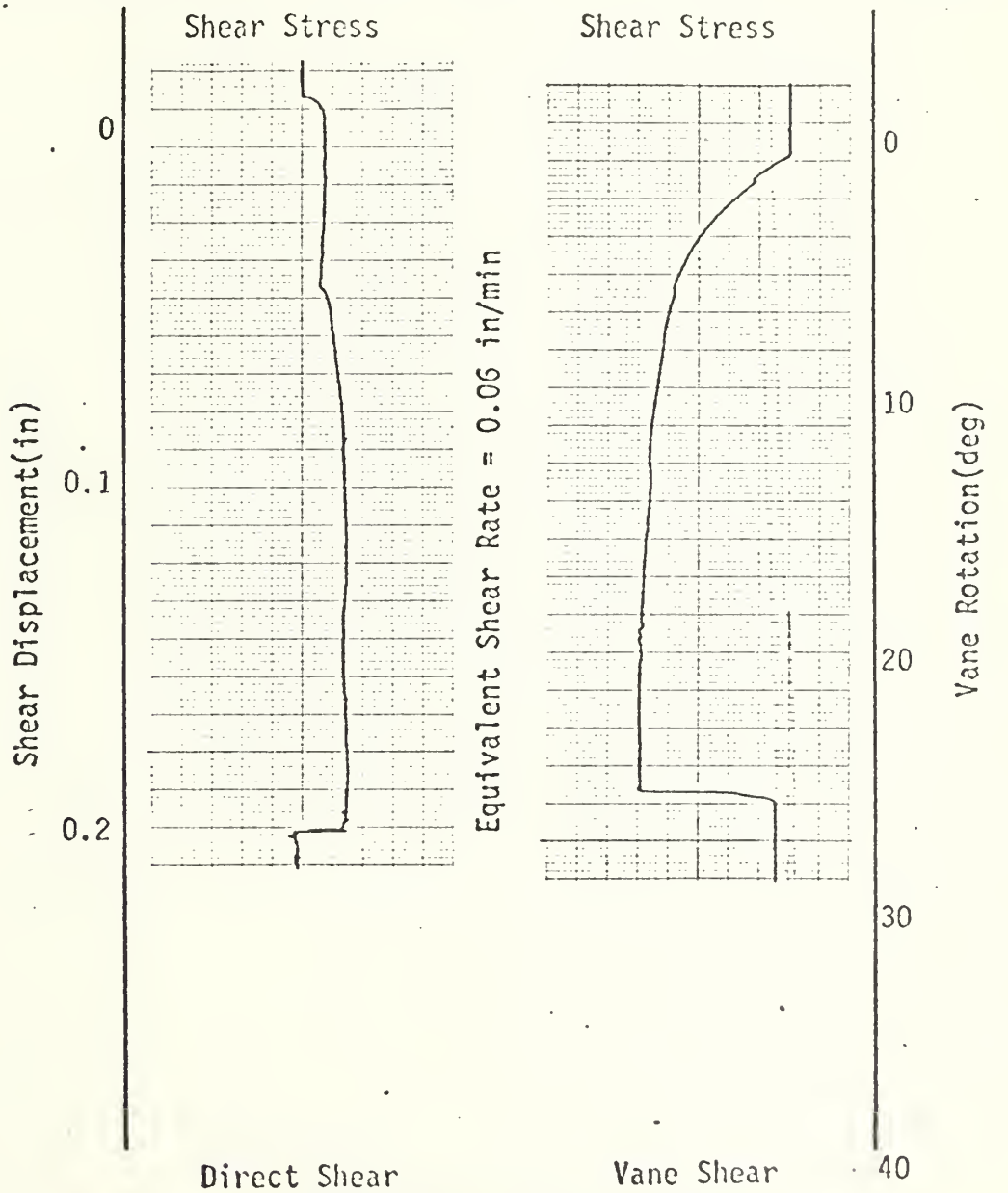

Figure A- 24 Test Results - Sample ATL

Date: 11/22/76		Tested by: J. Foster	
Sample #: ATL	Water depth: 1935 m	Sample depth: ± 11 m.	
25 mm/min	Chart speed	25 mm/min	
20 v	Signal Conditioner	6 v	
10 mv	Sensitivity	20 mv	
12.0psi	Normal Stress, Consolidation Pressure	12.0psi	
5.52 psi	τ_{max}	2.86 psi	

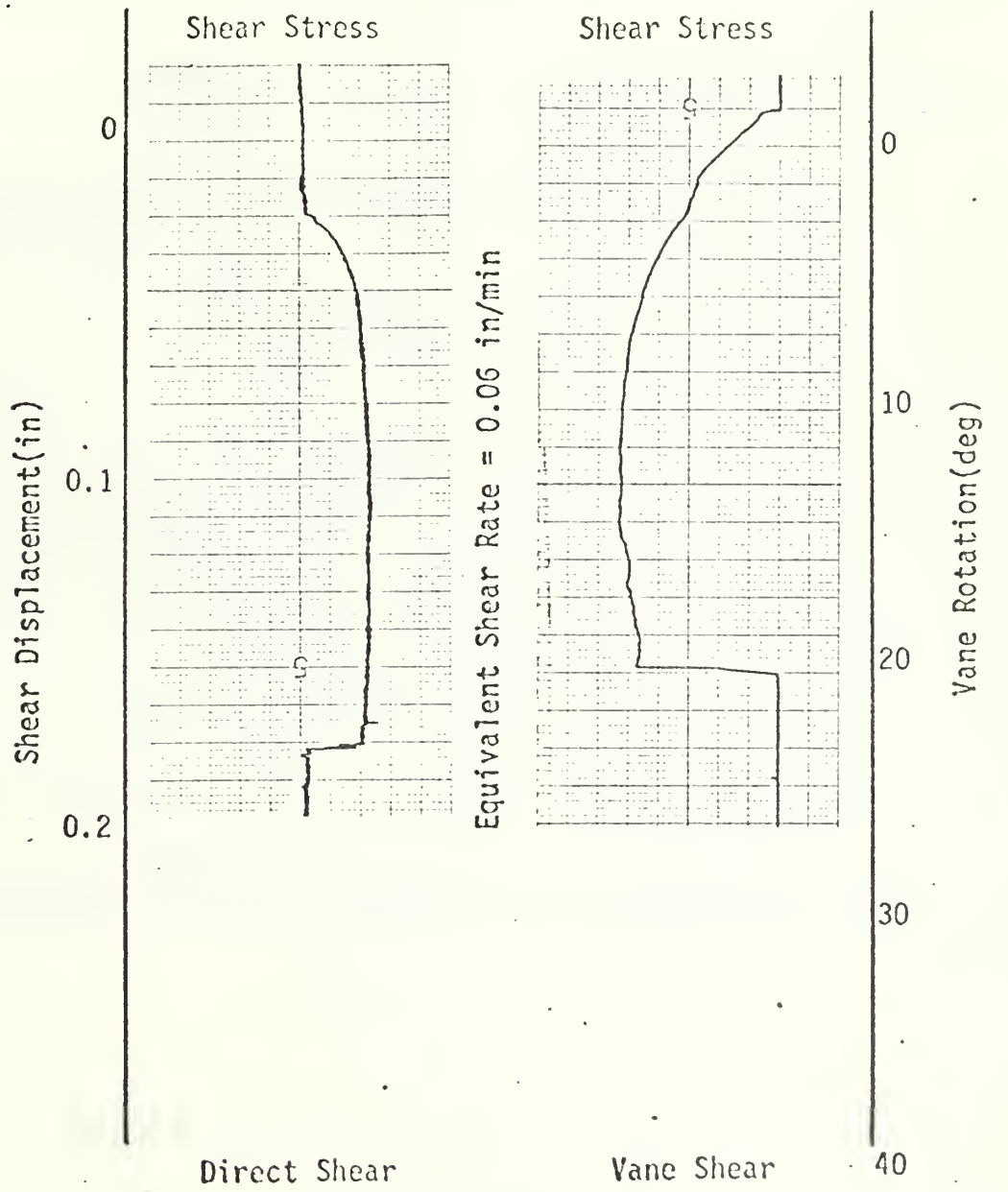

Figure A-25 Test Results - Sample ATL

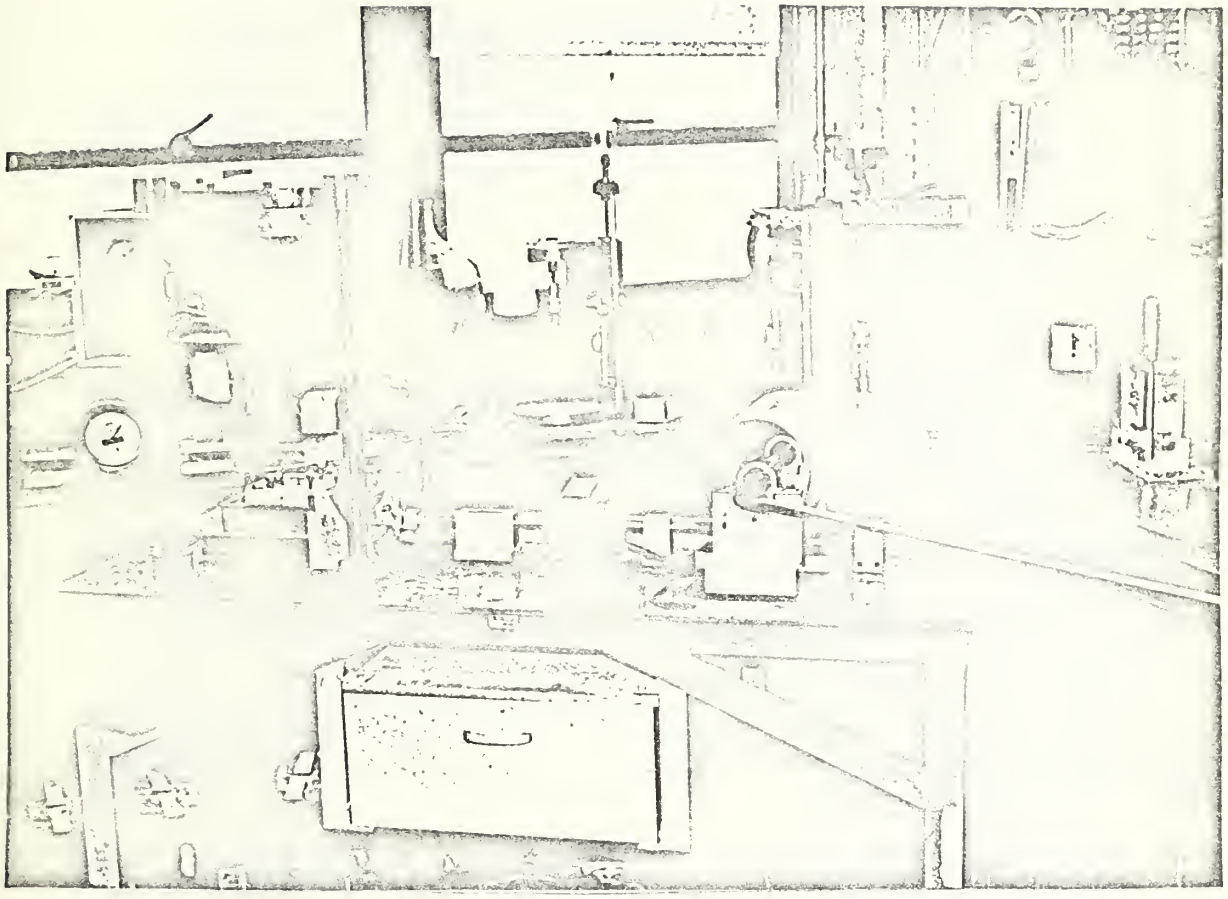

PLATE 1 DIRECT SHEAR TEST APPARATUS

PLATE 2 DIRECT SHEAR LOAD CELL

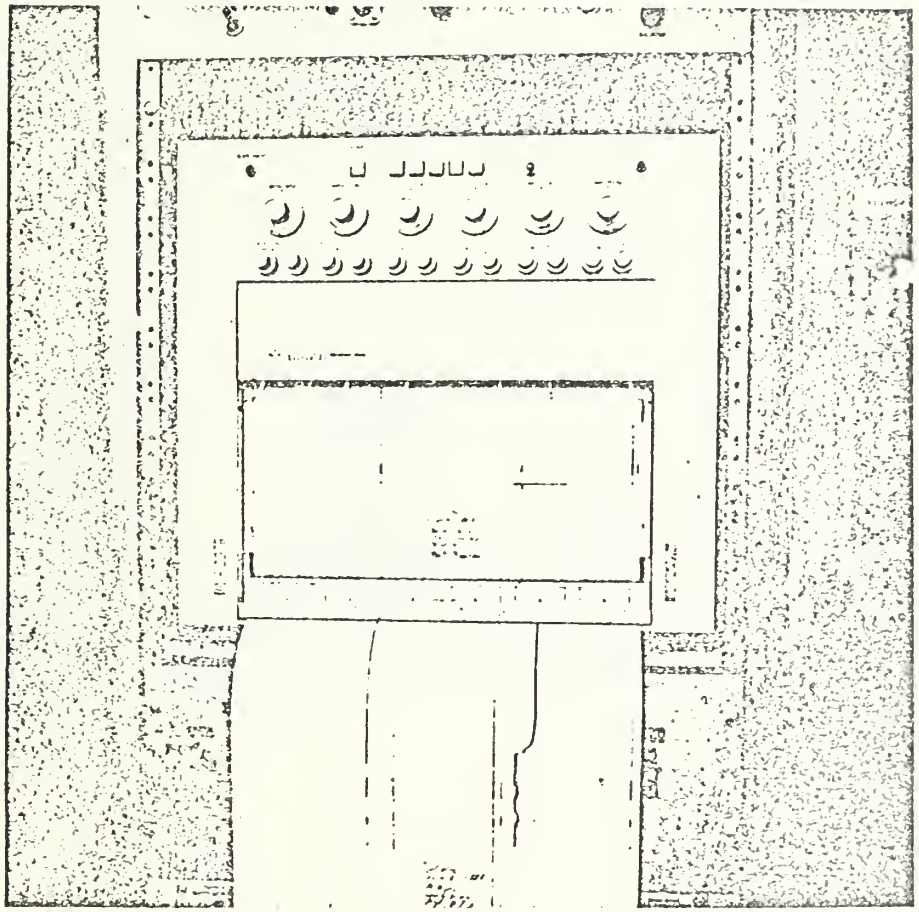

PLATE 3. Strain gage conditioner and data strip recorder

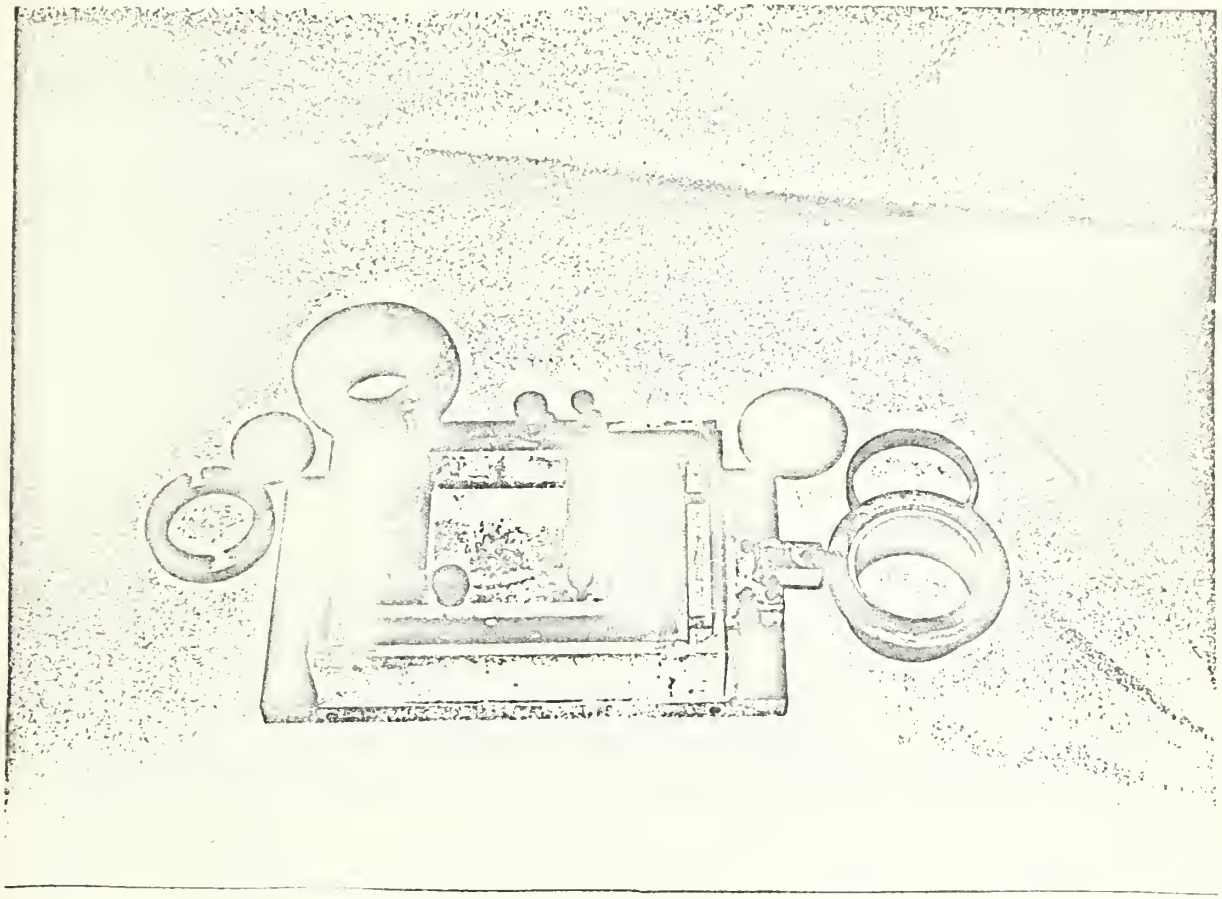

PLATE 4 DIRECT SHEAR BOX, RING ADAPTERS, AND PRESSURE PLATES

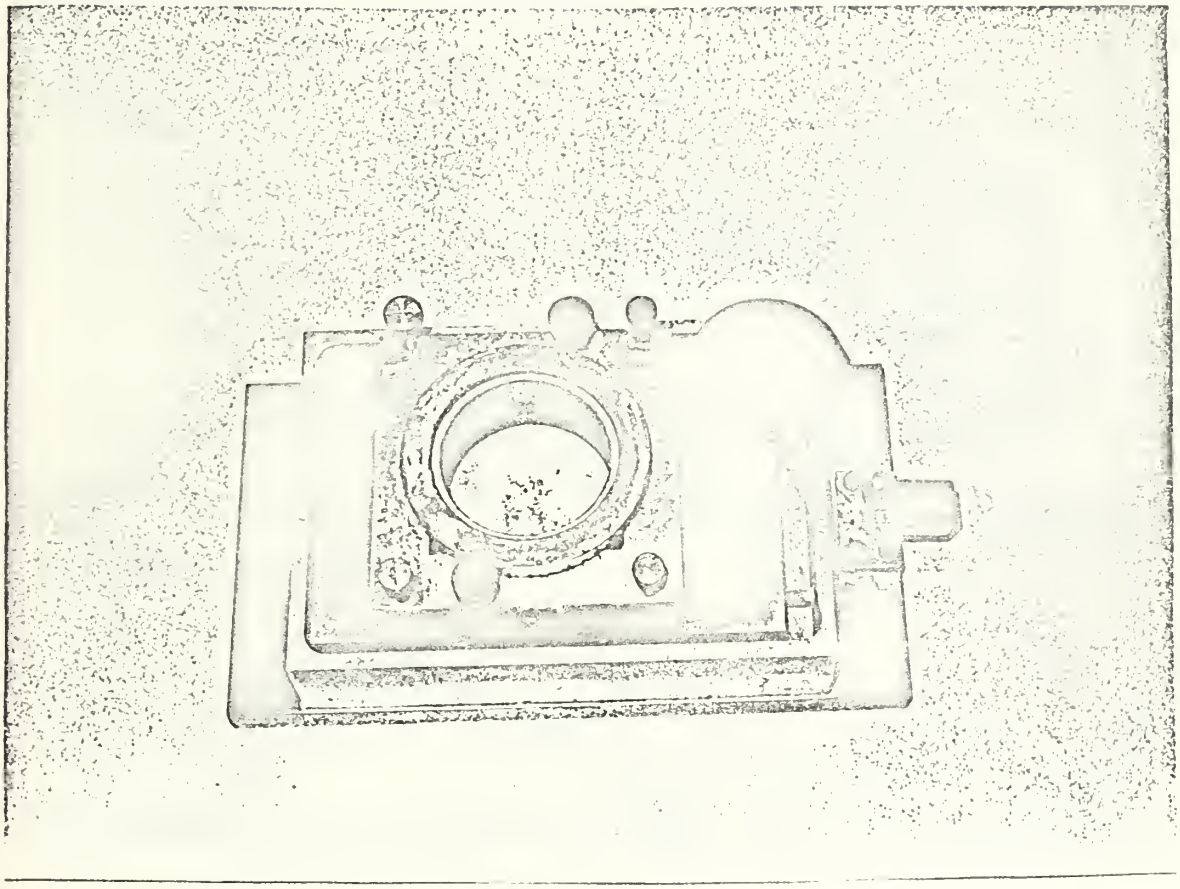

PLATE 5 ASSEMBLED MODIFIED DIRECT SHEAR BOX AND PRESSURE PLATE

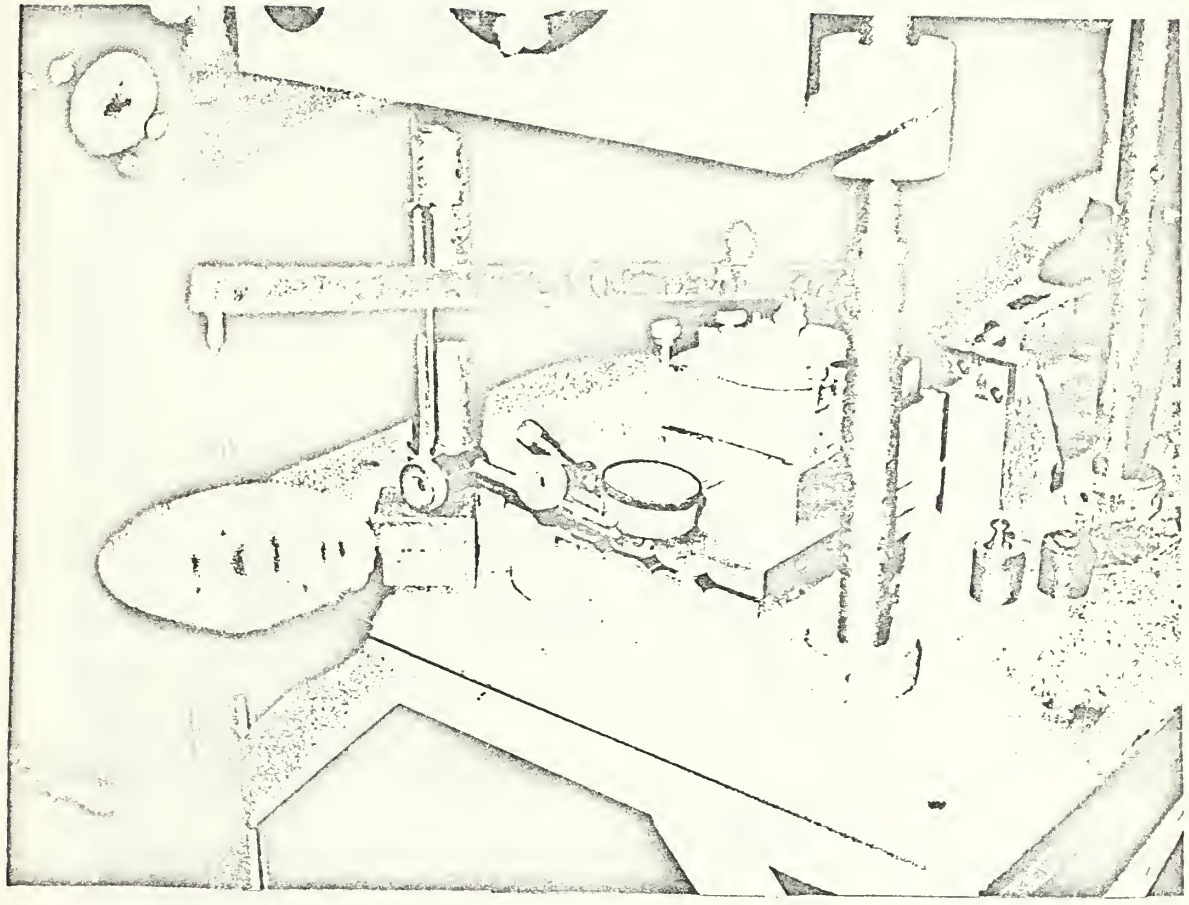

PLATE 6 CHECKING HORIZONTAL DISPLACEMENT DURING DIRECT SHEAR TEST

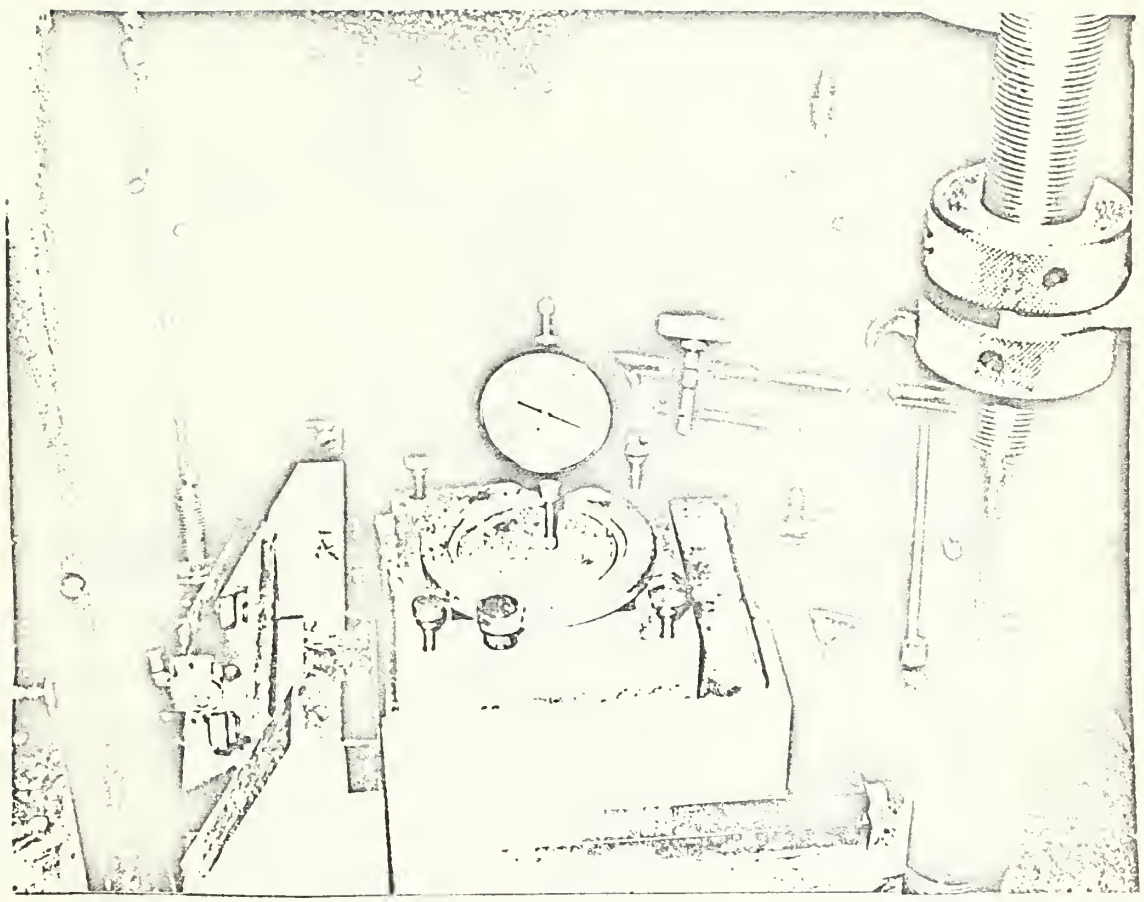

PLATE 7 MONITORING CONSOLIDATION IN DIRECT SHEAR MACHINE

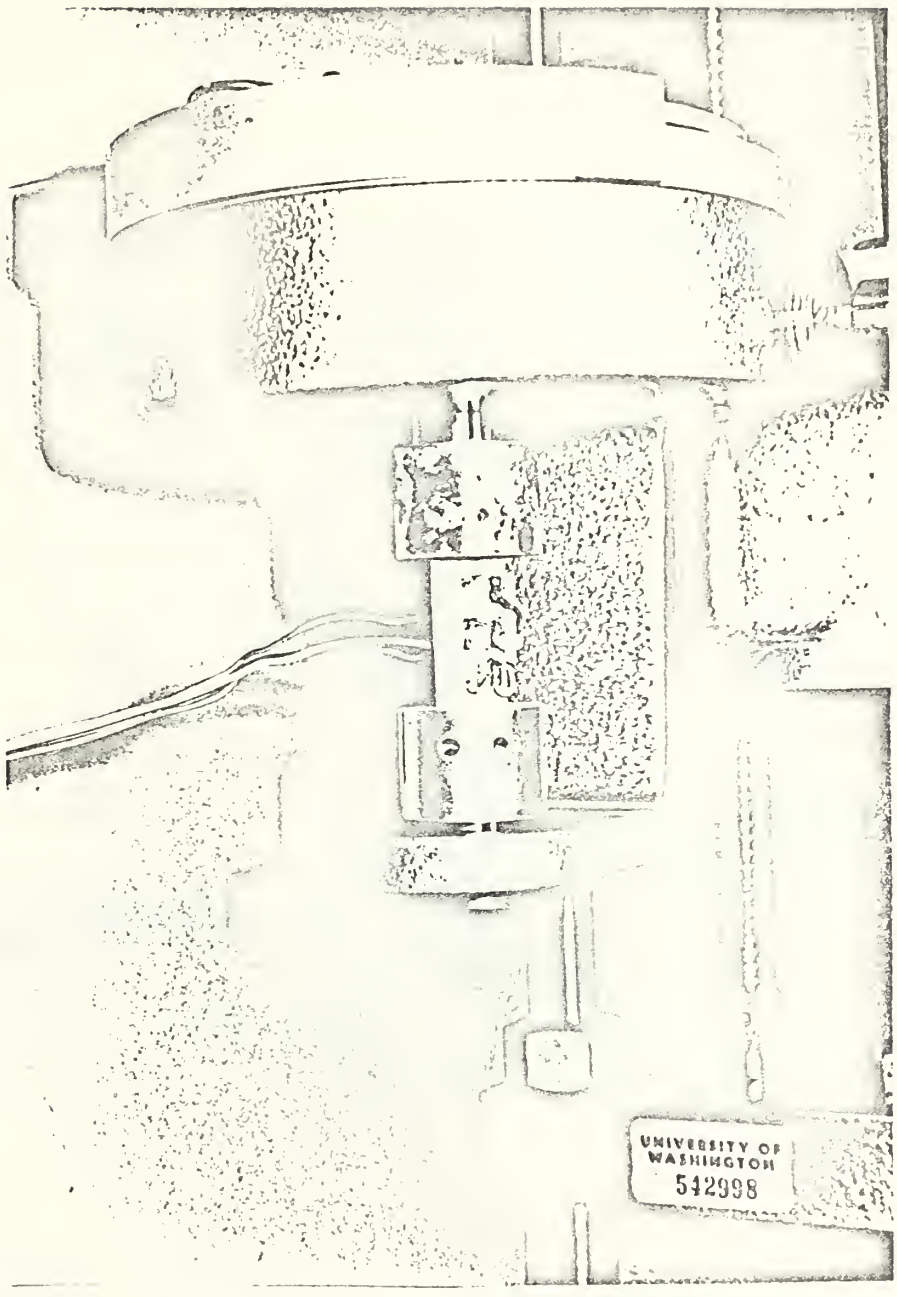

PLATE 8 VANE SHEAR MACHINE, STRAIN GAGE VANE TORQUE PICK-UP REPLACEMENT

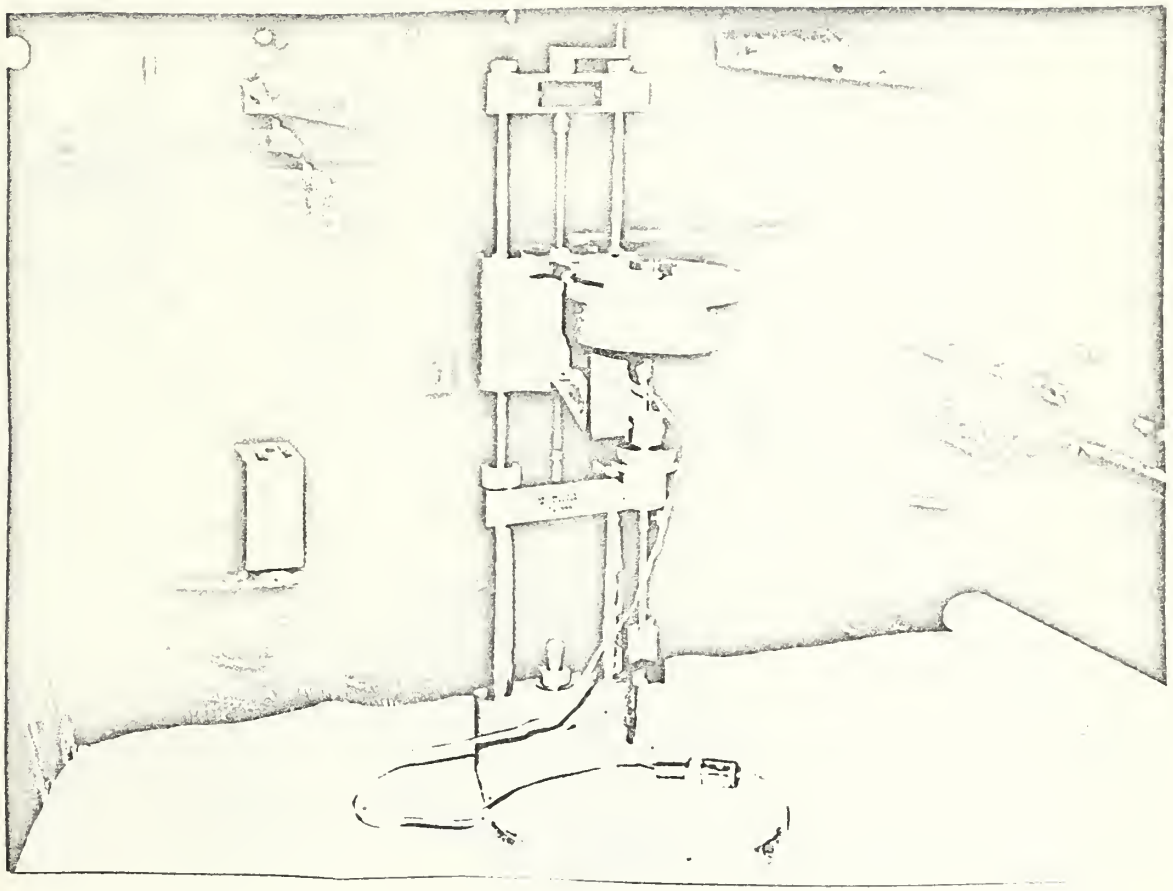

PLATE 9 MODIFIED WYKHAM-FARRANCE VANE SHEAR MACHINE

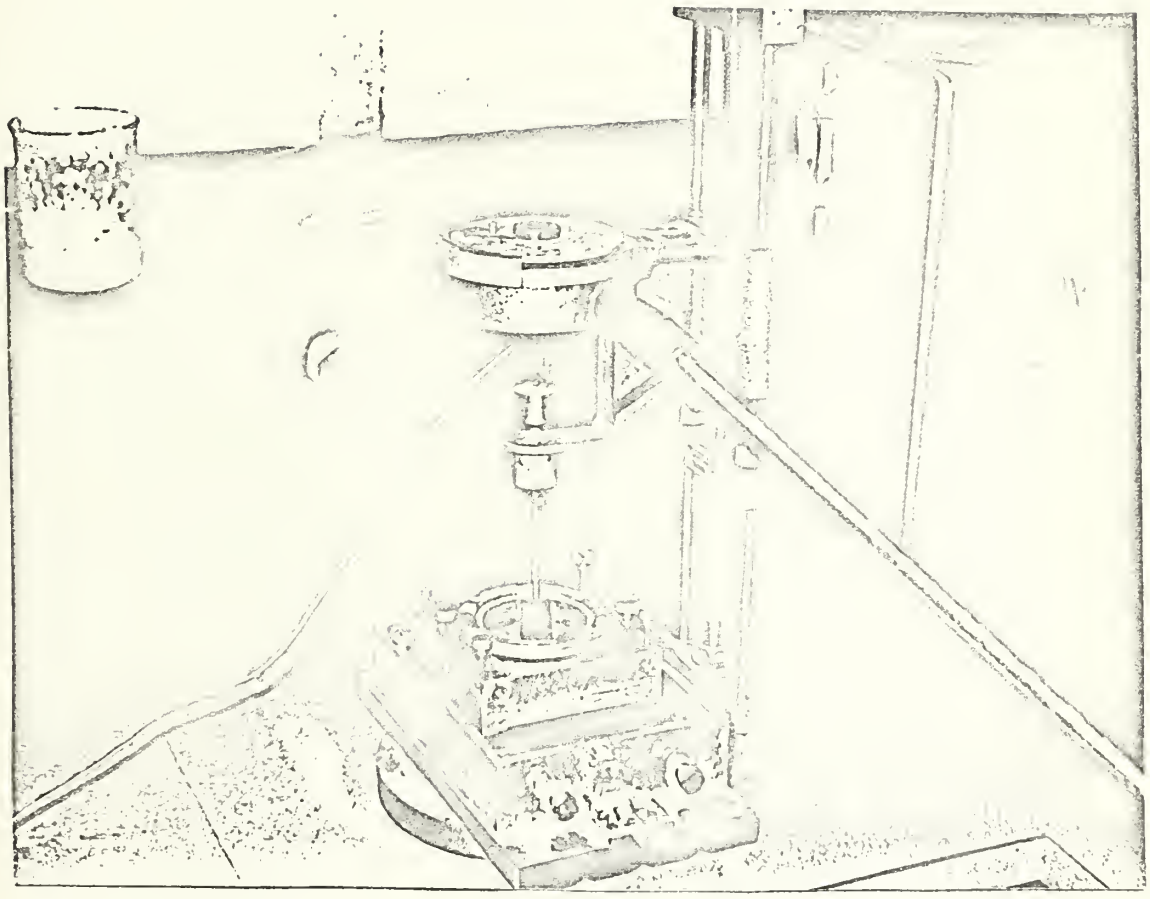

PLATE 10 VANE SHEAR TEST IN PROGRESS WITH SAMPLE IN DIRECT SHEAR BOX

Thesis
F654 Foster
Determination of undrained shear strength of marine clays by combined vane and direct shear analysis.
171265